UNIVERSIDAD AUTÓNOMA DE NUEVO LEÓN

FACULTAD DE CIENCIAS BIOLÓGICAS

TESIS

FORMULACIÓN Y EVALUACIÓN BIOLÓGICA DE NANOMEDICINAS CON EXTRACTO DEL CENIZO *Leucophyllum frutescens* (BERL.) I.M. JOHNSTON (SCROPHULARIACEAE) CONTRA *Mycobacterium tuberculosis*

POR

CLAUDIA JANETH MARTÍNEZ RIVAS

COMO REQUISITO PARCIAL PARA OBTENER EL GRADO DE DOCTOR EN CIENCIAS CON ACENTUACIÓN EN QUÍMICA DE PRODUCTOS NATURALES

NOVIEMBRE, 2018

UNIVERSITY CLAUDE BERNARD LYON 1

FORMULATION AND BIOLOGICAL EVALUATION OF NANOMEDICINS WITH CENIZO *Leucophyllum frutescens* (BERL.) I.M. JOHNSTON (SCROPHULARIACEAE) EXTRACT AGAINST *Mycobacterium tuberculosis*

BY

CLAUDIA JANETH MARTÍNEZ RIVAS

DOCTOR IN CHEMISTRY

NOVEMBER, 2018

UNIVERSIDAD AUTÓNOMA DE NUEVO LEÓN

FACULTAD DE CIENCIAS BIOLÓGICAS

UNIVERSIDAD AUTÓNOMA DE NUEVO LEÓN (MÉXICO)

Y

UNIVERSITÉ CLAUDE BERNARD LYON 1 (FRANCIA)

TESIS EN COTUTELA

FORMULACIÓN Y EVALUACIÓN BIOLÓGICA DE NANOMEDICINAS CON EXTRACTO DEL CENIZO *Leucophyllum frutescens* (BERL.) I.M. JOHNSTON (SCROPHULARIACEAE) CONTRA *Mycobacterium tuberculosis*

POR

CLAUDIA JANETH MARTÍNEZ RIVAS

COMO REQUISITO PARCIAL PARA OBTENER EL GRADO DE DOCTOR EN CIENCIAS CON ACENTUACIÓN EN QUÍMICA DE PRODUCTOS NATURALES

NOVIEMBRE, 2018

FORMULACIÓN Y EVALUACIÓN BIOLÓGICA DE NANOMEDICINAS CON EXTRACTO DEL CENIZO *Leucophyllum frutescens* (BERL.) I.M. JOHNSTON (SCROPHULARIACEAE) CONTRA *Mycobacterium tuberculosis*

Comité de Tesis

_____

Dr. Sergio Arturo Galindo Rodríguez

Presidente

_____

Dr. Abdelhamid Elaissari

Secretario

_____

Dra. Ma. Azucena Oranday Cárdenas

1ª. VOCAL

_____

Dra. Catalina Rivas Morales

2ª. VOCAL

_____

Dra. Ma. Adriana Nuñez González

3ª. VOCAL

FORMULACIÓN Y EVALUACIÓN BIOLÓGICA DE NANOMEDICINAS CON EXTRACTO DEL CENIZO *Leucophyllum frutescens* (BERL.) I.M. JOHNSTON (SCROPHULARIACEAE) CONTRA *Mycobacterium tuberculosis*

Dirección de Tesis

El presente trabajo fue dirigido por los abajo firmantes dentro de un convenio de colaboración para realizar tesis en cotutela entre la Facultad de Ciencias Biológicas (UANL) y el *Laboratoire d'Automatique et de Génie des Procédés* (UCBL-1), el cual fue firmado en junio del 2013. Como resultado del convenio, la sustentante, Claudia Janeth Martínez Rivas, obtendrá el grado de Doctor en Ciencias por ambas instituciones.

Dr. Sergio Arturo Galindo Rodríguez	Dr. Abdelhamid Elaissari
Director UANL	Director UCB-L1
Dra. Rocío Álvarez Román	Dr. Hatem Fessi
Co-directora UANL	Co-director UCB-L1

AGRADECIMIENTOS ACADÉMICOS

El presente trabajo fue apoyado por:

AIRD-France, Jeunes Équipes (JEAI-2011, NANOBIOSA).

PN-CONACYT-México/2014-248560 and PAICYT-UANL-México.

CJMR agradece a CONACyT por su apoyo a través de la beca no. 280212 y al Programa BECAS MIXTAS 2016 - MZO 2017 MOVILIDAD EN EL EXTRANJERO (291062) para la realización de una estancia de investigación.

Al Dr. Abdelhamid Elaissari y Dr. Hatem Fessi por su dirección durante el doctorado y la estancia de investigación en LAGEP, Université Claude Bernard Lyon 1, Francia.

A la Dra. Elvira Garza González por su dirección en la parte microbiológica de este trabajo en el Laboratorio de Gastroenterología del Hospital Universitario Dr. José Eleuterio González, Facultad de Medicina, UANL.

AGRADECIMIENTOS PERSONALES

María Luisa Rivas Ramírez y Martín Martínez García tienen mi infinito agradecimiento, porque su amor me ha formado e impulsado día a día, pero sobre todo me sustentó durante esta etapa de mi vida, Ustedes y yo sabemos todo lo que significó para mí. Los amo papás.

Igual de importantes son Gaby, Martín y Michelle quienes me vieron crecer en tantos sentidos de mi vida durante este tiempo, antes, mis hermanitos compañeros de cuarto, ahora, con una familia por quien luchar, espero haberles dado el mejor ejemplo.

A Juan Bernardo Pérez Arenas, quien me apoyó durante la mayor parte de estos estudios de doctorado, y ahora motivándome para el futuro. A la Sra. Juana María Arenas Solís, quien me dio un buen ejemplo en el tiempo en que convivimos.

Dr. Abdelhamid Elaissari gracias por todo lo que me enseñó, conocerlo ha sido todo un placer, sus palabras me hicieron crecer como persona no sólo como profesionista. Merci bien!

Gracias Lily por ser mi compañera incondicional y amiga, doy gracias a Dios por poner a una persona como tú en mi camino, todo fue mejor con tu presencia y consejo. Misael, gracias por estar ahí con nosotras cuando tenias el tiempo, y por seguir brindándome tu amistad. Caro, me alegro de que te hayan mandado a hacer tus pruebas al Nano, pues de eso resultó nuestra amistad. Y Sara, gracias por compartir conmigo durante el doctorado, nunca olvidaré ese gran viaje.

Gracias Dios por tu amor infinito y por esta lección de vida.

INDEX

INDEX OF TABLES

INDEX OF FIGURES

I. ABSTRACT

Tuberculosis is an emergency disease worldwide, the emergence of resistant strains to the treatment has produced the use of natural products as alternative. Studies have shown that *Leucophyllum frutescens* extracts present antimicrobial effect, but the disadvantage is that the extracts are recovered in a vehicle that contains organic solvents. The preparation of polymeric nanoparticles (NP) involves the elimination of the solvent in which the active is solubilized, which makes possible to use them as vehicles for the administration of the extracts. Therefore, the aim of this study was to design and develop formulations of NP with an extract of *L. frutescens*, and rifampicin (RIF), in order to evaluate the *in vitro* biological activity against *M. tuberculosis*. Firstly, the methanolic extract of leaves and roots of *L. frutescens* and its fractions were obtained. The anti-*M. tuberculosis* activity was determined, being the root extract (EMR) and its hexane fractions (FHR and RF1) the most actives with a MIC of 100, 40 and 40 µg/mL, respectively. RIF, EMH, FHR and RF1 were incorporated into NP by nanoprecipitation. NP of ≈180 nm with homogeneous size distribution were obtained. The NP were evaluated on *M. tuberculosis*, being the formulation of NP-PLGA-RIF (MIC=0.10 µg/mL) and NP-PLGA-RF1 (CMI=80 µg/mL) with better activity. Finally, the anti-*M. tuberculosis* activity of the combined form formulations was evaluated, the combination of RIF with NP-PLGA-RF1 produced better behavior, reducing the MIC of both without showing toxic effect. The studies carried out in this work showed the potential use of an NP formulation contains a vegetable fraction of *L. frutescens* in combination with RIF as an alternative against *M. tuberculosis*.

II. RÉSUMÉ

La tuberculose est une maladie d'urgence dans le monde, l'apparition de souches résistantes au traitement a produit l'utilisation de produits naturels comme alternative. Des études ont montré que les extraits de *Leucophyllum frutescens* présentaient un effet antimicrobien, mais l'inconvénient est que les extraits sont récupérés dans un véhicule qui contient des solvants organiques. La préparation de nanoparticules polymériques (NP) implique l'élimination du solvant dans lequel l'actif est solubilisé, ce qui permet les utiliser comme véhicules pour l'administration des extraits. Par conséquent, le but de cette étude a été design et développer des formulations de NP avec un extrait de *L. frutescens* et de la rifampicine (RIF), afin d'évaluer l'activité biologique *in vitro* contre *M. tuberculosis*. Premièrement, l'extrait méthanolique de feuilles et de racines de *L. frutescens* et ses fractions a été obtenu. L'activité contre *M. tuberculosis* a été déterminée, l'extrait de racines (EMR) et ses fractions hexanique (FHR et RF1) ont été les plus actives avec une CMI de 100, 40 et 40 µg/mL, respectivement. RIF, EMH, FHR et RF1 ont été incorporés dans NP par nanoprécipitation. Des NP de ≈180 nm avec une distribution de taille homogène ont été obtenus. Les NP ont été évaluées sur *M. tuberculosis*, les formulations de NP-PLGA-RIF (CMI=0,10 µg/mL) et NP-PLGA-RF1 (CMI=80 µg/mL) ont montré la meilleure activité. Finalement, l'activité des formulations combinées contre *M. tuberculosis* a été évaluée, la combinaison de RIF avec NP-PLGA-RF1 a produit le meilleur comportement, réduisant la CMI des deux sans montrer un effet toxique. Les études réalisées dans ce travail ont montré l'utilisation potentielle d'une formulation de NP contient une fraction végétale de *L. frutescens* en combinaison avec le RIF comme alternative contre *M. tuberculosis*.

III. INTRODUCTION

1. Tuberculosis

Tuberculosis (Tb) is an infectious disease caused by *Mycobacterium tuberculosis* (OMS, 2018), which is an acid-fast bacillus. It particularly affects the lungs, developing pulmonary Tb (Ruiz-Manzano *et al*., 2008). Since 1993, it is considered by the World Health Organization (WHO) as an emergency disease worldwide. In 2016, 10.4 million people became ill with tuberculosis and 1.7 million died from this disease (OMS, 2018).

The current therapeutic scheme against Tb is based on the administration of four first-line antibiotics: isoniazid (INH), rifampicin (RIF), pyrazinamide (PZA) and streptomycin or ethambutol, for 6 months (WHO, 2005). Specifically, RIF is the only bactericidal drug that has activity on different populations that the bacteria present in the organism.

One limitation of the treatment is that, due to its long duration many patients do not follow it adequately, which causes the appearance of drug-resistant strains. Therefore, to improve the pharmacological therapy and evade the resistance of the agent, it is urgent to find alternatives that reduce the time of treatment, or substances with a mechanism of action different to the existing drugs.

2. Natural Products

The plants have been used in traditional medicine to treat several diseases. WHO estimates that in many developed countries, from 70 to 80% of the population has resorted once to some form of alternative or complementary medicine (OMS, 2008).

Research in natural products has grown in recent years, numerous medicinal plant compounds that exhibit bioactivity have been described, including antimycobacterial activity (Camacho-Corona *et al.*, 2009).

For this reason and in response to the urgency of obtaining new drugs against strains of *M. tuberculosis*, several studies based on natural products have been developed. Some plants of the north of Mexico have been evaluated with favorable activity, among them, extracts of *Leucophyllum frutescens*, commonly named “cenizo”.

In the study by Molina-Salinas et al., extracts of *L. frutescens* against drug-resistant and drug-resistant strains of *M. tuberculosis* were tested. The extract of the leaves and

roots were obtained by maceration. The evaluation by microdilution in broth showed an activity of the root extract of 62.5 μg/mL, for the sensitive and the resistant strain. For the leaves, a MIC of 125 μg/mL was obtained. This study supports that, the selection of plants by ethnobotanical criteria increases the possibility of finding species with activity, not only against *M. tuberculosis*, but also against other microorganisms (Molina-Salinas *et al.*, 2007).

However, the disadvantage of the use of extracts is that they are recovered in vehicles containing organic solvents, therefore their application *in vivo* is not viable.

To overcome these limitations, new strategies have been proposed, including the use of polymeric nanoparticles (NP) as a vehicle for the administration of plant extracts.

3. Polymeric nanoparticles

NP (Figure 1) are particles of less than 500 nm in diameter that are prepared from natural or synthetic, biodegradable or non-biodegradable polymers. Drugs, proteins, peptides or nucleotides can be incorporated into these polymeric systems for their therapeutic application.

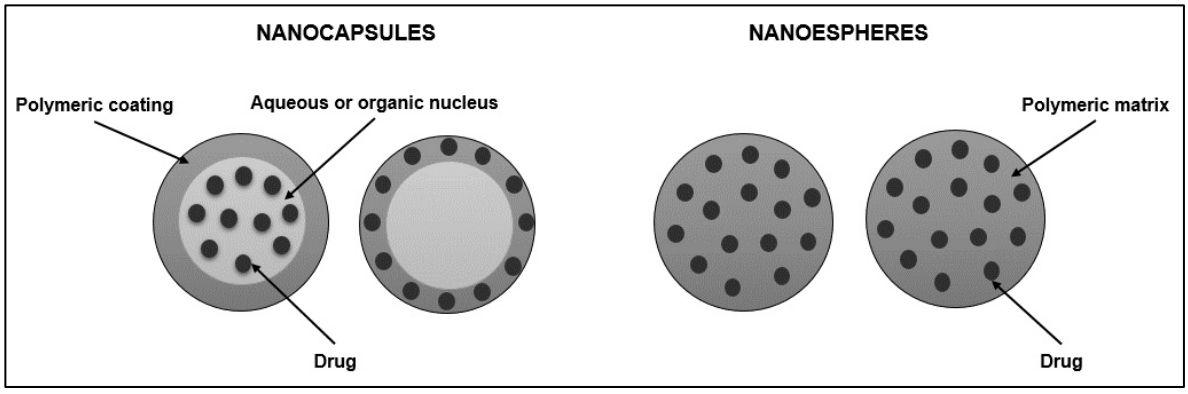

Figure 1. Structure of polymeric nanoparticles.

Among the features that stand out from these colloidal systems include the protection of the active, the targeting to an organ or cell and the sustained release of the encapsulated compound (Martínez Rivas *et al.*, 2017), this last virtue allows to reduce the frequency of treatment dose. On the other hand, the preparation of NP involves the elimination of the

solvent in which the active is solubilized (Figure 2), resulting in the encapsulation of the active compounds, free of organic solvents.

An additional advantage of NP is related to the versatility in their administration, depending their composition. NP can be applied topically (Martínez Rivas et al., 2017), oral or parenteral (Pilheu *et.al*., 2007).

Therefore, it is important to note that NP are a potential vehicle to increase the antimycobacterial activity of drugs used in the treatment of tuberculosis and to transport natural extracts that can not be administered directly to the body.

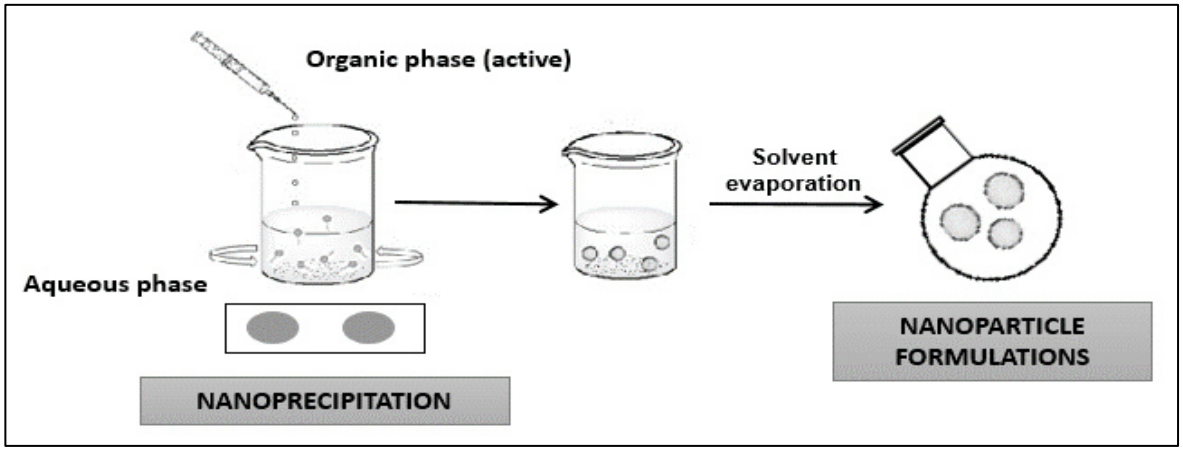

Figure 2. Preparation of polymeric nanoparticles by nanoprecipitation.

4. Encapsulation of natural compounds in polymeric nanoparticles

In recent years the interest in the encapsulation of plant extracts or derivatives has increased. An example of this, is the encapsulation of resveratrol. Yao *et al*. incorporated the compound in chitosan NP with free amino groups on the surface. NP had a particle size of 487 nm and an polydispersity index of 0.144; in addition, chitosan NP showed sustained release *in vitro* (Yao et al., 2006).

In another study, Uthaman *et al.* extracted boswellic acid from the rubber resin of *Boswellia serrata*. The volumetric analysis showed a total of boswellic acid in the extract of 60%. Subsequently, formulations of NP were formulated with boswellic acid by nanoprecipitation method. NP had a diameter of 259 nm and a Z potential of -42.88 mV. *In vitro* cytotoxicity assays were performed with different cancer cell lines (pancreas, brain, prostate and melanoma). The PC3 prostate cancer cell line showed favorable

cytotoxicity percentages. Therefore, they concluded that NP formulations containing boswellic acid can be used as potential anticancer agents in the treatment of prostate cancer (Uthaman *et al*., 2012).

5. Drugs for the treatment of tuberculosis loaded in polymeric nanoparticles

Different studies have verified the protective properties (Calleja-Avellanal *et al.*, 2003), targeting (Yolandy *et al*., 2010) and sustained release (Maksimenko *et al.*, 2010) from NP containing first-line drugs of the tuberculosis treatment, including RIF. NP improved the bioavailability of the drugs and reduced the frequency of the dose (Pandey *et al.*, 2003; Pandey y Khuller, 2006). In addition, there are several works that showed an effect against *M. tuberculosis* when they are encapsulated in NP. An example was observed in the study conducted by Yolandy *et al*., who demonstrated targeting of isoniazid (INH) in nanoparticulate delivery systems. *In vitro* tests were performed on THP-1 and U937 monocyte-macrophages and microscopic analysis showed that targeting was achieved. After 1 and 2 days of exposure of INH loaded NP, a significant inhibition in the growth of the microorganism was observed, but with a reduced value in the toxicity/efficiency ratio compared with free INH (Yolandy *et al*., 2010). And, Booysen *et al*. proved that RIF and INH loaded NP have activity against the strain of *M. tuberculosis* H37Rv. In addition, they carried out the oral administration of the formulations in mice and observed a sustained release of the drugs for 7 days. They also determined the distribution of RIF and INH in the liver and the lungs for up to 10 days. With these results, they conclude that NP containing drugs for the treatment of tuberculosis have the potential to improve Tb chemotherapy (Booysen *et al.*, 2013).

Therefore, the incorporation of plant compounds in NP as well as a first-line drug such as RIF is a promising alternative. In this context, the present work focused on the encapsulation of the extract and the fractions of *L. frutescens* in NP to generate a phytomedicine, as well as the incorporation of RIF, with the purpose of improving the activity against M. tuberculosis, and thus, proposing them as treatment for tuberculosis.

IV. JUSTIFICATION

Tb is considered since 1993, by WHO, a worldwide emergency disease. One of the main causes of the great number of deaths, reported each year because of this disease, is due to the resistance that the bacillus strains have acquired in consequence to the inadequate monitoring of the treatment.

For this reason, it is urgent to find alternatives that reduce the treatment time and actives with a mechanism of action different from the existing drugs, to treat resistant strains. In recent years, natural products have been studied for the molecules with biological activity it contains, but their application is limited to the presence of organic solvents with which extracts are recovered.

NP are a vehicle of biologically active compounds that offers multiple advantages, among them, the removal of the organic solvents in which the active compounds are dissolved. Therefore, the incorporation of plant compounds in NP is a promising alternative. In addition, NP provide sustained release to the encapsulated compound, making possible to reduce the dose frequency.

In this context, the present work is focused on incorporation of extracts and fractions of *Leucophyllum frutescens* plant to generate a phytomedicine, as well as encapsulation of RIF, in order to enhance the activity against *M. tuberculosis* and propose them as treatment for Tb.

V. HYPOTHESIS

The encapsulation of an extract or fraction of *L. frutescens* and rifampicin in polymeric nanoparticles allows the enhancement of the activity against *M. tuberculosis*.

VI. GENERAL OBJECTIVE

To design and develop NP formulations based on an extract or fraction of *L. frutescens* and RIF, in order to increase their biological activities against *M. tuberculosis*.

VII. SPECIFIC OBJECTIVES

- To obtain the methanol extracts of leaves and roots of *L. frutescens* by maceration and sonication and carry out the fractionation.

- To develop a chromatographic method validated by CLAR in order to characterize the extracts and their fractions and obtain their chromatographic profiles.

- To encapsulate the extracts and active fractions by nanoprecipitation technique in NP and perform their physicochemical characterizations according to the size, polydispersity index (PDI), zeta potential, surface morphology, drug loading and encapsulation efficiency.

- To encapsulate RIF in NP by nanoprecipitation technique and perform their physicochemical characterizations according to the size, PDI, zeta potential, surface morphology and incorporated compounds.

- To evaluate the *in vitro* biological activity of the NP formulations on *M. tuberculosis*, as well as to determine the synergistic effect of the drug and the vegetable samples, free and encapsulated.

- To evaluate the toxicity of NP formulations with better antimycobacterial activities.

CHAPTER 1. RIFAMPICIN AND *Leucophyllum frutescens*: ENCAPSULATION IN BIODEGRADABLE POLYMERIC NANOPARTICLES AND THEIR BIOLOGICAL EVALUATION AGAINST *Mycobacterium tuberculosis*

ABSRACT

Tuberculosis (Tb), is an emergency disease worldwide, caused by *Mycobacterium tuberculosis.* For its treatment four first-line drugs are administered; however, the emergence of resistant strains has led to the promising use of natural products as an alternative to combat the disease. Studies show that several plant extracts have action against *M. tuberculosis*, such as *Leucophyllum frutescens*. The disadvantage of the extracts is that they are recovered in vehicles as organic solvents, which makes difficult its application *in vivo*. The preparation of polymeric nanoparticles (NP) involves the elimination of the solvent in which the active is solubilized, it makes possible to use them as vehicles for the administration of extracts. While, RIF an antibiotic used in the treatment, is a model for the incorporation in NP. The objective of the present work was to formulate NP with the extract and fractions of *L. frutescens* and to evaluate its activity against *M. tuberculosis* in order to propose its use as a coadjuvant of the antituberculosis drug RIF. In parallel, a formulation of RIF loaded NP was developed with the aim of improving the therapeutic performance of the drug. Firstly, chromatographic profile of methanol extracts of leaves and roots and their fractions of *L. frutescens* were obtained by HPLC. For leaves, four peaks-components were appreciated, for roots seven peaks-components were appreciated. The screening of methanol extracts of leaves and roots and their fractions for anti-*M. tuberculosis* activity revealed that the best activities were shown with the extract of roots (EMR) and the hexane fractions (FHR and RF1) with a MIC=100, 40 and 40 μg/mL, respectively. Subsequently, EMR, FHR, RF1 and RIF were encapsulated. NP had sizes between 140 and 190 nm, with homogeneous distributions and negative zeta potential. Then, the formulations were tested on *M. tuberculosis*. The formulation of RIF with the best activity was PLGA-PVAL-NP with a MIC of 0.10 μg/mL compared with the free drug that showed a MIC of 0.20 μg/mL. While, among the vegetable samples, were the formulations of FHR-PLGA-NP and RF1-PLGA-NP which

presented the best activities with a MIC of 80 μg/mL for both. An assay combining free actives and formulations and were carried out. The combination of RIF and RF1-PLGA-NP reduced the MIC for both cases. Finally, the toxicity was measured by hemolysis, the results showed that EMR, FHR, RF1 free and formulated produced hemolysis but there is no presence of hemolysis with the combination of RIF and RF1-PLGA-NP. In this study, NP formulations containing RIF, active extract or active fractions of *L. frutescens* against *M. tuberculosis* were developed, finding promising the use of RF1-PLGA-NP as coadjuvant of the antituberculosis drug RIF.

INTRODUCTION

Tuberculosis (Tb), since 1993, is considered by the World Health Organization as an emergency disease worldwide. In 2016, 10.4 million people became ill with tuberculosis and 1.7 million died (OMS, 2018). Four first-line antibiotics are administered to treat the disease, including rifampicin (RIF). However, the daily administration of the drugs for more than 6 months orally (NOM NOM-006-SSA2-1993).

One limitation of the treatment is its long duration, patients do not follow it adequately, which causes the appearance of resistant strains to the drugs. Therefore, to improve drug therapy and to evade the resistance of the agent, it is urgent to find alternatives that reduce the time of treatment or find substances with a different mechanism of action from the existing drugs.

Plants have been used in traditional medicine to treat different diseases. WHO estimates that 70 to 80% of the population has ever resorted to one or another form of alternative or complementary medicine (OMS, 2008). The phytochemical study has grown in recent years and have been described numerous compounds obtained from medicinal plants that exhibit biological activity, including antimycobacterial activity described (Camacho-Corona *et al*., 2009).

For this reason, and in response to the urgency of obtaining new treatments against *M. tuberculosis* strains, natural products studies have been developed. Several plants in northern of Mexico have a favorable activity against this bacterium. Particularly, the extracts of *L. frutescens* plant, commonly known as "cenizo", were found among those that presents best activity.

Molina-Salinas *et al.*, evaluated the methanol extract from leaves and roots of *L. frutescens* on the sensitive and multi-drug resistant strain of *M. tuberculosis*. Leaves extract had no activity on the sensitive strain, whereas, in the resistant multi-drug strain showed a MIC of 125 µg/mL. Roots extract had a MIC of 62.5 µg/mL in both strains (Molina-Salinas et al., 2007).

However, the disadvantage of this type of extracts is they are recovered in vehicles that contain organic solvents, thus their application *in vivo* is not viable. To overcome this limitation, new strategies have been proposed such as polymeric nanoparticles (NP) use. NP are systems that present sustained release allowing the reduction of the frequency of

treatment doses; in addition, NP confer to the active: protection *(*Yoo *et al.*, 2011), targeting to specific tissues and controlled delivery (Maksimenko *et al*., 2010; Pandey y Khuller, 2006). For example, Yao *et al.*, carried out studies about the release of resveratrol (a compound present in grapes) incorporated in chitosan nanoparticles, the results showed that the nanoparticles had a sustained release and, therefore, a reduction in the frequency of the dose (Yao *et al*., 2006).

Antitubercular drugs have also been incorporated in NP for the enhancement of their activities. Booysen *et. al.* encapsulated RIF and isoniazid (INH) in polylactic-*co*-glycolic acid (PLGA) NP covered with polyethylene glycol (PEG) by the double emulsion technique and spray drying. They obtained nanoparticle sizes from 230 to 380 nm with zeta potentials of +12.45mV and the encapsulation efficiencies for RIF and INH were 68.48 and 55.2%, respectively. In addition, they proved that RIF loaded NP had activity against the strain of *M. tuberculosis* H37Rv. On the other hand, they carried out the oral administration of a dose of the formulations in mice and observed a sustained release of the drugs for 7 days and biodistribution of RIF in the liver and INH in the lungs after 10 days. With these results, they concluded that PLGA NP containing antituberculosis drugs have the potential to improve Tb therapy (Booysen *et al.*, 2013). For this reason, RIF being an antibiotic used in the treatment of Tb, is a model drug for its incorporation into NP.

The promising use of extracts or fractions is accompanied by the term biocompatibility. Two aspects that should be considered in the study of sample compatibility are: cytotoxicity and hemocompatibility. Knowing this last aspect, extracts or non-toxic fractions can be proposed for the use in an organism.

The aim of the present work was to take advantage of anti-*M. tuberculosis* activity that presents the extracts and fractions from *L. frutescens* plant to formulate them in NP in order to make viable its application against *M. tuberculosis*. In addition, the combined effect of extracts and fractions free and encapsulated was evaluated to propose the use of an extract or fraction of *L. frutescens* as coadjuvant of the antituberculosis drug RIF.

MATERIALS AND METHODS

Preparation of *Leucophyllum frutescens* extracts and their fractions

Leaves and roots of *L. frutescens* were collected in Monterrey, N. L., Mexico in July 2013. Consequently, the plant material was washed, dried at room temperature and pulverized. 50 g of powdered leaves or roots were weighed, 350 mL of methanol was added. The extracts were obtained by ultrasound (Ultrasonic Cleaners, VWR Symphony, USA). For a period of 1 h, the temperature for the extraction was increased from 25 to 60 ºC, once reached 60 ºC, three cycles of 10 min of sonication and 10 min of rest were performed. Subsequently, the samples were filtered to obtain the solvent, which was evaporated under reduced pressure (Laborota 4003 control, Heidolph) in order to obtain the methanol extract of leaves (EMH) and roots (EMR).

With respect to the fractionation of the extracts, two methods were used. In the method 1, EMH was solubilized in methanol, it was placed in a separatory funnel and hexane was added; subsequently, both solvents were mixed and the hexane part was recovered and evaporated under reduced pressure in order to obtain the hexane fraction (FHH). The same procedure was followed with the EMR in order to obtain the hexane fraction from roots (FHR).

In the method 2, hexane was added to the EMH and stirred to aid the solubilization of the compounds related to the solvent, then, it was filtered to obtain the solvent and evaporated obtaining the hexane fraction called HF1. Chloroform was added to the solid insoluble in hexane, stirred, filtered to obtain the solvent with the compounds related to chloroform and evaporated obtaining the chloroformic fraction (HF2). This procedure was repeated with other solvents of higher polarity (ethyl acetate, ethanol and methanol) in order to obtain the HF3-HF5 fractions.

The fractionation method 2 was also performed to the EMR, identifying the obtained fractions as RF1-RF5. The yield (%) of the extracts and the fractions were calculated according to equations 1 and 2, respectively:

$$\text{Yield of the extract (\%)} = \frac{W_{extract}}{W_{plant}} X\ 100 \qquad (1)$$

$$\text{Yield of the fraction (\%)} = \frac{W_{fraction}}{W_{extract}} X\ 100 \quad (2)$$

where, $W_{extract}$ is the weight (g) of the obtained extract once the solvent is evaporated, W_{plant} is the weight (g) of the dried and powdered leaves or roots, $W_{fraction}$ is the weught (g) of the obtained fraction once the solvent is evaporated, and $W_{extract}$ is the weight (g) of the extract for the fractionation.

Chromatographic analysis of the extracts and fractions of *Leucophyllum frutescens*

For the obtaining of the chromatographic profile of the EMH, EMR and fractions, the samples were dissolved separately in acetonitrile (J. T. Baker, USA)/methanol (Tedia, USA), each solution was filtered through a 0.45 µm filter (Millipore, USA) to be analyzed by HPLC (VARIAN 9065, 9012, ProStar 410, USA). A Synergi™ 4 µm Fusion-RP 80 Å (150 mm x 2.0 mm x 4 µm) column, a flow of 0.2 mL/min and 30 °C was used. The mobile phase was formic acid (purity: 90%, Millipore, USA) at 0.1% v/v and methanol with an isocratic elution of 45:55 for 40 min for leaves and 60 min for roots. The profiles were detected at λ=215 nm.

Chromatographic analysis of rifampicin

The RIF analysis (Sigma-Aldrich, USA) was carried out by HPLC using a Zorbax Eclipse XDB-C18 (150 mm x 2.1 mm x 5 µm) column, with a mobile phase formed by acetonitrile and water at 0.1% v/v of formic acid with an isocratic elution of 60:40 with a flow of 0.35 mL/min at 30 °C and at λ=334 nm.

Preparation of the calibration curve and method validation for the quantification of rifampicin

For the quantification of RIF a stock solution in acetonitrile was prepared. From this solution, the working solutions were prepared in a range from 5 to 30 µg/mL and filtered through a 0.45 µm membrane. The analysis was carried out by HPLC to obtain the calibration curve.

The chromatographic method was validated through the variables: linearity, limit of detection (LOD) and limit of quantification (LOQ) according to the International

Conference on Harmonization (ICH). For the establishment of the linearity, the calibration curve was prepared and analyzed in triplicate. The LOD and LOQ were calculated by the following equations:

$$\text{Limit of detection (LOD)} = \frac{3.3\,\sigma}{S} \qquad (3)$$

$$\text{Limit of quantification (LOQ)} = \frac{10\,\sigma}{S} \qquad (4)$$

where, σ is the standard deviation of the response and S is the slope of the calibration curve.

The repeatability was established with three levels of concentration, six times each one the same day, while the reproducibility was obtained with three levels of concentration, six times each one in two different days.

Preparation of the calibration curve of the methanol extract from roots and their hexane fractions of *Leucophyllum frutescens*

For the quantification of the plant samples in NP, calibration curves of the EMR, FHR and RF1 were prepared. The samples were prepared in a mixture of acetonitrile/methanol at a concentration of 600 – 1700 μg/mL, the solution was filtered through a 0.45 μm filter to be analyzed by HPLC.

Synergi™ 4 μm Fusion-RP 80 Å (150 mm x 2.0 mm x 4 μm) column was used. The mobile phase was formic acid at 0.1% v/v and methanol in an isocratic elution of 45:55 for 60 min with a flow of 0.2 mL/min, 30 ºC and at λ=220 nm.

The chromatographic method for the sample RF1 was validated through the variables: linearity, LOD and LOQ according to the ICH.

Encapsulation and characterization of rifampicin, methanol extract and hexanic fractions of *Leucophyllum frutescens* roots in biodegradable polymeric nanoparticles

Four different formulations of RIF loaded NP were prepared by the nanoprecipitation technique proposed by Fessi *et al.* (Fessi *et al.*, 1989). Briefly, the

organic phase was prepared containing polylactic acid (PLA; PURASORB) or polylactic-co-glycolic acid (PLGA; MEDISORB 85 15 DL) and 2 mg of RIF in 3 mL of a mixture of solvents (acetone:methanol). The organic phase was added to 10 mL of an aqueous phase, containing polyvinyl alcohol (PVAL) (Clariant, Mexico) or Lutrol F127 (BASF) as a tensoactive agent at a concentration of 1% (w/w).

Then, the organic solvent was evaporated under reduced pressure. In this way, four formulations of RIF loaded NP were obtained. The NP characterization was carried out determining the particle size and polydispersity index (PDI) by dynamic light scattering (Zetasizer Nano ZS90, Malvern Instruments, UK). The zeta potential was measured by electrophoretic light scattering (Zetasizer Nano ZS90, Malvern Instruments, UK).

Two different formulations EMR, FHR or RF1 in NP were prepared by the nanoprecipitation technique. The organic phase was prepared with the particle-forming polymer, 20 mg of PLA or 15 mg of PLGA, and the plant sample (8 mg for EMR or 4 mg for FHR or RF1) in solvent mixture (acetone: methanol). The organic phase was added to PVAL at 1% w/w in constant stirring. The NP characterization was carried out by determining the particle size, PDI and zeta potential.

To determine the drug loading and encapsulation efficiency (%L and %EE), the NP formulations were centrifuged at 25,000 rpm (Allegra 64R, Beckman Coulter, USA), the supernatant was decanted, and the pellets were lyophilized (Freeze Dry System, LABCONCO, USA). The lyophilized NPwere dissolved in acetonitrile for NP-RIF and acetonitrile:methanol for NP-EMR, NP-FHR and NP-RF1.

The obtained solutions were analyzed according to the chromatographic method previously described to quantify the samples from the calibration curves of each one. Subsequently, the %L and % EE for each formulation were determined by the following equations:

$$\text{Drug loading (\%L)} = \frac{Weight\ of\ the\ active\ in\ NP}{Weight\ of\ the\ NP\ pellet}\ X100 \quad (5)$$

$$\text{Encapsulation efficiency (\%EE)} = \frac{Weight\ of\ the\ active\ in\ NP}{Wight\ of\ RIF}\ X100 \quad (6)$$

All the analyzes were carried out in triplicate, only the analysis of NP-PLA-EMR and NP-PLA-FHR was performed in duplicate. The experimental results were expressed as mean±standard deviation ($\bar{X}\pm\sigma$, n=3).

Analysis by Scanning Electron Microscopy

The surface morphology of the NP was observed through the scanning electron microscopy (SEM) (FEI Quanta 250 FEG) from the "*Centre Technologique des Microstructures"* (CTμ) of the Claude Bernard University Lyon 1, France. For the preparation of the samples, one drop of each NP suspension was deposited in a metal sample holder and dried at room temperature. Finally, the samples were plated with platinum under vacuum.

Anti-*M. tuberculosis* activity

The anti-*M. tuberculosis* activity was evaluated on the susceptible strain of *M. tuberculosis* H37Rv by the alamar blue assay in a microplate adapting the methodology used by Molina-Salinas *et al*. (Molina-Salinas *et al*. 2007). The strain was cultivated in Middlebrock 7H9 broth enriched with OADC (Becton Dickinson and Co., Sparks, MD, USA) at 37 °C for 14 days. After, the strain was adjusted according to the standard scale no. 1 of McFarland and diluted 1:20 for use in the assay. On the other hand, a stock solution in DMSO was prepared at a concentration of 20 mg/mL. Work solutions were prepared from the stock solution. On the other hand, in a 96-well microplate, 200 µL of water was added to the wells in the periphery. While, in the work wells, 100 µL of Middlebrock 7H9 broth enriched with OADC was added. Subsequently, in the first well of each row, 100 µL of each previously prepared work solution was added. Once all the samples were added, serial dilutions 1:2 of each sample were performed, taking 100 µL of the first well and adding them to the second well of the row, then, of the second well, 100 µL was taken to add them to the third, this procedure was repeated until reaching the last well each row; the 100 µL taken from the last well was eliminated. Finally, 100 µL of the bacterial suspension was added to obtain a final volume in all wells of 200 µL. The final concentrations for the EMH, FHR and RF1 were from 0.7 to 400 µg/mL; for RIF from 0.1 to 50 µg/mL; for NP-RIF from 12.5 to 400 µg/mL; for NP-EMR, NP-FHR and

NP-RF1 from 5 to160 µg/mL. The microplates were incubated at 37 °C for 5 days. At day 5, 20 µL of the blue alamar reagent and 12 µL of 10% v/v of tween 80 were added to all the work wells, and the microplates were reincubated at 37 °C for 24 h. The minimum inhibitory concentration (MIC) was determined from the color change of the blue to pink reagent. All tests were carried out at least in triplicate.

In a second stage of the study, the RIF was combined with the EMR, FHR and RF1 in order to determine the mixture with the best activity. The work carried out by Avijgan (Avijgan *et al*., 2014). was taken as a reference. Then, RIF was combined with the formulation of NP-RF1 and NP-RIF formulation with NP-RF1 to determine if there was a synergism in the antimycobacterial activity. To carry out the evaluation, the concentration of RIF was varied by column and the concentration of the vegetable samples was varied by row. For example, for the RIF and RF1 combination, the RIF concentration was varied in the 1st row and the volume of the solution was kept constant with RF1 for a final concentration of 40 µg/mL; in the 2nd row the concentration of RIF was varied, and the volume of the solution was kept constant with RF1 for a final concentration of 20 µg/mL and, thus, downwards.

All analyzes were carried out in triplicate, except for the combination of RIF with EMR (n=1).

Hemolytic activity assay

The assay of hemolytic activity was carried out according by UNE-EN ISO 10993-4. A blood sample, from a healthy patient, was placed in a tube with ethylenediaminetetraacetic acid (EDTA), as an anticoagulant. The sample was centrifuged, discarding the plasma and the white cell pack, and preserving only the red blood cells (RBC) package. The RBC were washed three times with PBS (pH 7.4) in a 1:1 ratio (RBC:PBS). After washing, the supernatant was discarded and the RBC were resuspended in PBS in a 1: 1 ratio (RBC:PBS) in order to obtain the working suspension of RBC. On the other hand, stock solutions of EMR and hexane fractions were dissolved in DMSO/PBS at a concentration of 1 mg/mL. Different concentrations of these samples were prepared from the stock solution, as well as NP formulations that showed the best activity against *M. tuberculosis* (NP-RIF and NP-RF1) in a range of 10 to 200 µg/mL in

DMSO from 0.1 to 2% v/v. The negative control to the hemolysis was prepared with 975 µL of PBS and the positive control to the hemolysis was prepared with 975 µL of milli-Q water. 25 µL of the RBC suspension was added to all samples, including controls. The samples were incubated at 37 ° C for 1 h (VORTEMP 56, Labnet International, Inc., USA). After this time, the samples were centrifuged at 10,000 rpm for 10 min (Spectrafuge 24D, Labnet International, Inc., USA), recovering the supernatant of all the samples and adding them to a 96-well microplate. Finally, the absorbance of the supernatants was measure at λ = 575 nm in a microplate reader (Epoch, BioTek Instruments, Inc., USA). The hemolytic activity was expressed as a percentage according to equation 7:

$$\text{Hemolysis (\%)} = \frac{ABS_{sample} - ABS_{neg}}{ABS_{pos}} X\ 100 \qquad (7)$$

where, ABS_{sample} is the absorbance of the supernatant from the sample, ABS_{neg} is the absorbance of the negative control, and ABS_{pos} is the absorbance of the positive control. All analyzes were carried out at least in triplicate. The experimental results were expressed as $\bar{X}\pm\sigma$, n=3.

RESULTS AND DISCUSION

Yields of extracts of Leucophyllum frutescens and their fractions

The methanol extracts from the leaves and roots of *L. frutescens* were obtained by ultrasound. As shown in Table I, the highest yield was obtained with the leaves. In the study published by Sultana *et al*. the same tendency is observed, there was a higher yield in leaves than in roots. They obtained the methanol extracts from leaves and roots of *Moringa oleifera* by two extraction techniques, with an orbital agitator at room temperature and under reflux in a water bath for 6 h, obtaining a yield with *M. oleifera* leaves of 9.6 and 16.6%, respectively. The yields in roots were of 3.2 and 5.1%, respectively (Sultana *et al.*, 2009). Even, the yields for EMH is higher than EMR, 19.30 and 7.92%, respectively.

The ultrasound used during the extraction of EMH and EMR can facilitate the swelling and solvation causing the enlargement of the pores of the cell wall. The greater swelling will improve the rate of mass transfer and, occasionally, it will break the cell walls, which leads to an increase in extraction efficiency and/or reduction in extraction time (Huie, 2002). Soares-Melecchi *et. al*. optimized the technique of extraction by ultrasound to obtain the extract from flowers of *Hibiscus tiliaceus* L They weighed 5 g of flowers and added 150 mL of methanol (1:30 ratio), reaching the highest yield (17.10%) in 5 h of extraction (Soares Melecchi *et al*., 2006). In our case, the ultrasound method developed to obtain the methanol extracts from leaves and roots of *L. frutescens* required less time (2 h). The percentages of yield of the fractions, with the methodology described above, are shown in Table I. When the hexane fraction is obtained, by any method, there was a higher yield in the hexane fractions from roots, it is possible to attribute greater number of related compounds in hexane by roots than leaves. While, increasing the polarity of the solvents, yields of leaves are observed higher than roots.

Table I. Percentage of yield of methanol extracts from leaves and roots of *Leucophyllum frutescens* and its fractions

Leaves	EMH	FHH	HF1	HF2	HF3	HF4	HF5
Yield (%)	19.30±4.20	3.46±0.09	2.55±0.31	6.10±4.34	1.17±0.28	33.05±3.09	3.48±0.12
Roots	EMR	FHR	RF1	RF2	RF3	RF4	RF5
Yield (%)	7.92±0.38	9.62±5.04	10.46±0.99	7.19±0.36	0.40±0.05	13.99±4.06	16.27±0.56

Chromatographic profiles of the extracts and fraction of *Leucophyllum frutescens*

The extracts and fractions from leaves and roots were analyzed by CLAR to obtain their chromatographic profile. The variability within the plants of the same species depends on the collection station and the origin of the plant, among other factors (Nguyen Hoai *et al*., 2009). For this reason, the determination of the chromatographic profile is useful for the quality control of plant extracts (He *et al*., 2015; Kim *et al*., 2015; Xie *et al*., 2007, Yang *et al*., 2013).

The extract and fractions obtained from leaves of the plant reveal the presence of 4 main peaks (Figure 1), while the chromatographic profiles of the extract and fractions from roots reveal the presence of 7 main peaks (Figure 2).

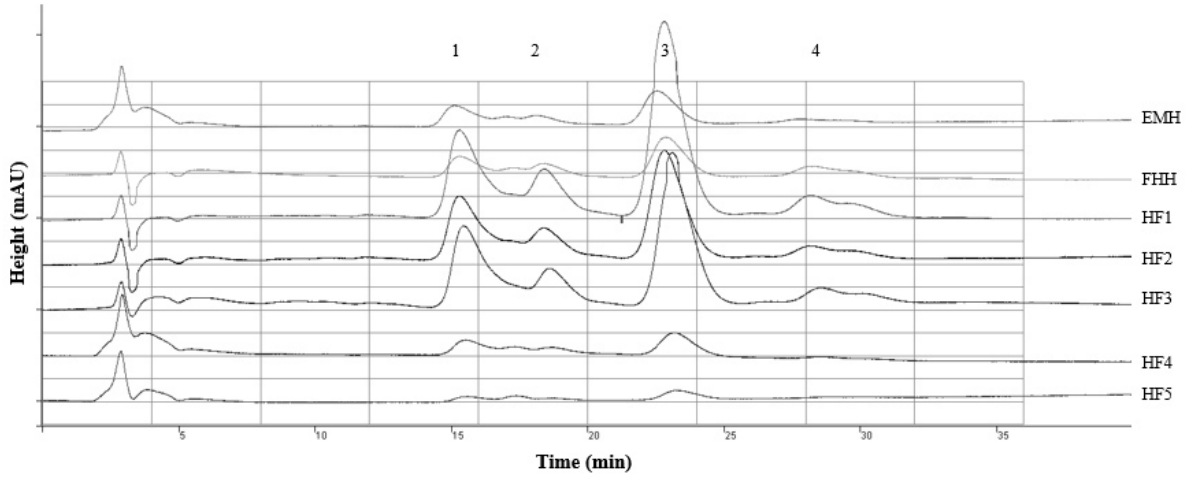

Figure 1. Chromatographic profile of methanol extract from leaves of *Leucophyllum frutescens* (EMH) and its fractions (FHH, HF1, HF2, HF3, HF4 y HF5) at 400 µg/mL analyzed by HPLC.

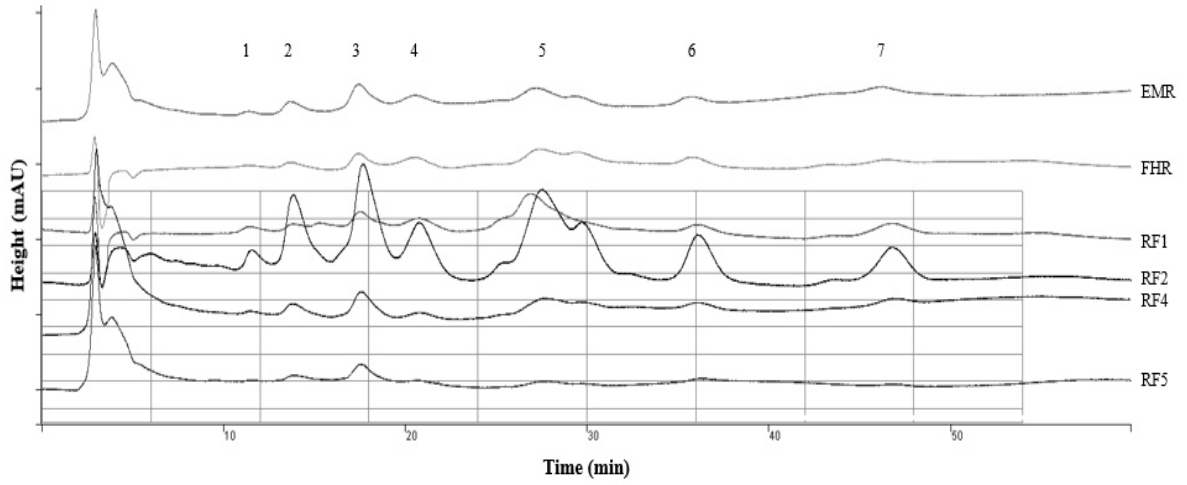

Figure 2. Chromatographic profile of methanol extract from roots of *Leucophyllum frutescens* (EMR) and its fraction (FHR, RF1, RF2, RF4 y RF5) at 400 µg/mL analyzed by HPLC.

Anti-*M. tuberculosis* activity of the extracts and fractions obtained from de *Leucophyllum frutescens*

The activity of extracts and fractions of *L. frutescens* against M. tuberculosis H37Rv was evaluated by the alamar blue microplate method. MIC obtained from the assay are presented in Table II. EMH had a MIC value above 200 µg/mL while EMR had a MIC value of 100 µg/mL. In the study by Molina-Salinas *et al.* similar trends are reported, because in leaves the tested concentrations did not show activity, while in roots MIC was of 62.5 µg/mL (Molina-Salinas et al., 2007). Compared with our result, this variability in activity may be due to factors such as collection time or place of collection (Nguyen Hoai *et al*., 2009).

Table II. Anti-*M. tuberculosis* activity H37Rv of the methanol extracts from leaves and roots of *Leucophyllum frutescens* and their fractions

Leaves	EMH	FHH	HF1	HF2	HF3	HF4	HF5
MIC (µg/mL)	>200	>200	>200	>200	>200	>200	>200
Roots	EMR	FHR	RF1	RF2	RF3	RF4	RF5
MIC (µg/mL)	100	40	40	200	200	>200	>200

The best activity against *M. tuberculosis* was collected with the hexane fractions from roots (FHR and RF1) at a MIC of 40 µg/mL. Comparing the methods of fractionation 1 and 2, FHR and RF1, respectively, both demonstrate the same efficiency to the extract compounds related to hexane with antituberculosis activity. Previously, the isolation and identification of a compound extracted from roots with potent anti-*M. tuberculosis* activity was reported (Molina-Salinas *et al*., 2011), this fraction of interest was obtained with hexane, with a similar methodology to the fractionation method 1 performed in this work. However, an easy and rapid fractionation method was also developed (fractionation method 2), for the obtaining the fraction of interest preserving its antimycobacterial activity.

MIC achieved by FHR and RF1 is comparable to MIC reported in studies with other plants. Gemechu *et al*. investigated five medicinal plants in Ethiopia: roots of *Calpurnia aurea*, seeds of *Ocimum basilicum*, leaves of *Artemisia abyssinica*, *Croton macrostachyus*, and *Eucalyptus camaldulensis* used locally to fight tuberculosis. Methanol extracts of the plant materials were obtained by maceration and evaluated on *M. tuberculosis* strains such as: H37Rv, SIT73, SIT149, SIT149, SB1176 and SB1953, which were comparatively the most susceptible to the extracts with MIC of ≤50 µg/mL (Gemechu *et al.*, 2013). However, Nguta *et al*. evaluated the antimycobacterial activity of the hydroethanol extract from leaves of *Solanum torvum Aloe vera var*. *barbadensis*, *Dissotis rotundifolia, Chenopodium ambrosioides* and rizosimas of *Zingiber officinale* Roscoe on *M. tuberculosis* H37Ra and H37Rv. It was determined that the leaves of *S. torvum* were the best potential anti-*M. tuberculosis*, since, they showed a MIC of 156.3 and 1,250 µg/mL against *M. tuberculosis* H37Ra and H37Rv, respectively (Nguta *et al*., 2016). Likewise, Kahaliw *et al*. obtained the chloroform extracts from roots of different plants, among them *Pterolobium stellatum*, which showed the highest MIC. The fractionation of this extract was carried out by solvent partition, in order to obtain the hexane and ethyl acetate fractions. In this case, the activity given by the fractions was greater than the extract (Kahaliw *et al*., 2017).

According to the results published with other plants, root fractions are potential plant samples against *M. tuberculosis.* Following the mentioned chromatographic profile (Figure 2), in roots there are more peaks than in leaves.

RF3 fraction was discarded for the determination of the chromatographic profile, antioxidant and haemolytic activity, due to experimentally a low percentage of yield and low anti-*M. tuberculosis* H37Rv were obtained.

Chromatographic analysis of rifampicin

Among the analytical methods, HPLC highlight, it allows the separation of the compounds according to their physiochemical characteristics, even if they are in a polymeric matrix (Moreno-Exebio y Grande-Ortiz, 2014).

Initially, the chromatographic conditions that allowed the detection of RIF were developed. Figure 3 showed that the molecule was detected at a retention time of 2.0 min.

This result is close to the obtained retention time by Glass *et al*., who optimized a chromatographic method for the quantification of antituberculosis drugs. The retention time of RIF was 2.85 min using acetonitrile: tetrabutylammonium hydroxide (42.5:57.5, v / v) (0.2 mM) at a pH of 3.10 (Glass *et al*., 2007).

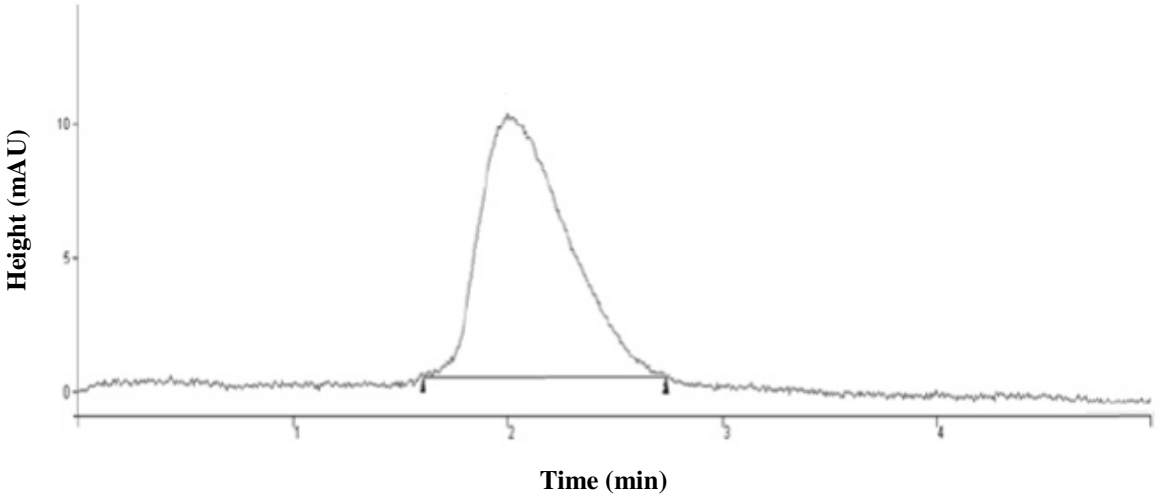

Figure 3. Rifampicin chromatogram (30 ppm) obtained by HPLC (retention time=2 min).

Preparation of the calibration curve and method validation for the quantification of rifampicin

The validation was carried out to ensure that the analytical procedure is accurate for the quantification of RIF. Table 3 shows the validation parameters established for the developed method. The concentration range (5-30 µg/mL) had linearity, with a correlation coefficient greater than 0.99. LOD was 0.71 µg/mL, while LOQ was 2.14 µg/mL. On the other hand, repeatability and reproducibility were measured, obtaining a variation of 5.97 and 6.79%, respectively. These values are acceptable, below the ±15% previously established (Glass *et al*., 2007), therefore the method is accurate.

Table III. Validation parameters of the chromatographic method for the quantification of rifampicin

Regression equation	Correlation coefficient (r)	LOD (µg/mL)	LOQ (µg/mL)	Repeatability (RSD, %)	Reproducibility (RSD, %)
y = 8.8983x - 9.2698	0.99	0.71	2.14	5.97	6.79

Preparation of the calibration curve of the methanol extract from leaves and roots of *Leucophyllum frutescens*

As part of the characterization, from the chromatographic methods previously developed, the calibration curve of each plant sample (EMR, FHR and RF1) was analyzed in order to quantify the most abundant peaks in them, being selected the peak no. 5 in all the samples, and the peaks no. 6 and 7 in RF1. The method for RF1 quantification was validated by linearity, LOD and LOQ (Table IV).

For extracts or fractions from plants, the known compounds of the plant are selected, and the chromatographic method is developed for their quantification. For example, in the Amorim *et al*. study, three flavonoids were identified in the hydroethanol extract from the aerial part of *Tonina fluviatilis* (6,7-dimethoxyquercetin- 3-*O*-β-D-glucopyranoside, 6-hydroxy-7-methoxyquercetin-3-*O*-β-D-glucopyranoside and 6-methoxyquercetin-3-*O*-β-D-glucopyranoside) and a chromatographic method was developed and validated to quantify these compounds in the plant. For the preparation of the calibration curve, solutions of the three flavonoids were prepared and the regression equation for each was determined. LOD and LOQ of the calibration curves were below 30 µg/mL (Amorim *et al*., 2014).

For RF1 with the developed method, LOD and LOQ are superior because internal marker compounds of the fraction are used, it was possible preparing solutions of different concentrations of this hexane fraction for the preparation of the calibration curve, instead of standard solutions. The validation was carried out to ensure that the analytical procedure is accurate for the quantification of RF1 once it was loaded in NP (Martínez-Rivas *et al*. 2017).

Table IV. Validation parameters of the chromatographic method for the quantification of the vegetable samples from *Leucophyllum frutescens*

Active	*No. Peak*	Regression equation	Correlation coefficient *(r)*	*LOD (µg/mL)*	*LOQ (µg/mL)*
EMR	5	y = 1.712x – 355.49	0.99	ND	ND
FHR	5	y = 1.4231x – 591.75	0.99	ND	ND
RF1	5	y = 2.0497x – 105.57	0.99	209.22	634.00
	6	y = 0.3646x – 38.803	0.99	427.35	1295.00
	7	y = 1.3158 – 224.39	0.99	103.98	315.10

(ND=no determinado)

Encapsulation and characterization of rifampicin, methanol extract and hexanic fractions from roots of *Leucophyllum frutescens* loaded in polymeric nanoparticles

Nanotechnology has emerged as a promising area to target the active to reservoirs such as macrophages (Nasiruddin *et al*., 2017). *M. tuberculosis* resides for a long period of time in the alveolar macrophages of the lungs (Jain *et al.*, 2013).

Due to the NP size, they are a promising vehicle for distribution through the body and to reach the target cells or organs. Nahar and Jain prepared NP with sizes of 150-200 nm and negative zeta potential. Subsequently, they determined the targeting of Amphotericin B in PLGA NP conjugated with mannose and PEG to organs rich in macrophages (liver, kidney, spleen, lung and lymph nodes) in a bioavailability study. Swiss albino adult mice and males were injected with NP formulations, after the treatment they were sacrificed to analyze the organs. The results showed targeting of NP to organs rich in macrophages (Nahar y Jain, 2009). Comparing these results with our work, these characteristics of size and surface charge are favorable for their potential use. Table V describes the characterization parameters of RIF loaded NP. For the four formulations developed to encapsulate RIF, a particle size in a range of 140 – 180 nm was obtained, with homogeneous size distributions and negative zeta potential.

The surface charge measured by the zeta potential is important because it is related to the stability of NP and drug release profiles (Honary y Zahir, 2013). The use of some

emulsifiers (surfactants) modifies the surface charge, although the emulsifiers used in this work are neutral (Mura *et a*l. 2011), and their charge is modified depending on the pH of the medium. For example, PVAL has acetates groups that are negatively ionized as the medium change from pH 3 to pH 9 (Wiśniewska *et al*. 2016). Honary and Zahir prepared PLGA NP with two non-ionic surfactants, PVAL and Pluronic F68 (PF68). They obtained NP with negative zeta potential. The result obtained with PLGA-PVAL-NP was -5±1 mV and with PLGA-PF68-NP was -24±1 mV (Honary y Zahir, 2013), this formulation with PVAL presents a similar result compared with our work with this formulation (-5.57±1.35 mV).

Table V. Characterization parameters of the biodegradable polymeric nanoparticles containing rifampicin prepared by nanoprecipitation

Polymer	***Emulsifier agent***	***Size (nm)***	***PDI***	***Zeta Potential (mV)***	***%L***	***%EE***
PLA	Lut	142.8±15.4	0.210±0.042	ND	2.8±0.1	30.4±0.3
PLGA	Lut	163.0±4.6	0.113±0.019	-15.93±3.10	0.7±0.1	6.0±1.0
PLA	PVAL	178.5±4.1	0.168±0.045	-7.89±1.82	2.2±0.1	35.9±1.0
PLGA	PVAL	176.3±9.4	0.139±0.007	-5.57±1.35	0.5±0.1	4.0±0.5

(Lut: Lutrol F127 NF: PVAL: polyvinyl alcohol); ND=not determined

($\bar{x}$±σ, n=3)

Then, the formulations were analyzed by CLAR for the quantification of the drug, this HPLC method was developed to detect RIF without interference from the polymeric matrix. As seen in Table V, the encapsulation percentages changed according to the polymer and surfactant involved in particle formation. NP formulation with the highest encapsulation of RIF was PLA-PVAL-NP formulation, with an encapsulation efficiency of 35.9%, which indicates that 35.9% of total RIF is encapsulated in NP. While, the lowest encapsulation was PLGA-PVAL-NP. This difference is given, because the polymer PLA has lower hydrophilic affinity than PLGA (Dalpiaz et al., 2016). Therefore, PLA is more related to hydrophobic drugs such as RIF. NP preparation technique used in this work

(nanoprecipitation) with the formulation parameters used, are favorable for formulating NP with RIF.

Due to the results shown in the studies against *M. tuberculosis*, EMR and its fractions FHR and RF1 were selected to be encapsulated in NP. Table VI describes the characterization parameters of NP with plant samples. For the two formulations that were developed to encapsulate the EMR, FHR or RF1, a particle size in a range of 160 – 190 nm was obtained, with homogeneous size distributions and negative zeta potential.

As already mentioned, NP from 150 to 200 nm with negative zeta potential have shown targeting towards the organs rich in macrophages such as the lungs (Nahar y Jain, 2009), NP with EMR, FHR or RF1 obtained in our work, are potential formulations to reach the lungs. Likewise, they have the characteristics for the internalization by the alveolar macrophages that contain the tuberculosis bacterium. Nicolete *et al.* observed that their blank PLGA NP with zeta potential of -17.2±6.1 mV were internalized by J774 macrophages at 4 h. Therefore, they conclude that the size and surface chemistry of the particles influences their absorption (Nicolete *et al.*, 2011).

The peak no. 5 was selected to be quantified in NP, for being an abundant component in plant samples. The peak was encapsulated in all formulations, which indicates that the NP preparation method is favorable for the encapsulation of extracts or fractions extracted from *L. frutescens* plant. Some researchers have encapsulated plant compounds in NP such is the case of do Nascimento *et al*., who encapsulated the red propolis extract in five formulations of poly-ε-caprolactone (PCL) NP and quantified five flavonoids (liquiritigenin, pinobanksin, isoliquiritigenin, formononetin and biochanin A) by UPLC. %EE of the flavonoids in NP had an average value of 75% (do Nascimento *et al*., 2016). However, in this work the chromatographic method was designed to detect the components of interest of the extracts and fractions obtained from *L. frutescens* and using them as internal markers for their quantification in NP.

Table VI. Characterization parameters of the biodegradable polymeric nanoparticles containing methanol extract and hexane fractions from *Leucophyllum* prepared by nanoprecipitation

Active	*Polymer*	*Size (nm)*	*PDI*	*Zeta Potential (mV)*	*No. Peak*	*%EE*
EMR	PLA	160.7±2.7	0.259±0.045	-9.79±036	5	78.10±11.67
	PLGA	176.0±7.0	0.150±0.018	-6.11±1.16	5	57.94±5.08
FHR	PLA	189.8±2.2	0.114±0.019	-11.23±1.86	5	21.65±1.60
	PLGA	171.5±10.6	0.127±0.025	-7.76±1.64	5	21.63±1.01
RF1	PLA	180.5±2.1	0.110±0.013	-10.77±2.69	5	83.82±3.61
					6	81.42±16.53
					7	83.42±8.16
	PLGA	170.3±4.4	0.094±0.012	-7.73±1.49	5	77.71±1.0
					6	55.47±10.86
					7	63.72±7.84

($\bar{x}\pm\sigma$, n=3 and n=2)

Finally, the surface morphology of the NP by MEB was determined. Figure 4 shows the micrographs obtained from the blank NP, RIF NP and RF1 NP. NP had a spherical shape and a smooth surface, with a size around 80 nm and homogeneous distribution in all formulations.

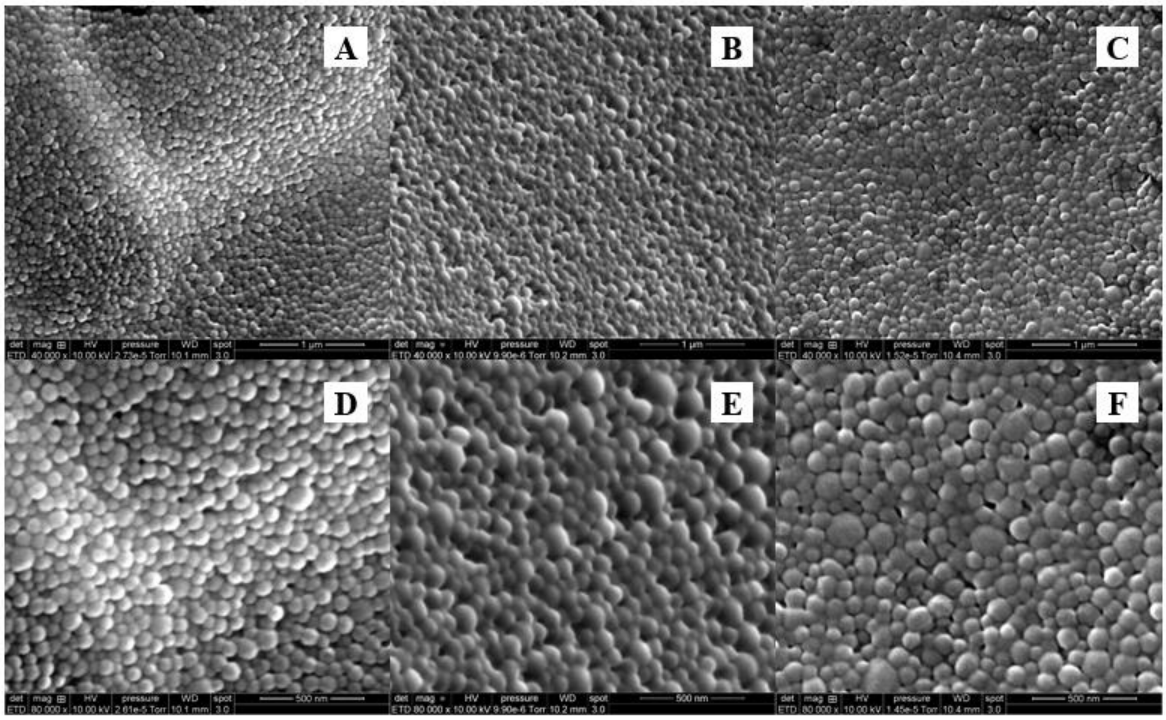

Figure 4. MEB image of PLGA nanoparticles prepared by nanoprecipitation. A and D blank nanoparticles; B and E: nanoparticles with rifampicin; C and F: nanoparticles with the hexane fraction of *Leucophyllum frutescens* roots (A, B, and C: scale bar represents 1 μm; D, E and F: scale bar represents 500 nm).

Anti-*Mycobacterium tuberculosis* activity of the nanoparticle formulations

Once the formulations of NP were obtained, they were evaluated against *M. tuberculosis*. In Table VII, MIC of the formulations of NP with RIF are shown, the complete formulations (encapsulated and non-encapsulated active) and the formulations with the encapsulated active were evaluated. Likewise, MIC for RIF was determined (0.20 μg/mL). PLGA NP showed the best encapsulation, and it is the PLGA-PVAL formulation with encapsulated active that had the highest activity (0.10 μg/mL) even compared with the free drug. This enhancement in the antibacterial activity of the drug encapsulated in PLGA NP compared with its free form has already been observed in other studies.

As example is the work carried out by Darvishi *et al.*, who incorporated 18-β-glycyrrhetinic acid (GLA) in PLGA NP with a size around 200 nm and negative zeta potential to test them against: *Pseudomonas aeruginosa*, *Staphylococcus aureus* and *Staphylococcus epidermidis.* MIC of NP with GLA and free GLA for *P. aeruginosa* was around 75 and 20 μg/mL, respectively; for *S. aureus* was of 75 and 35 μg/mL, respectively; and, for *S. epidermidis* was of 35 and 10 μg/mL, respectively. The results revealed that GLA NP had better activity than free GLA (Darvishi *et al*., 2015).

Table VII. Minimal inhibitory concentration (MIC) of biodegradable polymeric nanoparticles containing rifampicin (n=3)

	MIC	
Formulations	***Encapsulated non-encapsulated rifampicin (μg/mL)***	***Encapsulated rifampicin (μg/mL)***
RIF-PLGA-Lut	0.20	0.30
RIF-PLA-PVAL	0.40	0.90
RIF-PLGA-PVAL	0.20	0.10

As mentioned, the best antimycobacterial activities were given by EMR, FHR and RF1 (MIC=100, 40 and 40 μg/mL, respectively), so they were selected to be formulated in NP. Table VIII shows the results of the assay for the determination of the activity of the NP formulations containing EMH, FHR or RF1, being FHR-PLGA-NP and RF1-PLGA-NP with the best activities. These results suggest that PLGA-PVAL-NP enhanced the activity against *M. tuberculosis* compared to free forms of RIF, FHR and RF1.

Table VIII. Minimal inhibitory concentration (MIC) of biodegradable polymeric nanoparticles containing the vegetable actives (n=3)

Formulations	*MIC encapsulated and non-encapsulated active (µg/mL)*
EMR-PLA	400
EMR-PLGA	400
FHR-PLA	160
FHR-PLGA	80
RF1-PLA	160
RF1-PLGA	80

Subsequently, the combined effect between RIF and EMR, FHR or RF1 was evaluated, the best combination was achieved with RIF and RF1, MIC decreased from 0.20 to 0.10 µg/mL and 40 to 10 µg/mL, respectively (Table VIII). From this favorable combination, the combined effect of RIF with RF1-PLGA-NP and RIF-PLGA-NP with RF1-PLGA-NP was tested. The combination RIF-PLGA-NP with RF1-PLGA-NP did not have a better effect than the free combination. However, the combination of RIF with RF1-PLGA-NP, showed a better MIC for both, from 0.20 to 0.10 µg/mL and 80 to 20 µg/mL, respectively. It means, when RF1 is in NP, it is possible to enhance the effect of its free form. These results suggested that the combination of RIF with a hexane fraction from roots of *L. frutescens* against *M. tuberculosis* is favorable. The combination of drugs with natural agents increases the spectrum of activity and decreases the risk of emergence of resistant strains (Avijan *et al.*, 2014).

Table IX. Minimal inhibitory concentration (MIC) of rifampicin with methanol extract and hexane fractions from *L. frutescens* roots against *M. tuberculosis*

	MIC of rifampicin (μg/mL)		*MIC of vegetable samples (μg/mL)*
EMR	0.10	+	100
FHR	0.10	+	20
RF1	0.10	+	10
RF1-PLGA-NP	0.10	+	20

Hemolysis assay

One of the techniques for measuring compatibility can be through the determination of hemolysis (Fischer et al., 2003). The test of the extracts and their fractions was carried out according by UNE-EN ISO 10993-4 which establish that a percentage lower than 5% is considered non-hemolytic, considering the value of 100% to the total amount of hemoglobin present in the RBC sample added. RF5 showed no hemolysis at the concentrations analyzed. In contrast, RF2 and RF4 maintain a non-hemolytic effect at ≤100 μg/mL, and EMR at ≤25 μg/mL, Finally, the hexane fractions FHR and RF1 are non-hemolytic at ≤10 μg/mL (Figure 5).

Comparing the results of hemolytic activity with the *M. tuberculosis* activity, in EMR, FHR and RF1 there was presence of hemolysis at the established MIC (100, 40 and 40 μg/mL, respectively). Vega Menchaca *et al*. Vega Menchaca *et al.* evaluated the acute toxicity of the methanol extract from *L. frutescens* leaves. They carried out the evaluations in *Artemia salina*, reporting a LD_{50} of 196.37 μg/mL, , and in the VERO cell line, reporting an IC_{50} of 58.0 μg/mL (Menchaca *et al*., 2013). These results suggest the presence of toxicity in the plant.

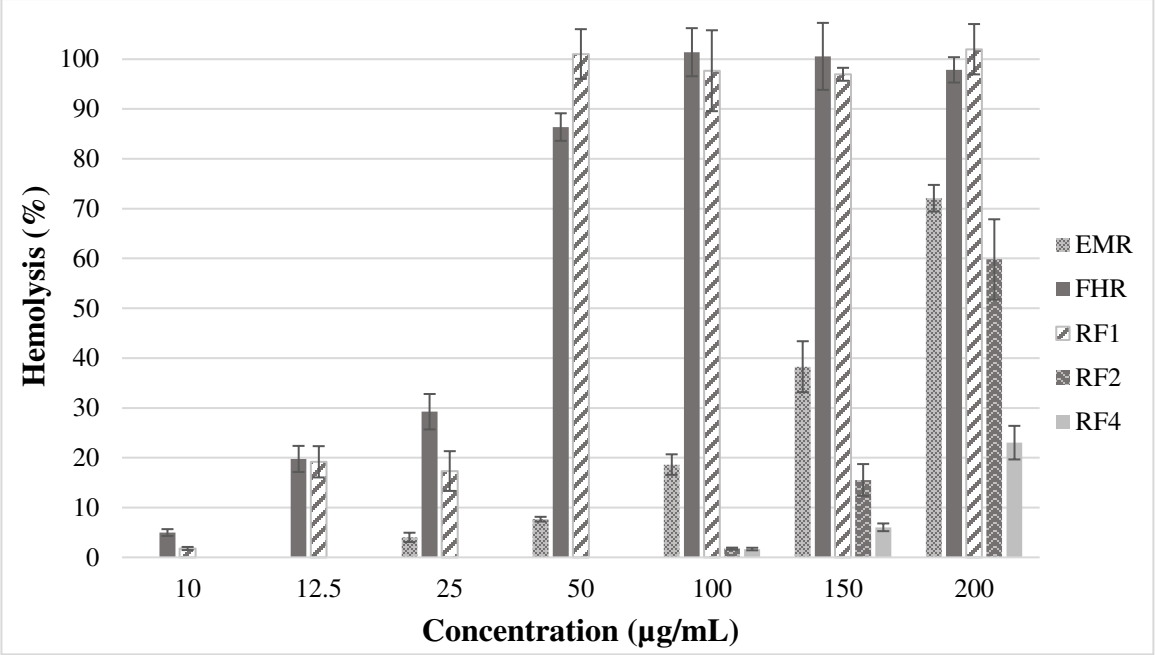

Figure 5. Hemolytic activity of the vegetables samples from *Leucophyllum frutescens*: methanol extract and fractions ($\bar{x}\pm\sigma$, n=3).

Also, the hemolysis percentage was determined as an indicator of the toxicity of RIF and NP formulations. For the concentration of RIF with activity against *M. tuberculosis* MIC were determined: *i)* free form (0.20 µg/mL), *ii)* in combination (0.10 µg/mL) and *iii)* RIF-PLGA-PVAL, being the formulation with the best activity. The results showed there was no presence of hemolysis. While, RF1 and RF1-PLGA-NP at the MIC against *M. tuberculosis* (40 and 80 µg/mL, respectively) are hemolytic. However, when RF1 is combined with RIF, the concentrations decreased from 40 to 10 µg/mL for RF1 and from 80 to 20 µg/mL for the NP formulation, and at these concentrations there was no presence of hemolysis (Figure 6). Additionally, Figure 6 showed that the encapsulation of RF1 in NP favors the reduction of its toxicity.

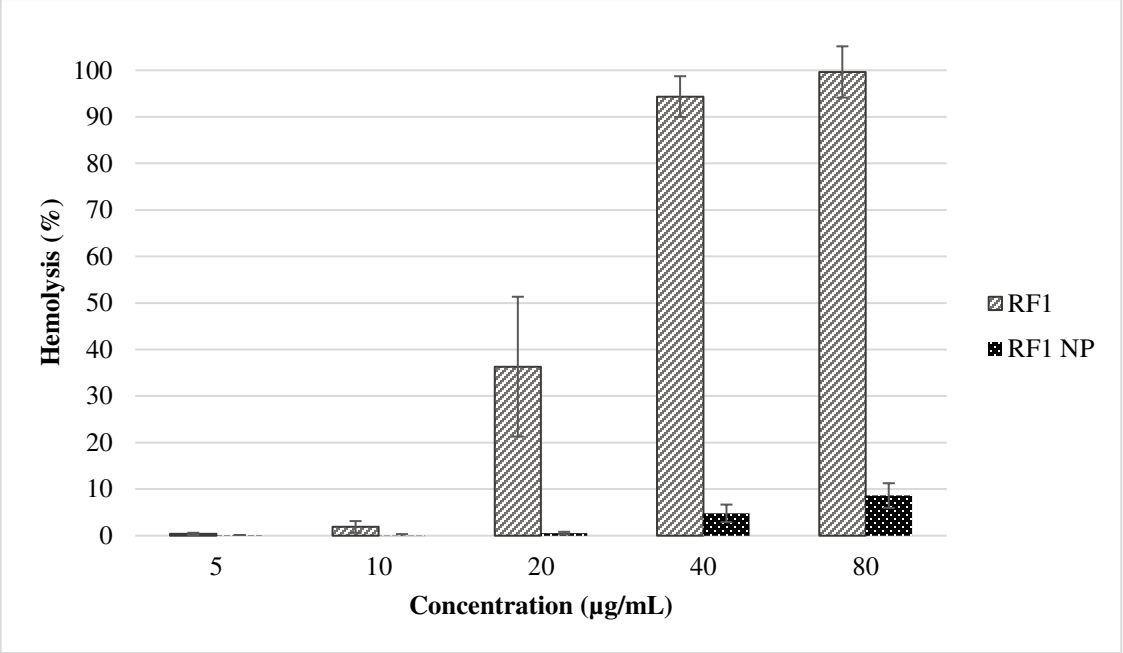

Figure 6. Hemolytic activity of the encapsulated hexane fraction from roots of *Leucophyllum frutescens* (RF1 NP) and non-encapsulated (RF1) ($\bar{X}\pm\sigma$, n=3).

Table X. Percentage of hemolysis of rifampicin, hexane fraction from roots of *Leucophyllum frutescens* and nanoparticles

ANTITUBERCULOSIS ACTIVE	*CONCENTRATION (µg/mL)*	*HEMOLYTIC ACTIVITY (%)*
RIF	0.20	N/H
RIF	0.10	N/H
RIF-PLGA-NP (E+NE)	0.20	N/H
RIF-PLGA-NP (E)	0.10	N/H
RF1	40	94.35±4.37
RF1	10	N/H
RF1-PLGA-NP (E+NE)	80	8.62±2.65
RF1-PLGA-NP (E+NE)	20	N/H

(E+NE=complete batch; E=encapsulated active)

($\bar{X}\pm\sigma$, n=3)

CONCLUSION

In this study several evaluations were carried out in order to have a broader knowledge about the biological activity of *L. frutescens*. The ultrasound method developed to obtain the methanol extract of leaves and roots of the plant allowed to achieve a good performance in a short time (2 h). Two different fractionation methods were developed in order to obtain the hexane fraction of leaves and roots, the percentage of yield obtained with both methods was very close. However, method 2 was selected to continue with the following partitions because it is faster and easier to execute.

The chromatographic profiles of the extracts and fractions were obtained by HPLC, these results revealed that there was the same number of peaks of the extract (leaves or roots) and the fractions obtained from it; as well as, particularly in roots, the greatest number of peaks was found.

The evaluation of the activity against *M. tuberculosis* of the extracts and the fractions revealed that the roots are more active, specifically, EMR, FHR and RF1 with MIC of 100, 40 and 40 μg/mL, respectively. However, hemolysis occurred at these concentrations.

On the other hand, biodegradable NP of RIF and plant samples (EMR, FHR and RF1) of *L. frutescens* were prepared by nanoprecipitation. The characterization of the formulations showed NP from140 to 190 nm, with homogeneous distributions and negative zeta potential. When RIF is encapsulated in PLGA-PVAL-NP enhanced its activity against *M. tuberculosis* (0.10 μg/mL) compared to the PLA-PVAL-NP and the free drug. The extract and fractions had a higher MIC when they are encapsulated. The most active formulations were with the fractions, showing better activity with PLGA NP (80 μg/mL) compared to PLA NP (160 μg/mL).

The combination of plant samples with RIF decreased the MIC in both cases, demonstrating a better effect. At the active concentrations against *M. tuberculosis*, RIF and RIF loaded NP did not present hemolysis. Whereas, RF1 and RF1 loaded NP showed hemolysis at the active concentrations against *M. tuberculosis*. However, when RF1 is combined with RIF, the concentrations decreased from 40 to 10 μg/mL for RF1 and from 80 to 20 μg/mL for the NP formulation, and at these concentrations there is no presence of hemolysis.

This suggests that the encapsulation of RF1 in NP favors the reduction of its toxicity. Therefore, an alternative to make use of these fractions, with potential activity against the bacteria causing tuberculosis and without hemolytic effect is to combine it with conventional antituberculosis drugs.

CHAPTER 2. POTENTIAL USE OF *Leucophyllum frutescens* AS ANTIOXIDANT AGENT AND ITS ENCAPSULATION IN POLYMERIC NANOPARTICLES

ABSTACT

Leucophyllum frutescens has been studied mainly for its activity against *Mycobacterium tuberculosis* but other biological properties in the plant have been less studied. In addition, for advance in the investigation of the plant to the application in some organism, it would be promising to transport the natural components in polymeric nanoparticles (NP), thus avoiding the use of organic solvents. It should be noted that NP have different advantages that improve the biological activity of the contained active. The objective of this work was to encapsulate an extract or fraction, with antioxidant activity, obtained from the methanol extract of *L. frutescens*. With nanoencapsulation, the vegetable sample is incorporated in a vehicle free of organic solvents, without losing its property, making possible to administer it in the body. First, the antioxidant activity of the extracts and fractions from leaves and roots of *L. frutescens* were evaluated to select the ethanolic fraction from leaves (HF4) as the most active. The chromatographic profile of the ethanol fraction of leaves was determined by High Performance Liquid Chromatography (HPLC), selecting four peaks-components for their use as internal markers in order to quantify them once the plant sample was encapsulated in NP. For quantification of the component peaks in NP, firstly, the chromatographic method was partially validated. The regression equations of the four peaks were obtained, with correlation coefficients greater than 0.99. In addition, the limit of detection and limit of quantification of each peak was determined resulting in 43.09 and 130.58, 38.62 and 117.03, 22.29 and 67.53 and, 45.86 and 138.97 μg/mL, for peaks 1, 2, 3 and 4, respectively. Suspensions of HF4 loaded NP were obtained by the nanoprecipitation method. NP had particle sizes around 200 nm with homogeneous distributions. While, the percentage of encapsulation of peaks 1, 2, 3 and 4 was 20, 23, 61 and 80%, respectively. Then, the antioxidant activity was evaluated using the oxidant peroxyl, 2,2-azo-bis-(2-amidinopropane) dihydrochloride (AAPH) in red blood cells. The fraction HF4 presented antioxidant activity at 100 μg/mL and when HF4 was encapsulated

in NP, the activity was preserved. Finally, through the hemolysis test was concluded that HF4 and HF4-NP are not toxic to the active concentrations. Therefore, the potential use of HF4 loaded NP as an antioxidant agent is promising.

INTRODUCTION

Several compounds with biological activity from plants, have been isolated and identified. One of the most common examples is Taxol®, which was obtained from the plant called *Taxus breuifolia* (Wani *et al*., 1971). The large number of plants existing in the earth leads to the acquisition of new compounds or the promising discovery of activities not yet known in species not yet studied.

Leucophyllum frutescens, de la familia Scrophulariaceae, of the family Scrophulariaceae, is a plant commonly known as "cenizo". In Nuevo León it is the bush par excellence. In Texas it is called "shrub barometer" because its flowering depends on humidity in the environment and rainfall (Zaragoza, 2009). *L.* has been studied mainly for its activity against *Mycobacterium tuberculosis* (Alanís-Garza *et al*., 2012; Molina-Salinas *et al*., 2007, 2011). Some studies suggest other biological properties present in the metabolites of the plant.

However, a property not yet studied is its antioxidant capacity. Throughout the antioxidant effect, the body is protected from oxidative stress caused by free radicals. Free radicals play a fundamental role in different diseases such as cancer, inflammatory diseases or neurological disorders caused by age (Lobo *et al*., 2010).

There are several studies focused on the investigation of the antioxidant activity of plants. Generally, the antioxidant properties are attributed to a chemical group called polyphenols (Özkan y Özcan, 2017). In the study by Saeed *et al*., some extracts were obtained from the plant *Torilis leptophylla*, were studied, where the presence of phenols were found, which were related to their antioxidant activity. Likewise, an *in vivo* study suggested that methanol extract could be used against oxidative damage caused by carbon tetrachloride (CCl_4) by its antioxidant property (Saeed *et al*., 2012).

To produce free radicals using the peroxyl initiator, 2,2-azo-bis-(2-amidinopropane) dihydrochloride (AAPH) in red blood cells (RBC) causes hemolysis, however, adding an antioxidant prevents hemolysis. Therefore, this system is an adequate model to determine the antioxidant activities of extracts or fractions of plants (An *et al.*, 2014). This method allowed to Jiang *et al*. to investigate the protection conferred by the aqueous extract of *Pueraria thomsonii* and *Pueraria lobata* on the RBC damage of rats caused by free radicals. No antioxidant activity was shown by the aqueous extract of *P.*

thomsonii, with an IC_{50} around 1000 µg/mL. In contrast, the extract of *P. lobata* exhibited a potent activity, with an IC_{50} of 194.0±6.9 µg/mL (Jiang *et al.*, 2005).

A limitation in the use of plant extracts with potential as antioxidant agents is on their *in vitro* or *in vivo* application because they are obtained in an organic solvent, which cannot be administered to an organism. A proposal to transport natural components is the use of polymeric nanoparticles (NP), because they show different advantages that improve the biological activity of the sample (Christofoli *et al*., 2015).

For this reason, the aim of this work was to encapsulate an ethanol fraction obtained from the methanol extract of *L. frutescens* leaves, with antioxidant activity in order to contain it in a vehicle free of organic solvents without loss of activity, and thus to obtain a formulation with potential administration in an organism.

MATERIALS AND METHODS

Obtaining of the extracts of *Leucophyllum frutescens* and their fractions

Chapter 1 describes the procedure for obtaining the extracts from leaves and roots of *L. frutescens* and its fractions. Briefly, *L. frutescens* plant was collected in Monterrey, N. L., Mexico in July 2013. Consequently, the plant material was washed, dried at room temperature and pulverized. 50 g of powdered leaves or roots were weighed, 350 mL of methanol was added. The extracts were obtained by ultrasound (Ultrasonic Cleaners, VWR Symphony, USA). For a period of 1 h, the temperature for the extraction was increased from 25 to 60 ºC, once reached 60 ºC, three cycles of 10 min of sonication and 10 min of rest were performed. Subsequently, the samples were filtered to obtain the solvent, which was evaporated under reduced pressure (Laborota 4003 control, Heidolph) in order to obtain the methanol extract of leaves (EMH) and roots (EMR). With respect to the fractionation of the extracts, two methods were used. In the method 1, EMH was solubilized in methanol, it was placed in a separatory funnel and hexane was added; subsequently, both solvents were mixed, and the hexane part was recovered and evaporated under reduced pressure in order to obtain the hexane fraction (FHH). The same procedure was followed with the EMR in order to obtain the hexane fraction from roots (FHR).

In the method 2, hexane was added to the EMH and stirred to aid the solubilization of the compounds related to the solvent, then, it was filtered to obtain the solvent and evaporated obtaining the hexane fraction called HF1. Chloroform was added to the solid insoluble in hexane, stirred, filtered to obtain the solvent with the compounds related to chloroform and evaporated obtaining the chloroformic fraction (HF2). This procedure was repeated with other solvents of higher polarity (ethyl acetate, ethanol and methanol) in order to obtain the HF3-HF5 fractions. The fractionation method 2 was also performed to the EMR, identifying the obtained fractions as RF1-RF5.

Determination of the antioxidant activity of the extracts and fractions from *Leucophyllum frutescens*

The antioxidant activity was measured by the damage of RBC producing free radicals with AAPH, the methodology described by Abajo *et al*. (2004). was used as reference. A blood sample, from a healthy patient, was placed in a tube with ethylenediaminetetraacetic acid (EDTA), as an anticoagulant. The sample was centrifuged, discarding the plasma and the white cell pack, preserving only the RBC package. RBC were washed three times with a solution of phosphates with salt (PBS, pH 7.4) in a ratio of 1:1 (RBC: PBS). After the washing, the supernatant was discarded, and the RBC were resuspended in PBS to subsequently dilute them 1:10 (RBC:PBS) in order to obtain the working suspension of RBC.

On the other hand, stock solutions of EMH, EMR and fractions in DMSO were prepared. Also, one solution of AAPH at 400 mM in PBS was prepared. Then, a volume of each sample was taken to obtain the final concentrations in a range of 10 to 200 μg/mL in DMSO (0.15 to 3% v/v). The antioxidant control was ascorbic acid (AA), which was prepared at the same concentrations as the plant samples. 375 μL of the AAPH solution and 250 μL of the RBC suspension were added to all the samples.

The oxidant control was PBS, 375 µL of the AAPH solution and 250 µL of the RBC suspension. Two controls were added, one negative to the hemolysis (750 µL of PBS and 250 µL of RBC) and another positive to hemolysis (750 µL of milli-Q water and 250 µL of RBC). All test samples had a final volume of 1000 µL. Samples and controls were incubated at 37 ° C for 2.5 h with constant agitation (300 rpm) (VORTEMP 56, Labnet International, Inc., USA). After this time, the samples were centrifuged at 10,000 rpm for 10 min (Spectrafuge 24D, Labnet International, Inc., USA), recovering the supernatant of all the samples and adding them to a 96-well microplate. Finally, the absorbance of the supernatants at λ=575nm was measured in a microplate reader (Epoch, BioTek Instruments, Inc., USA). The oxidative damage was determined by equation 1:

$$\text{Oxidative damage } (\%) = \frac{ABS_{sample} - ABS_{ox}}{ABS_{pos}} \; X \; 100 \qquad (1)$$

where, ABS_{sample} is the absorbance of the supernatant of the sample, ABS_{ox} is the absorbance of the supernatant of the oxidant control and ABS_{pos} is the absorbance of the supernatant of the positive control to the hemolysis. From this result the antioxidant activity was determined:

$$\text{Antioxidant activity } (\%) = 100 - oxidative\ damage\ (\%) \qquad (2)$$

All analyzes were carried out at least in triplicate. The experimental results were expressed as mean±standard deviation ($\bar{X}\pm\sigma$, n=3).

Determination of the hemolytic activity of the extracts and fractions from *Leucophyllum frutescens*

The assay of hemolytic activity was carried out according by UNE-EN ISO 10993-4. A blood sample, from a healthy patient, was placed in a tube with ethylenediaminetetraacetic acid (EDTA), as an anticoagulant. The sample was centrifuged, discarding the plasma and the white cell pack, and preserving only the red blood cells (RBC) package. The RBC were washed three times with PBS (pH 7.4) in a 1:1 ratio (RBC:PBS). After washing, the supernatant was discarded and the RBC were

resuspended in PBS in a 1: 1 ratio (RBC:PBS) in order to obtain the working suspension of RBC.

On the other hand, stock solutions of EMR and hexane fractions were dissolved in DMSO/PBS at a concentration of 1 mg/mL. Different concentrations of these samples were prepared from the stock solution, as well as NP formulations that showed the best activity against *M. tuberculosis* (NP-RIF and NP-RF1) in a range of 10 to 200 µg/mL in DMSO from 0.1 to 2% v/v. The negative control to the hemolysis was prepared with 975 µL of PBS and the positive control to the hemolysis was prepared with 975 µL of milli-Q water. 25 µL of the RBC suspension was added to all samples, including controls. The samples were incubated at 37 ° C for 1 h (VORTEMP 56, Labnet International, Inc., USA). After this time, the samples were centrifuged at 10,000 rpm for 10 min (Spectrafuge 24D, Labnet International, Inc., USA), recovering the supernatant of all the samples and adding them to a 96-well microplate. Finally, the absorbance of the supernatants was measure at λ = 575 nm in a microplate reader (Epoch, BioTek Instruments, Inc., USA). The hemolytic activity was expressed as a percentage according to equation 3:

$$\text{Hemolysis } (\%) = \frac{ABS_{sample} - ABS_{neg}}{ABS_{pos}} \; X \; 100 \qquad (3)$$

where, ABS_{sample} is the absorbance of the supernatant from the sample, ABS_{neg} is the absorbance of the negative control, and ABS_{pos} is the absorbance of the positive control. All analyzes were carried out at least in triplicate. The experimental results were expressed as $\bar{x}\pm\sigma$, n=3.

Chromatographic analysis

For the obtaining of the chromatographic profile of HF4, it was dissolved in acetonitrile (J. T. Baker, USA)/methanol (Tedia, USA), the solution was filtered through a 0.45 µm filter (Millipore, USA) to be analyzed by HPLC (VARIAN 9065, 9012, ProStar 410, USA). A Synergi™ 4 µm Fusion-RP 80 Å (150 mm x 2.0 mm x 4 µm) column, a flow of 0.2 mL/min and 30 °C was used. The mobile phase was formic acid (purity: 90%,

Millipore, USA) at 0.1% v/v and methanol with an isocratic elution of 45:55 for 40 min for leaves and 60 min for roots. The profiles were detected at λ=224 nm.

Preparation of the calibration curve and method validation

HF4 was weighted and disolved in methanol (Tedia, USA), to obtain a stock solution at 2000 µg/mL. From the stock, the working solutions were prepared in the range from 100 to 700 µg/mL and filtered through a 0.45 µm membrane (Millipore, USA), they were analyzed by the HPLC method before mentioned to obtain the calibration curve.

The chromatographic method was validated through the variables: linearity, limit of detection (LOD) and limit of quantification (LOQ) according to the International Conference on Harmonization (ICH). For the establishment of the linearity, the calibration curve was prepared and analyzed in triplicate. The LOD and LOQ were calculated by the following equations:

$$\text{Limit of detection (LOD)} = \frac{3.3\,\sigma}{S} \qquad (4)$$

$$\text{Limit of quantification (LOQ)} = \frac{10\,\sigma}{S} \qquad (5)$$

where, σ is the standard deviation of the response and S is the slope of the calibration curve.

Encapsulation of the ethanol fraction from leaves of *Leucophyllum frutescens* in polymeric nanoparticles and its characterization

Once the validation parameters were established, NP containing HF4 were prepared by the nanoprecipitation technique proposed by Fessi *et al.* (Fessi *et al.*, 1989). Briefly, the organic phase was prepared dissolved 15 mg of polylactic-co-glycolic acid (PLGA; MEDISORB 85 15 DL) and 4 mg of HF4 in 3 mL of a mixture of solvents (acetone:methanol). The organic phase was added to 10 mL of an aqueous phase, containing polyvinyl alcohol (PVAL) (Clariant, Mexico) as a stabilizer agent at a concentration of 1% w/w. Then, the organic solvent was evaporated under reduced

pressure. The NP characterization was carried out determining the particle size and polydispersity index (PDI) by dynamic light scattering (Zetasizer Nano ZS90, Malvern Instruments, UK). To determine the drug loading and encapsulation efficiency (%L and %EE), the NP formulations were centrifuged at 25,000 rpm (Allegra 64R, Beckman Coulter, USA), the supernatant was decanted, and the pellets were lyophilized (Freeze Dry System, LABCONCO, USA). The lyophilized NP were dissolved in acetonitrile and methanol. The obtained solutions were analyzed by HPLC to quantify the peaks encapsulated from the calibration curve of each one, the results obtained were substituted in the following equations:

$$\text{Drug loading (\%L)} = \frac{Weight\ of\ the\ active\ in\ NP}{Weight\ of\ the\ NP\ pellet}\ X100 \quad (6)$$

$$\text{Encapsulation efficiency (\%EE)} = \frac{Weight\ of\ the\ active\ in\ NP}{Wight\ of\ RIF}\ X100 \quad (7)$$

All the analyzes were carried out in triplicate. The experimental results were expressed as $\bar{x}\pm\sigma$, n=3.

Determination of the antioxidant activity of the ethanol fraction from *Leucophyllum frutescens* leaves in polymeric nanoparticles

To evaluate the antioxidant activity of HF4 loaded NP, a suspension of RBC was prepared as previously described. For the preparation of the samples, solutions of AA and HF4 were prepared, the volume of the NP dispersion containing HF4 was taken to obtain the final concentrations of 25 to 200 µg/mL. 375 µL of the AAPH solution and 250 µL of the RBC suspension were added to all the samples. The antioxidant control was ascorbic acid (AA), which was prepared at the same concentrations of the plant samples. 375 µL of the AAPH solution and 250 µL of the RBC suspension were added to all the samples.

The oxidant control was PBS, 375 µL of the AAPH solution and 250 µL of the RBC suspension. Two controls were added, one negative to the hemolysis (750 µL of PBS and 250 µL of RBC) and another positive to hemolysis (750 µL of milli-Q water and 250 µL of RBC). All test samples had a final volume of 1000 µL. Samples and controls were

incubated at 37 ° C for 2.5 h with constant agitation. After this time, the samples were centrifuged at 10,000 rpm for 10 min, recovering the supernatant of all the samples and adding them to a 96-well microplate. Finally, the absorbance of the supernatants at λ=575nm was measured in a microplate reader. The results of the assay was determined by equation 1 and 2.

All analyzes were carried out at least in triplicate. The experimental results were expressed as $\bar{x}\pm\sigma$, n=3.

Determination of the hemolytic activity of the etanol fraction from *Leucophyllum frutescens* leaves in polymeric nanoparticles

To evaluate the hemolytic activity of the HF4 in NP, a suspension of RBC was prepared as previously described. For the preparation of the samples, the necessary volume of the dispersion of NP containing HF4. The samples were tested in a concentration range from 25 to 200 μg/mL. The negative control to the hemolysis was prepared with 975 μL of PBS and the positive control to the hemolysis was prepared with 975 μL of milli-Q water. 25 μL of the RBC suspension was added to all samples, including controls. The samples were incubated at 37 ° C for 1 h. After this time, the samples were centrifuged at 10,000 rpm for 10 min, recovering the supernatant of all the samples and adding them to a 96-well microplate. Finally, the absorbance of the supernatants was measure at λ=575 nm in the microplate reader. The hemolytic activity was expressed as a percentage according to equation 3. The experimental results were expressed as $\bar{x}\pm\sigma$, n=3.

RESULTS AND DISCUSION

Determination of the antioxidant activity of the extracts and fractions of *Leucophyllum frutescens*

Adding AAPH to RBC, free radicals are generated by oxidative damage in the lipids of the cell membrane, consequently, the hemolysis of the cell is induced. The hemolysis can be avoided with the presence of antioxidant substances. The extracts and fractions that exhibit antioxidant activity can protect the cell against oxidative damage, as a result, the RBC lysis is avoided. Paiva-Martins *et al*., for example, made use of this

method to determine the inhibition of the oxidative lysis of RBC. They obtained the compound called and 3,4-dihydroxyphenylethanol-elenolic acid dialdehyde (3,4-DHPEA-EDA) of olive oil and synthesized its metabolite 3,4-DHPEA-EDAH_2. Its objective was to induce the oxidative stress of RBC by AAPH, and to add the compounds obtained to measure the capacity of them to protect the cells. Both compounds showed RBC protection from oxidative hemolysis at concentrations ranging from 10 to 80 µM. 4-DHPEA-EDA achieved 70% of protection at 80 µM (Paiva-Martins *et al*., 2015).

In the present study with *L. frutescens*, the samples with the best activity were obtained from leaves. The EMH, and the fractions HF1, HF2, HF3 and HF4 reached a protection around 80% from 50 µg/mL. While, the HF5 fraction reached this percentage from 100 µg/mL (Figure 1).

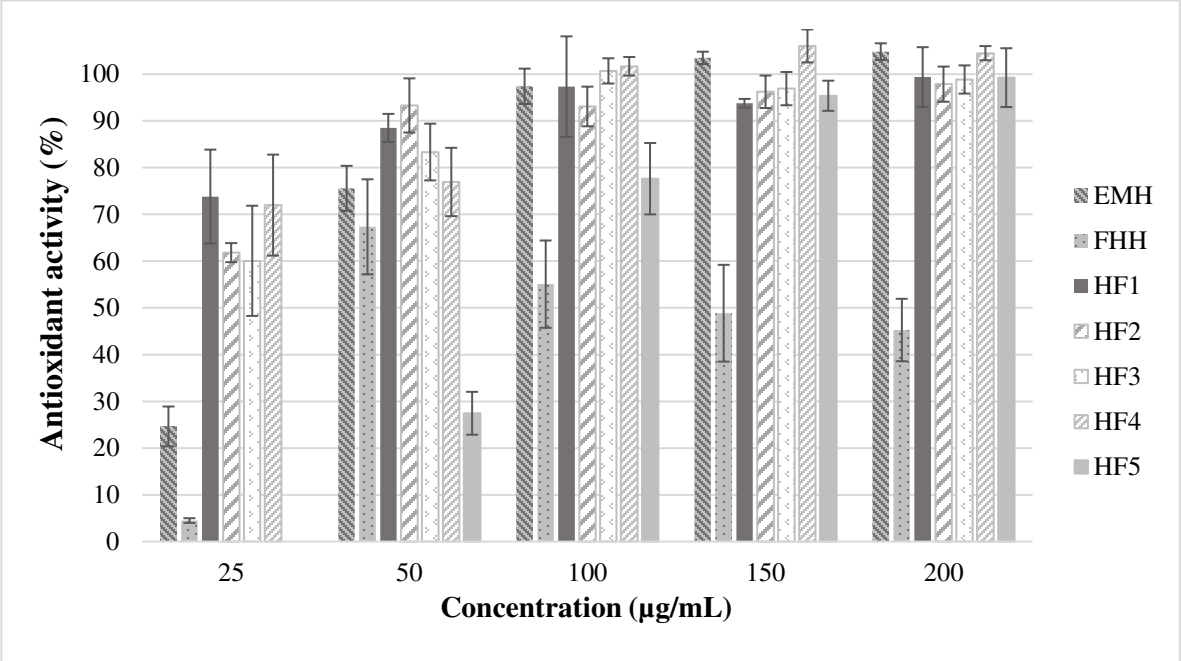

Figure 1. Percentage of the antioxidant activity of the methanol extract from leaves of *L. frutescens* and its fractions ($\bar{x}\pm\sigma$, n=3).

The ascorbic acid (AA) control presents antioxidant activity from 50 µg/mL (Figure 2). The results with *L. frutescens* revealed a protective effect at concentrations close to plants commonly reported with antioxidant activity. Karimi *et al*. investigated the aqueous and ethanol extracts of seeds of *Nigella sativa* L. and the aerial part of *Portulaca*

oleracea L. in order to evaluate the cytoprotective effect of the extracts against the hemolytic damage induced by the free radical initiator AAPH. In general, the concentrations tested were from 25 to 1800 µg/mL, being from 150 µg/mL where an antioxidant effect is observed in the extracts (Karimi *et al.*, 2011). In contrast, FHH reached its highest protection capacity (around 70%) at 50 µg/mL, at higher concentrations this property decreases. This percentage decreases because at the same time, it has a hemolytic effect. Despite being obtained with the same solvent (hexane), the results for FHH and HF1 are different, therefore the fractionation method influenced the antioxidant activity of each fraction.

On the other hand, EMR reached 80% of protection from 25 to 50 µg/mL, however, when the tested concentration was 100 µg/mL, its antioxidant activity decreases (Figure 2).

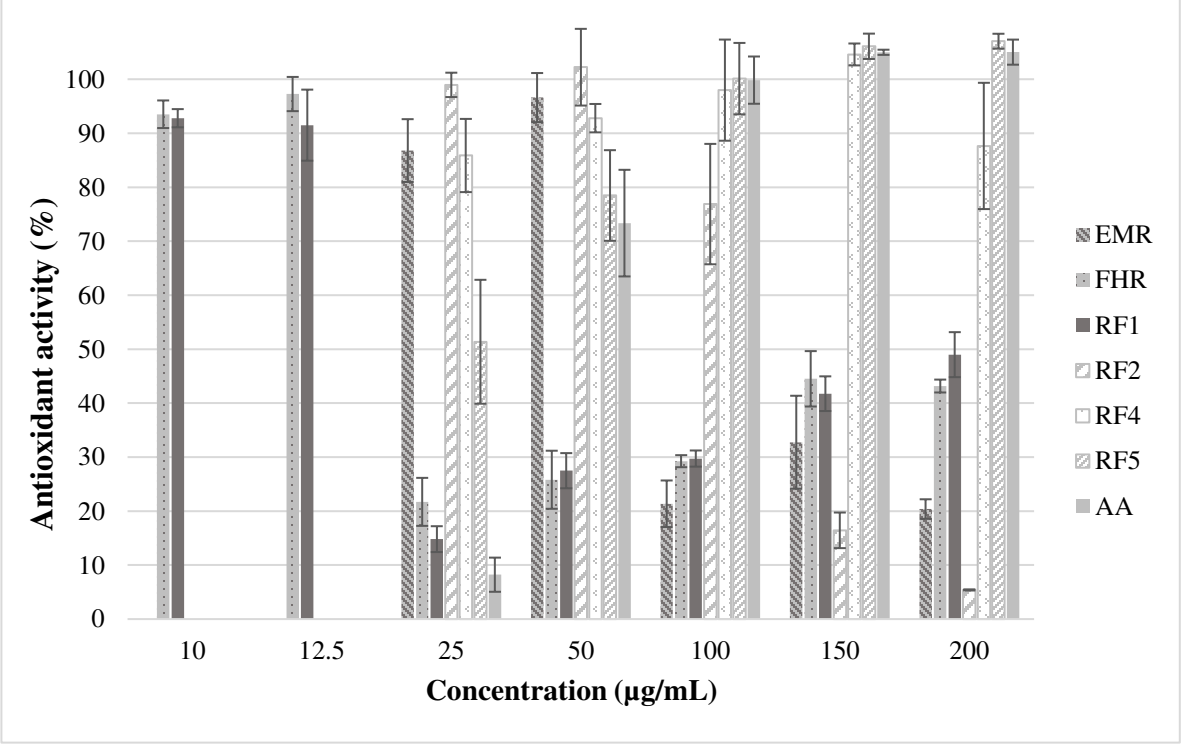

Figure 2. Percentage of the antioxidant activity of the methanol extract from roots of *L. frutescens* and its fractions ($\bar{X}\pm\sigma$, n=3).

As evidenced in Figure 2, the same behavior of EMR can be seen in its fractions. In the hexane fractions FHR and RF1, protection above the 80% is maintained in the range

of 10 to 12.5 µg/mL, for RF2 and RF4 from 25-50 µg/mL and 50-150 µg/mL, respectively. In contrast, the antioxidant activity in RF5 is maintained from 50 to 200 µg/mL. Probably, the protection of the EMR, FHR, RF1, RF2 and RF4 samples decreased as presented in Chapter 1, they have a hemolytic effect, while in RF5 there is no presence of hemolysis. All these results demonstrated that, the EMH, HF1, HF2, HF3, HF4, HF5 and RF5, could be used in a range from 25 to 200 µg/mL and obtain an antioxidant effect, even, this effect can be comparable to AA control. Meanwhile, FHH, EMR, FHR, RF1, RF2 and RF4 could be used at specific concentrations.

Determination of the hemolytic activity of the methanol extract from leaves of *Leucophyllum frutescens* and its fractions

Because, extracts and fractions obtained from *L. frutescens* leaves showed greater antioxidant activity, we proceeded to the determination of toxicity by hemolysis.

The test of the extracts and their fractions was carried out according to UNE-EN ISO 10993-4, which states that a percentage lower than 5% is considered non-hemolytic. TEMH, HF1, HF2, HF3, HF4 and HF5 did not show hemolysis at the analyzed concentrations (25-200 µg / mL), while the FHH was not hemolytic below 25 µg/mL.

Chromatographic analysis

Of all the plant samples with antioxidant activity evaluated in the present work, HF4 fraction was selected to be encapsulated in NP. Firstly, it was analyzed by a HPLC to observe its chromatographic fingerprint or its peak profile, which is a useful tool for quality control, as well as to determine the amount of peaks or components present in the vegetable sample (Bian *et al*., 2013).

The chromatographic method developed allowed the separation of four peaks or components of interest in HF4 (Figure 3). This method was validated in order to use it for the quantification of peaks 1-4, once the fraction in the NP was encapsulated.

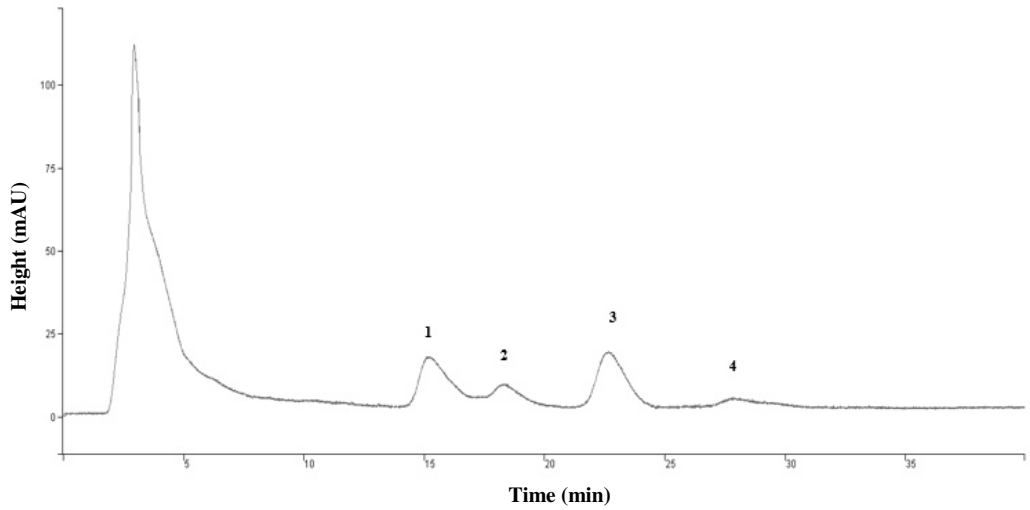

Figure 3. Chromatographic profile of the ethanol fraction from *Leucophyllum frutescens* leaves (700 µg/mL) obtained HPLC, showing four peaks-components of interest (retention times: 15.10, 18.20, 22.60 and 27.80 min, respectively).

Calibration curve of HF4 and validation of the chromatographic method

The regression equation of each peak-component (1-4) was obtained from the calibration curve shown in Figure 4. As shown in Table 1, the correlation coefficients for the calibration curve of each peak-component were greater than 0.99. LOD and LOQ for each peak 1, 2, 3 and 4 were 43.09 and 130.58, 38.62 and 117.03, 22.29 and 67.53 and, 45.86 and 138.97 µg/mL, respectively.

In the area of natural products, when it is required to quantify a peak from a known molecule present in an extract, it is compared with the standard analyzed by the same chromatographic method. Such is the case of Assunção *et al*. who developed and validated a method by CLAR for the quantification of ellagic acid in the ethanol extracts from leaves of *Eugenia uniflora* L. (Myrtaceae) (Assunção *et al*., 2017). In our work a chromatographic method was developed and validated by CLAR using peaks-components as internal markers for the quantification of HF4 in NP.

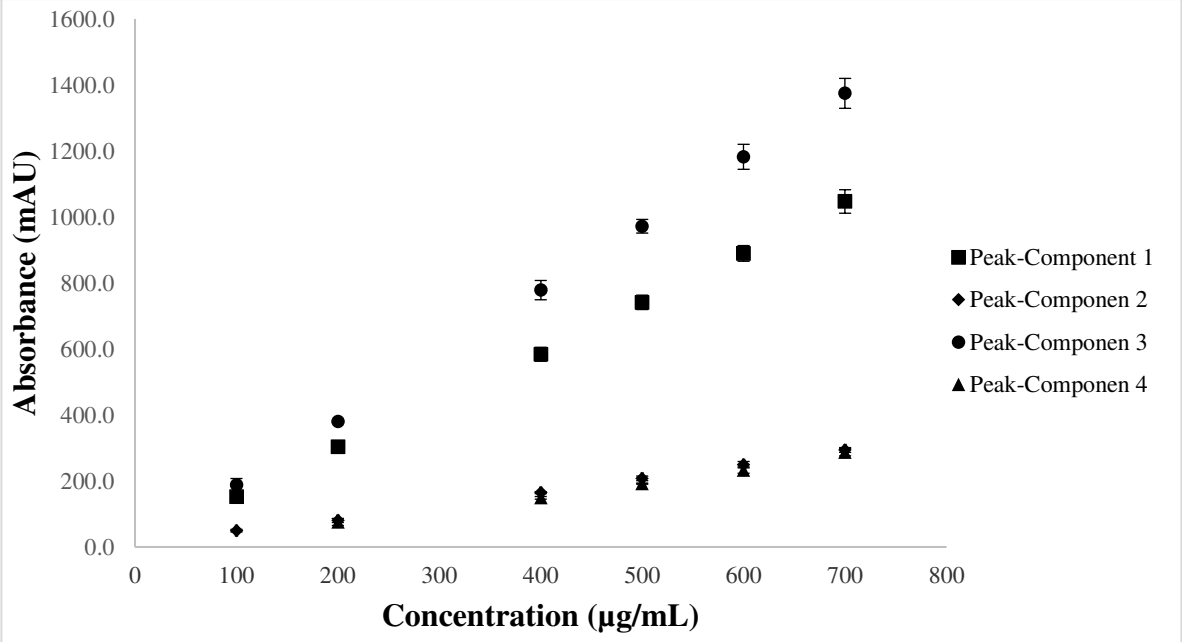

Figure 4. Calibration curve of the four peaks-components of interest present in the ethanol fraction from *Leucophyllum frutescens* roots ($\bar{X}\pm\sigma$, n=3).

Table I. Validation parameters of the four peaks-components of interest present in the ethanol fraction from *Leucophyllum frutescens* roots by HPLC

Peak-Component	Regression equation	Correlation coefficient (r)	LOD (µg/mL)	LOQ (µg/mL)
1	y = 1.4826x + 1.8489	0.99	43.83	130.58
2	y = 0.4121x + 2.5638	0.99	38.62	117.03
3	y = 1.9841x – 14.17	0.99	22.29	67.53
4	y = 0.4178x – 13.207	0.99	45.86	138.97

Encapsulation and characterization of the ethanol fraction from *Leucophyllum frutescens* leaves in polymeric nanoparticles

Once the method was validated, HF4 was encapsulated in NP by the nanoprecipitation method. The characterization of the formulation of NP with HF4 is shown in Table 2. NP sizes were obtained around 200 nm with a homogeneous size

distribution (0.118). The lyophilized NP pellet with HF4 was dissolved in a mixture of acetonitrile: methanol, and the obtained solution was analyzed by HPLC. The area under the curve of each peak was replaced in its regression equation (Table 1), in order to obtain the concentration of the four component peaks in NP. Consequently, equations 6 and 7 were used to determine %L and %EE of peaks 1, 2, 3 and 4 in NP, being 4.13 and 19.83, 4.89 and 23.48, 12.81 and 61.52 and, 16.56 and 79.53%, respectively.

The encapsulation of the peaks increased as the hydrophobic nature of the peaks increased, the highest hydrophobicity was observed with peak 4 and therefore the highest encapsulation. Sanna *et al.*, obtained white tea extract by infusing the leaves in distilled water, after, it was encapsulated in poly-ε-caprolactone NP (PCL) and alginate as particle-forming polymers using the nanoprecipitation technique. The optimal formulation had a size around 380 nm and a unimodal distribution. They determined the %EE of two catechins, (-)-epigallocatechin gallate and (-)epicatechin gallate, with values of 30.62 and 32.60%, respectively (Sanna *et al*., 2015). In our work, higher %EE were determined, probably due to the nature of the components present in the *L. frutescens* fraction.

Table II. Polymeric nanoparticles characterization containing the ethanol fraction from *Leucophyllum frutescens* leaves

			Quantification	
Size (nm)	***PDI***	***Peak-Component***	***%L***	***%EE***
206.4±3.3	0.118±0.026	1	4.13±0.76	19.83±3.76
		2	4.89±0.86	23.48±4.25
		3	12.81±2.19	61.52±11.17
		4	16.56±3.21	79.53±16.21

($\bar{x}$±σ, n=3)

Determination of the antioxidant and hemolytic activity of the etanol fraction from *Leucophyllum frutescens* leaves

The method used to determine the antioxidant activity of the HF4 NP was by the induction of oxidative damage of RBC with the reagent AAPH which generates hemolysis. Hemolysis of the RBC damage can be avoided with the presence of antioxidant substances. Figure 5 shows the antioxidant activity of HF4, HF4 NP and AA. HF4 fraction revealed around 80% of protection against oxidative damage (antioxidant activity) at 50 µg/mL. Achieving 100% antioxidant activity above 100 µg/mL. If this concentration is compared with the AA molecule evaluated as an antioxidant control, HF4 had better activity. When HF4 is encapsulated in NP, at 50 µg/mL the activity is around 80%; while 100% of antioxidant activity is reached at 100 µg/mL. In free HF4, total antioxidant activity is revealed at 100 µg/mL. Therefore, it is demonstrated that, although this fraction is formulated in NP, the antioxidant property is preserved.

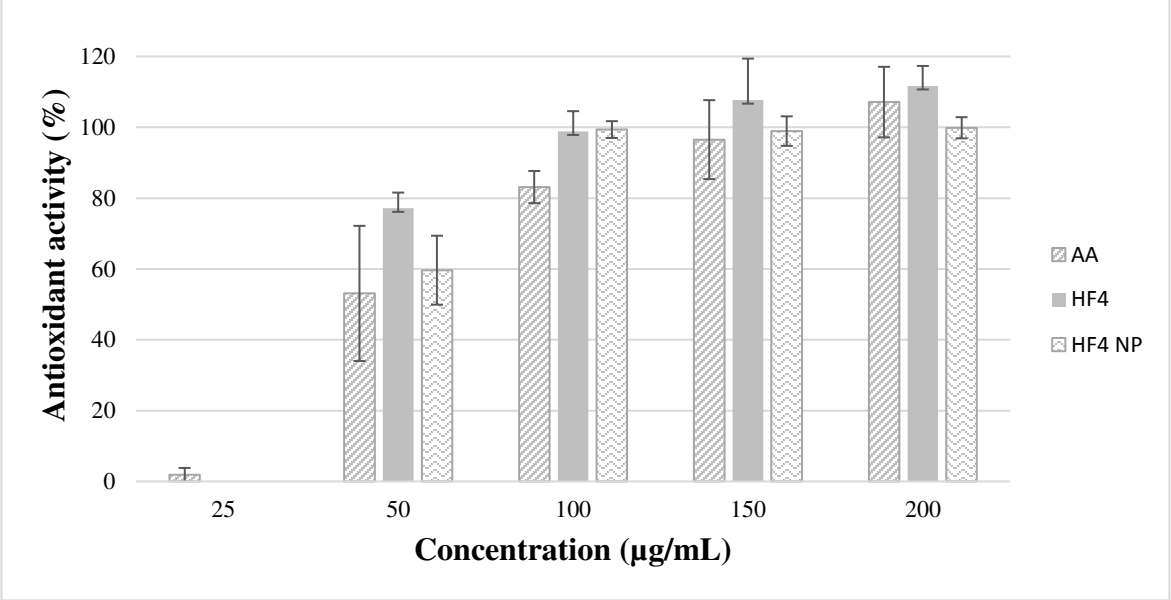

Figure 5. Antioxidant activity of the ethanol fraction from leaves of *Leucophyllum frutescens* (HF4) in its non-encapsulated and encapsulated form in biodegradable polymeric nanoparticles (NP). Ascorbic acid (AA) was taken as an antioxidant control ($\bar{x}\pm\sigma$, n=3).

In the aforementioned research by Sanna *et al.*, the antioxidant activity of the white tea extracts was evaluated by the *in vitro* 2,2-diphenyl-1-picrylhydrazyl (DPPH) method.

The best activity of PCL NP was of DPPH, observed at 300 μg/mL with 60% of inhibition compared to the free extract that shoed 100% of inhibition of DPPH at 25 μg/mL.

They attributed this difference to the low release of polyphenols from PCL NP (Sanna *et al*., 2015). Less activity is obtained at a higher concentration if it is compared with our result, this may be due to the nature of the polymers, because PCL has a slower degradation rate compared with polylactics (Mahapatro y Singh, 2011), which is related to his low release. Likewise, the toxicity was evaluated by the hemolytic activity at active concentrations, determining that there is no presence of hemolysis. This test results in the potential use of HF4 fraction formulated or not formulated in NP for administration in the organism, however, it is in NP where the use of the organic solvents is avoided.

CONCLUSION

The extracts and fractions of *L. frutescens* plant showed protection, avoiding the lysis of RBC caused by the oxidation induced with the AAPH reagent. However, FHH, EMR, FHR, RF1, RF2 and RF4, presented their maximum antioxidant activity at low concentrations and, subsequently, decreased when they were tested at higher concentrations. While, EMH, HF1, HF2, HF3, HF4, HF5 and RF5 were plant samples with antioxidant activity from 25 to 200 μg/mL and non-hemolytic effect. HF4 fraction was selected for the studies that proceeded. This fraction was of interest for the antioxidant activity that it presented at a concentration of 100 μg/mL, showing better activity than the reference antioxidant molecule AA.

A method was developed to obtain the chromatographic profile of HF4 by HPLC. The chromatographic method was validated to be used for the quantification of four peaks-components in NP presented in the fraction. The encapsulation of the four peaks in NP was determined, it revealed a favorable incorporation of the *L. frutescens* fraction.

Suspensions of NP loaded with HF4 were obtained by the nanoprecipitation method, which had a particle size around 200 nm with a homogeneous distribution. Likewise, when HF4 was incorporated in NP the activity is conserved. Because the encapsulation of the fraction is achieved, the incorporation of HF4 in NP is of potential use as an antioxidant agent, its properties are preserved, and it is non-toxic at the active concentrations.

CHAPTER 3. RIFAMPICIN AND AN ACTIVE FRACTION OF *Leucophyllum frutescens* LOADED NANOEMULSIONS, CHARACTERIZATION AND POTENTIAL USE AGAINST *Mycobacterium tuberculosis*

ABSTRACT

The interest on the use of nanoemulsions (NE) is related to its application as drug delivery systems. NE have shown several advantages such as the incorporation of hydrophobic drugs into a hydrophilic dispersion medium, the targeting to an organ or cell, the cellular uptake and the increased bioavailability. In recent years, special interest has been placed on the encapsulation of natural products such as extracts and essential oils obtained from plants to improve their biological effects. Among the plants that have been investigated is included *Leucophyllum frutescens* commonly named "cenizo", it has been demonstrated effect against the microorganism *Mycobacterium tuberculosis*, causal agent of tuberculosis. For this reason, the aim of this work was to optimize and characterize a NE to encapsulate an active fraction from roots of *L. frutescens* (RF1), as well as, the antituberculosis drug rifampicin (RIF), and to evaluate their activity *in vitro* against *M. tuberculosis*. NE were prepared by ultrasonic emulsification and the influence of different preparation variables was tested. The results showed that at a longer time of sonication, the size and the polydispersity index (PDI) of NE globules decreased. The increase in the surfactant concentration, decreased the size and increased slightly the PDI. The increase in the amount of oil phase, increased the size and decreased slightly the PDI. The formulation of NE with a particle size around 180 nm and with homogeneous size distribution, was used for the encapsulation of the actives (RF1 and RIF). In a previous study, RF1 was determined as an active fraction against *M.* tuberculosis. The characterization of the loaded NE showed a particle size of 180 nm. For the determination of the percentage of the encapsulation efficiency of RF1, most abundant peaks were selected, being encapsulated at least 70%, while RIF was encapsulated at 99%. For the anti-*M*. tuberculosis activity were tested the blank NE, RF1-NE and RIF-NE, where, the blank NE showed inhibition at the same concentration as RF1-NE and RIF-NE, this behavior can be attributed to the presence of oleic acid as the oil phase. With this work the encapsulation and characterization of a vegetal sample (RF1) and RIF in NE are

achieved. The optimal NEs characterized and tested are promising in the inhibition of *M. tuberculosis*.

INTRODUCTION

NE are systems thermodynamically unstable and kinetically stable are on nanometric scale (Gupta *et al*., 2016). The interest for NE is related to the prospects of applications such disperse systems in medicine, in pharmaceutical and cosmetic industries (Koroleva y Yurtov, 2012). A nanoemulsion is constituted by oil, water and emulsifier (Gupta *et al*., 2016). The emulsifier or emulsifying agent is a surfactant that reduces the interfacial tension between the immiscible phases, provide a barrier around the droplets and prevent coalescence of the droplets (Manoharan *et al.*, 2010).

The methods for the emulsion preparation are classified in high- and low-energy. The high-energy methods include mechanical shear such as that produced by high-shear stirring, ultrasonic emulsification, high-pressure homogenization. The low-energy method most widely used is phase inversion temperature (Koroleva y Yurtov, 2012).

They can be administrated by oral (Devalapally *et al*., 2013), intranasal (Kumar *et al*., 2008), topical (Hussain *et al*., 2016) and parenteral routes (Araújo *et al*., 2011). They can be formulated in variety of formulations such as foams, creams, liquids, sprays (Jaiswal *et al*., 2015) or gels (Hussain *et al*., 2016). As drug delivery systems studies have demonstrated many advantages such as incorporation of hydrophobic drug into a hydrophilic medium, targeting, cellular uptake and bioavailability.

A study carried out by Kumar *et al.,* has demonstrated it with an antipsychotic drug. A risperidone nanoemulsion (RNE) was prepared using capmul MCM as the oily phase and tween 80 as surfactant. A mixture of transcutol and propylene glycol was used as co-surfactant and distilled water as the aqueous phase. A risperidone mucoadhesive nanoemulsion (RMNE) was prepared by addition of chitosan. The globule size range was 15.5–16.7 nm. They proved the biodistribution of RNE, RMNE and risperidone solution (RS) in the brain and blood of Swiss albino rats by intranasal (i.n.) and intravenous (i.v.) administration. The brain/blood ratios of 0.617, 0.754, 0.948, and 0.054 of RS (i.n), RME (i.n), RMME (i.n) and RME (i.v), respectively, at 0.5 h are indicative of direct nose to brain transport bypassing the blood–brain barrier. Also, they obtained scintigraphy images following intravenous administration of RNE and intranasal administration of RNE and RMNE. The scintigrams demonstrate the accumulation of formulations in brain administered via respective routes. Major radioactivity accumulation was seen in brain

following intranasal administration of RMNE as compared to intravenous administration of RNE. For mucoadhesive nanoemulsions indicated more effective and best brain targeting of RSP. Added, significant quantity of risperidone was quickly and effectively delivered to the brain by intranasal administration of formulated. This study conducted in rats clearly demonstrated effectiveness of intranasal delivery of risperidone as an antipsychotic agent (Kumar *et al*., 2008).

Another study by Hussain *et al*. reveal controlled and extended release profile and non-irritant properties of NE contained a broad-spectrum fungicidal antibiotic used primarily in the treatment of life-threatening systemic fungal infections. They prepared a NE and NE gel for topical delivery of amphotericin B (AmB) using sefsol-218 oil, Tween 80 and Transcutol-P. Then, NE was incorporate into the carbopol gel (1% w/w) formulation. The *in vitro* drug release for AmB NE was 42.12% and AmB NE gel was 10.96%. Formulation had shown 2.0- and 9.12-fold slower drug release, respectively, as compared to AmB solution (99.97%) in first 2 h suggesting controlled. The *in vitro* skin permeation study revealed NEs increase permeation rate. The cumulative amount of drug permeated at the end of 24 h was found to be 254.161± 1.45 mg, 870.42±4.2 mg and 999.81±7.3 mg for AmB DS, NE (pH 7.4) and AmB-NE gel, respectively. Also, the irritation potential of topical formulations was evaluated on Wistar albino rats. In this study, the results showed that no severe irritation symptoms such as erythema (redness) and edema (swelling) during 72 h except reference positive (Hussain *et al*., 2016).

In recent years, special interest has been placed in the encapsulation of natural products as extracts and essential oils obtained from plants to enhance their biological effects (Blanco-Padilla *et al*., 2014). Donsì *et al*. proved the activity of different essential oil components: carvacrol, limonene and cinnamaldehyde in the sunflower oil droplets of nanoemulsions. The antimicrobial activity was measured against three different microorganisms, such as *Saccharomyces cerevisiae* (ATCC 16664), *Escherichia coli* (ATCC 26) and *Lactobacillus delbrueckii sp. Lactis* (ATCC 4797). The microorganisms, centrifuged at 6500 rpm for 5 min at 4 ◦C, were resuspended in sterile distilled water to a final concentration of 10^4 CFU/mL in test tubes, where the nanoemulsions were added to the desired final antimicrobial concentrations. The testtubes were hence incubated at 32 ◦C for *S. cerevisiae* and *L. delbrueckii* and at 30 ◦C for *E. coli*. After 2 h and 24 h, the

surviving cells were evaluated by standard plate count method. The antimicrobial activity of formulations was evident over a longer time scale (24 h) (Donsì *et al*., 2012). Tsai y Chen extracted catechins from tea leaf waste of *Camellia sinensis* (L.) Kuntze. The catechin extract was incorporated in NE and tested in human prostate cancer cell PC-3 and human fibroblast cell CCD-986SK. After 72 h incubation catechin nanoemulsion exhibited a lower toxicity toward CCD-986SK cells than catechin extract. While, catechin nanoemulsion had a major inhibitory effect in prostate cancer cell PC-3 proliferation with the IC_{50} being 8.5 µg/mL than catechin extract with IC_{50} being 15.4 µg/mL (Tsai y Chen, 2016).

Some studies have focused on the use of plants against the microorganism *M. tuberculosis*, causal agent of tuberculosis, with the aim of reducing the large number of new cases and mortalities that occur per year. The plant known as "cenizo" *L. frutescens* has been studied for this purpose. Molina-Salinas *et al*. determined that the methanol extracts from leaves and roots showed activity against *M. tuberculosis* (Molina-Salinas et al., 2007). However, few compounds obtained from *L. frutescens* have been identified (Alanís-Garza *et al*., 2012; Molina-Salinas *et al*., 2011).

In this context, the aim of the study was to optimize and characterize of a NE to encapsulate an active fraction obtained from the methanol extract of roots of *L. frutescens*, as well as, the antituberculosis drug RIF, and the *in vitro* evaluation against *M. tuberculosis.*

MATERIALS AND METHODS

Preparation of *Leucophyllum frutescens* hexane fraction

Roots of *L. frutescens* were collected in Monterrey, N. L., Mexico in July 2013. Consequently, the plant material was washed, dried at room temperature and pulverized. 50 g of powdered leaves or roots were weighed, 350 mL of methanol was added. The extracts were obtained by ultrasound (Ultrasonic Cleaners, VWR Symphony, USA). For a period of 1 h, the temperature for the extraction was increased from 25 to 60 ºC, once reached 60 ºC, three cycles of 10 min of sonication and 10 min of rest were performed. Subsequently, the samples were filtered to obtain the solvent, which was evaporated under

reduced pressure (Laborota 4003 control, Heidolph) in order to obtain the methanol extract of roots (EMR). Hexane was added to the EMR, stirred to aid the solubilization of the compounds related to the solvent, filtered to obtain the solvent and evaporated obtaining the hexane fraction called RF1.

Preparation, optimization and characterization of nanoemulsions

Briefly, oleic acid (OA) as oil phase was emulsified in a tween 80 solution as aqueous phase with ultrasonic emulsification (Homogeneizador, OPTIC IVYMEN SYSTEM) with 80% amplitude. The influence of different variables in the preparation of emulsions were proved. Firstly, different times of sonication (3, 5, 6, 7 and 8 min) were tested with 4g of oleic acid and 96g of a tween 80 solution at 2%w/v. Then, the concentration of tween 80 was changed (1, 1.5, 2, 3 and 4% w/v). Finally, different amounts in oil/aqueous phase were proved (1.5/98.5, 2/98, 3/97, 3.5/96.5 and 4/96 g). All the formulations were prepared in triplicated. The hydrodynamic diameter, polydispersity index (PDI) and zeta potential of each emulsion were measured by dynamic light scattering (Zetasizer Nano ZS90, MALVERN). Zeta potential was determined at 5 different pH (3, 5, 7, 9 and 11). Their stabilities were followed by hydrodynamic diameter, PDI and the separation of oil/aqueous phases over time.

Preparation and characterization of hexane fraction of *Leucophyllum frutescens* and rifampicin loaded emulsions

Different formulations of RF1 and RIF were prepared by ultrasonic emulsification. Briefly, the organic phase containing RF1 or RIF in oleic acid was emulsified in the aqueous phase containing a solution of T-80 (1% w/v). Then, NE were characterized by the measurement of hydrodynamic diameter, polydispersity index (PDI), zeta potential and stability. The actives in NE were quantified by high performance liquid chromatography (HPLC) (WATERS).

RF1 quantification was carried out indirectly, centrifuging the samples (Eppendorf 5415 centrifuge) at 5000 rpm for 30 min, to separate the aqueous phase from the globules. The aqueous phase was taken and analyzed on a Phenomenex C_{18} column with a flow of

0.2 mL/min at 30 °C. The mobile phase was water (A) and methanol (B) in a isocratic elution 45:55 (A: B) for 60 min. The detection of the RIF peak was at λ=210 nm.

RIF quantification was carried out indirectly, centrifuging the samples (Eppendorf 5415 centrifuge) at 5000 rpm for 30 min, to separate the aqueous phase from the globules. The aqueous phase was taken and analyzed on a Phenomenex C_{18} column with a flow of 0.35 mL/min at 30 °C. The mobile phase was water (A) and acetonitrile (B) in a isocratic elution 40:60 (A: B) for 15 min. The detection of the RIF peak was at λ=334 nm.

Anti-*Mycobacterium tuberculosis* activity of the active fraction of *Leucophyllum frutescens* and rifampicin loaded in the nanoemulsions

The anti-*M. tuberculosis* activity was evaluated on the susceptible strain of *M. tuberculosis* H37Rv by the alamar blue assay in a microplate adapting the methodology used by Molina-Salinas *et al*. (Molina-Salinas et al., 2007). The strain was cultivated in Middlebrock 7H9 broth enriched with OADC (Becton Dickinson and Co., Sparks, MD, USA) at 37 °C for 14 days. After, the strain was adjusted according to the standard scale no. 1 of McFarland and diluted 1:20 for use in the assay. On the other hand, in a 96-well microplate, 200 µL of water was added to the wells in the periphery. While, in the work wells, 100 µL of Middlebrock 7H9 broth enriched with OADC was added. In the first well of each row, 100 µL of each sample (NE blank, NE-RF1 and NE-RIF) and control samples (RF1, RIF and tween 80 solution) were added. Once all the samples were added, serial dilutions 1:2 of each sample were performed, taking 100 µL of the first well and adding them to the second well of the row, then, of the second well, 100 µL was taken to add them to the third, this procedure was repeated until reaching the last well each row; the 100 µL taken from the last well was eliminated. Finally, 100 µL of the bacterial suspension was added to obtain a final volume in all wells of 200 µL. All samples were prepared in duplicate in the same day. The microplates were incubated at 37 °C for 5 days. At day 5, 20 µL of the blue alamar reagent and 12 µL of 10% v/v of tween 80 were added to all the work wells, and the microplates were reincubated at 37 °C for 24 h. The minimum inhibitory concentration (MIC) was determined from the color change of the blue to pink reagent. All tests were carried out at least in triplicate.

RESULTS AND DISCUSION

Preparation, optimization and characterization of nanoemulsions

The emulsions were prepared with oleic acid as oil phase and tween 80 as surfactant. Oleic acid was chosen due to *M. tuberculosis* has shown the ability to utilize this fatty acid complexed with triton as a source of carbon for growth was determined (Hedgecock, 1970), and with a nanocarrier based in oleic acid will be possible *M. tuberculosis* takes it more effectively than others.

As part of the optimization, different preparation variables of NE were evaluated. Firstly, the influence of the sonication time (3, 5, 6, 7 and 8 min) on the particle size and PDI was determined (Figure 1). When time was increased the hydrodynamic diameter and PDI decreased from 215.7±3.2 nm to 155.6±0.2 nm and from 0.319±0.025 to 0.244±0.009, respectively. The ultrasonic emulsification is very efficient in reducing droplet size. Here, the energy is provided through a sonicator probe. It contains piezoelectric quartz crystal which can expand and contract in response to alternating electric voltage. As the tip of sonicator contacts the liquid, it produces mechanical vibration and cavitation occurs. Cavitation is the formation and collapse of vapour cavities in liquid. Thus, ultrasound can be directly used to produce emulsion (Jaiswal *et al*., 2015). It means, more exposure time to emulsification more energy that allows smaller droplet size. The stability tests showed in the range of 5 to 8 min, a size change around 30 nm from day 0 to day 77 (data not shown), being from 7 min where a homogeneous size distribution was maintained during this period.

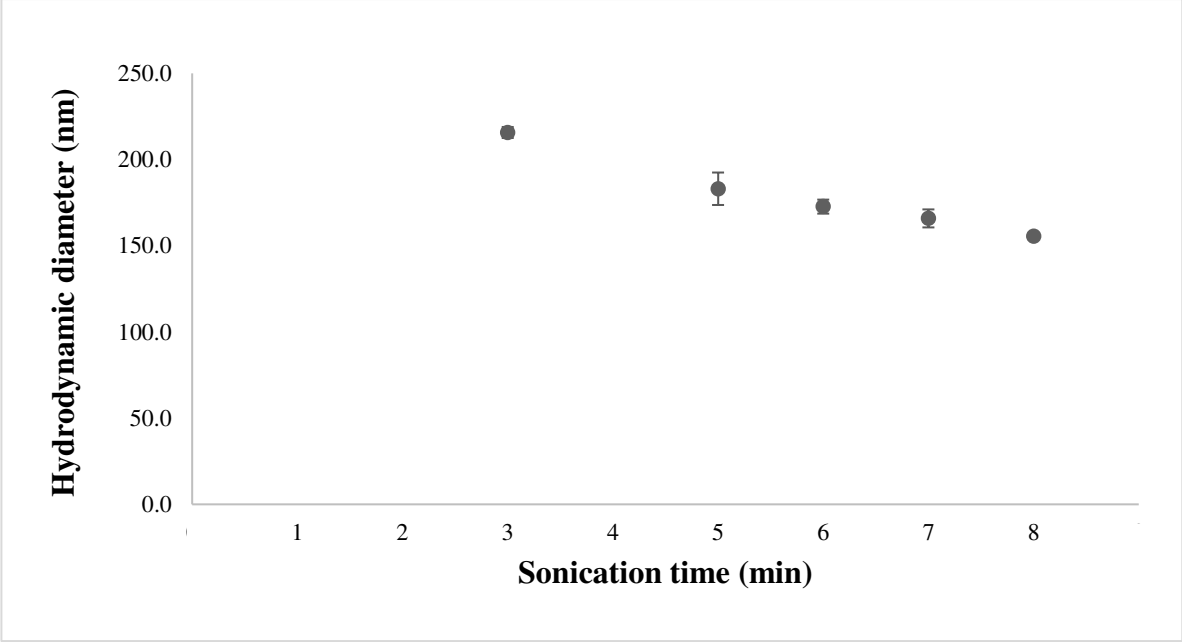

Figure 1. Effect of the sonication time on the hydrodynamic diameter ($\bar{x}\pm\sigma$, n=3).

To continue with the influence of T-80 concentration was used a time sonication of 7 min and 4g of OA. The increased of tween 80 concentration from 1 to 4% w/v decreased the droplet size from 195.1±1.4 nm to 156.1±4.1 nm but the PDI increased slightly from 0.201±0.006 to 0.285±0.005 (Figure 2). The same behaviors on the droplet sizes were observed in the study carried out by Ghosh *et al.* They prepared NE by ultrasonic emulsification with an oil phase containing cinnamon oil and Tween 80 as surfactant. Three different cinnamon oil and Tween 80 as surfactant ratios (1:1, 1:2 and 1:3 v/v) were proved at 10, 20 and 30 min of ultrasonic emulsification and steady decrease in droplet size of emulsion was observed from ~400 to 250 nm, ~250 to 96 nm and ~200 to 65 nm, respectively. T-80 concentration also played a major role in droplet size of nanoemulsion. Increasing surfactant concentration resulted in decrease in droplet diameter. Formulation with 6% surfactant concentration after sonication for 30 min was found to be 254 nm, whereas formulation with 12% surfactant was 96 nm and formulation with 18% surfactant has lowest droplet diameter of 65 nm after a sonication period of 30 min (Ghosh *et al.*, 2013).

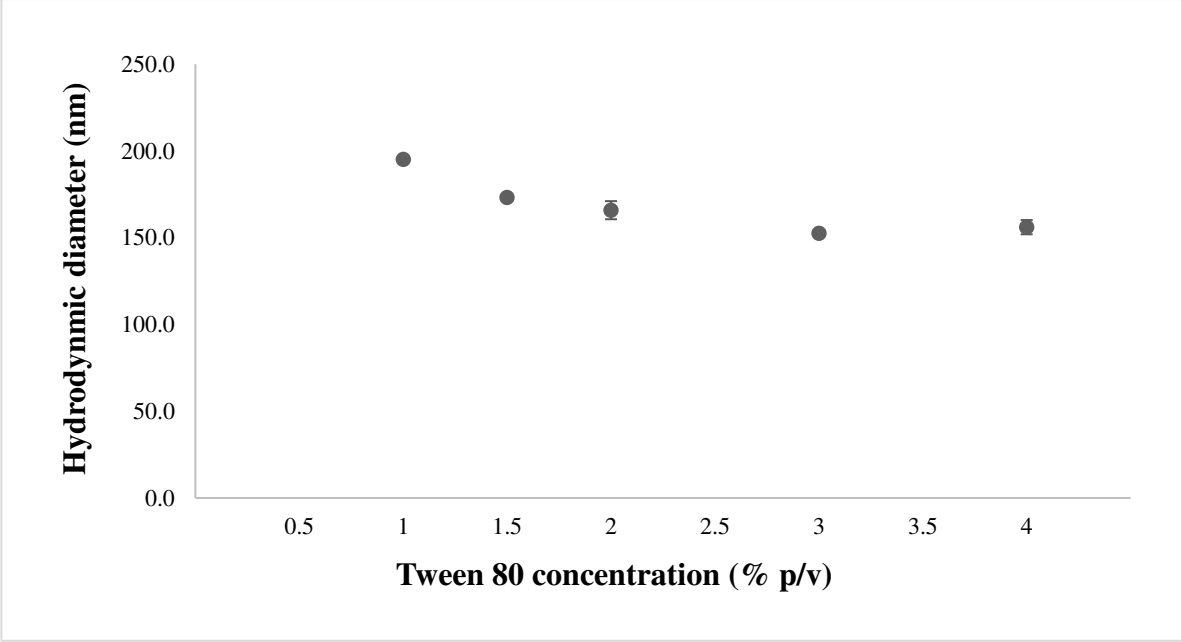

Figure 2. Effect of the concentration of Tween 80 solution on the hydrodynamic diameter ($\bar{X}\pm\sigma$, n=3).

Finally, the influence of the oil and aqueous phase amount on hydrodynamic diameter was evaluated, maintaining a sonication time of 7 min and tween 80 solution at 1% w/v. When the oil amount increased while aqueous phase decreased the droplet size at the same time from 126.3±0.7nm to 195.1±1.4 nm (Figure 3) and the PDI decreased slightly from 0.259±0.003 to 0.201±0.006. 0.259 ± 0.003 to 0.201 ± 0.006. Mantena *et al*. found this influence on size who prepared NE by aqueous phase titration method. Capryol 90 as oil, Tween 20 as surfactant and Transcutol P as cosurfactant. They maintained a constant percentage of surfactant (30%) and co-surfactant (10%) in the formulation and the percentage of oil was 10, 15 and 20% at the same time the percentage of water changed in 50, 45 and 40%. The size increased from 234.9 nm to 285.8 nm (Mantena *et al.*, 2015). The size of the NE droplets supposes an increase, when increasing the oil ratio, the amount of phase is reduced, as a consequence the chains of the surfactant are reduced, increasing the interfacial tension (Du *et al.*, 2016).

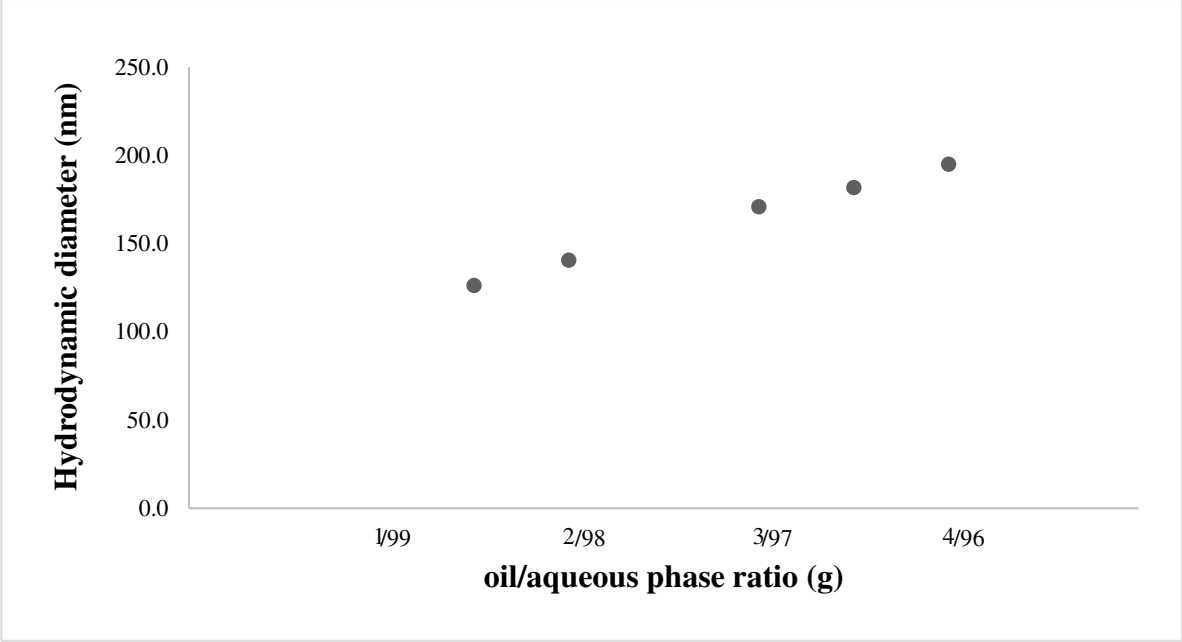

Figure 3. Effect of the ratio on the amount of oleic acid (oil phase) and 1% w/v of Tween 80 solution (aqueous phase) on the hydrodynamic diameter ($\bar{X}\pm\sigma$, n=3).

The NE prepared for the evaluation of the influence of the preparation variables were stable up to 77 days, likewise, all the formulations showed a negative zeta potential. The negative value can be explained by the presence of negatively charged carboxyl groups of oleic acid (Laouini *et al*., 2012). The negative value can be explained by the presence of negatively charged carboxyl groups of oleic acid (DeRuiter, 2005). The pKa of oleic acid is 5.02 (Pubchem). This explain when we compared at pH 3 the zeta potential is closer 0 (around -3 mV) with pH 5 to pH 11 (-40 to -70 mV) a greatly increased in the negativity can be observed.

Preparation and characterization of the hexanic fraction of *Leucophyllum frutescens* and rifampicin loaded in nanoemulsions

Subsequently, an optimal NE was selected for the preparation of two formulations, for the encapsulation of RF1 and RF1. For the preparation of RF1-NE and RIF-NE the sonication time of 7 min, the concentration of T80 at 1% w/v and the ratio in the amount of oleic acid and aqueous phase of 3.5/96.5 were selected. g. The obtained particle size with these variables was around 180 nm (Table I) and a homogeneous size distribution (Figure 4).

Table I. Characterization of nanoemulsions containing rifampicin and the hexane fraction from *Leucophyllum frutescens* roots

Active	*Hydrodynamic diameter (nm)*	*PDI*	*Encapsulation efficiency (%)*	
RIF	179.3±3.5	0.213±0.014	99.9±0.0	
RF1	179.1±1.4	0.217±0.002	*Peak* 5	75.8±3.5
			Peak 9	86.5±4.7
			Peak 10	72.8±0.4
			Peak 14	70.6±17.4
			Peak 15	84.7±5.3

($\bar{X}$±σ, n=3)

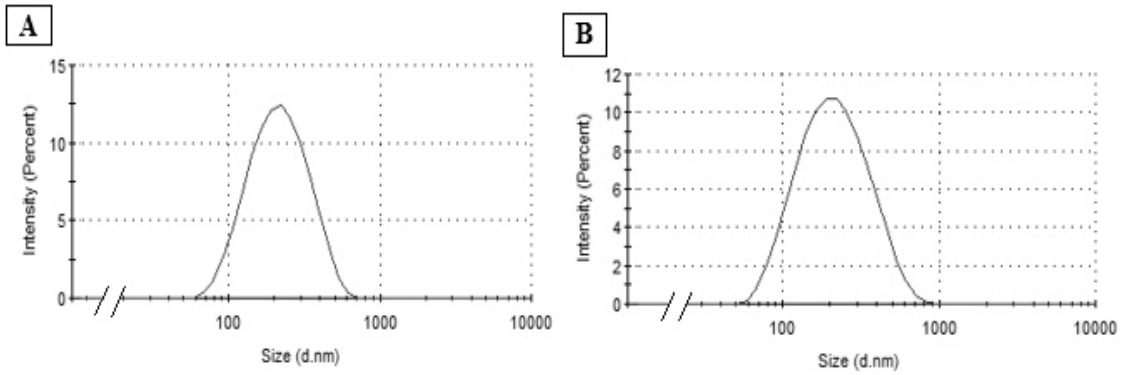

Figure 4. Size distribution of nanoemulsions by intensity percentage: (A) rifampicin loaded nanoemulsion; (B) hexane fraction from roots of *Leucophyllum frutescens*.

Lately, the encapsulation of both active in NE was determined by CLAR. In Figure 5 the chromatogram with the RIF peak in an aqueous solution is observed. When the sample obtained from the centrifugation of the NE was analyzed, it was determined that the molecule is 99% encapsulated. Ahmed *et al*. prepared a NE with RIF using Sefsol 218 as oil and T80 as emulsifier and tween 85 as a co-emulsifier. They found an encapsulation efficiency of around 100% with stability for more than 19 months (Ahmed *et al*., 2008).

On the other hand, RF1 was dissolved in methanol in order to observe its chromatographic profile, it showed 15 peaks (Figure 6). The peaks 5, 9, 10, 14 and 15 were selected for their quantification within the NE, obtaining an encapsulation efficiency greater than 70%. Similar results were obtained by Ha *et al*. when determined the encapsulation of lycopene in a tomato extract formulated in NE, which was 51 to 65% (Ha *et al*., 2015). For both formulations, a negative zeta potential (Figure 7) and stability (without phase separation) were observed over 77 days (Figure 8).

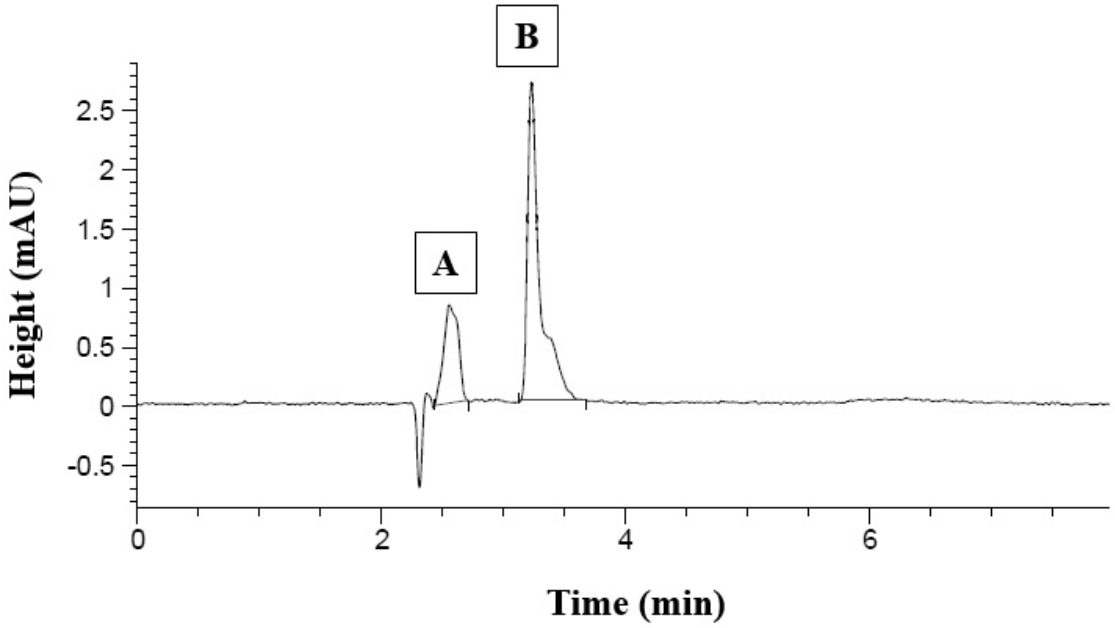

Figure 5. Chromatogram of rifampicin in water (9 µg/mL) obtained by CLAR: (A) water peak; (B) rifampicin peak, retention time = 3.2 min.

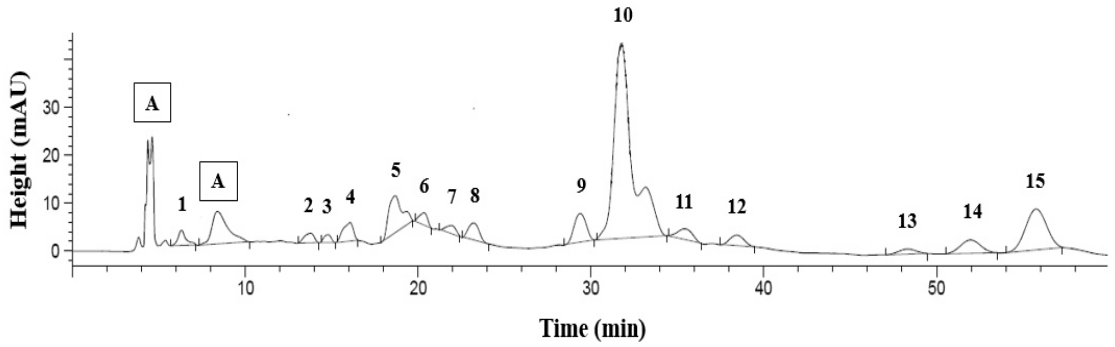

Figure 6. Chromatogram of the hexane fraction from roots of *Leucophyllum frutescens* (230 µg/mL) obtained by CLAR: (A) peaks of methanol.

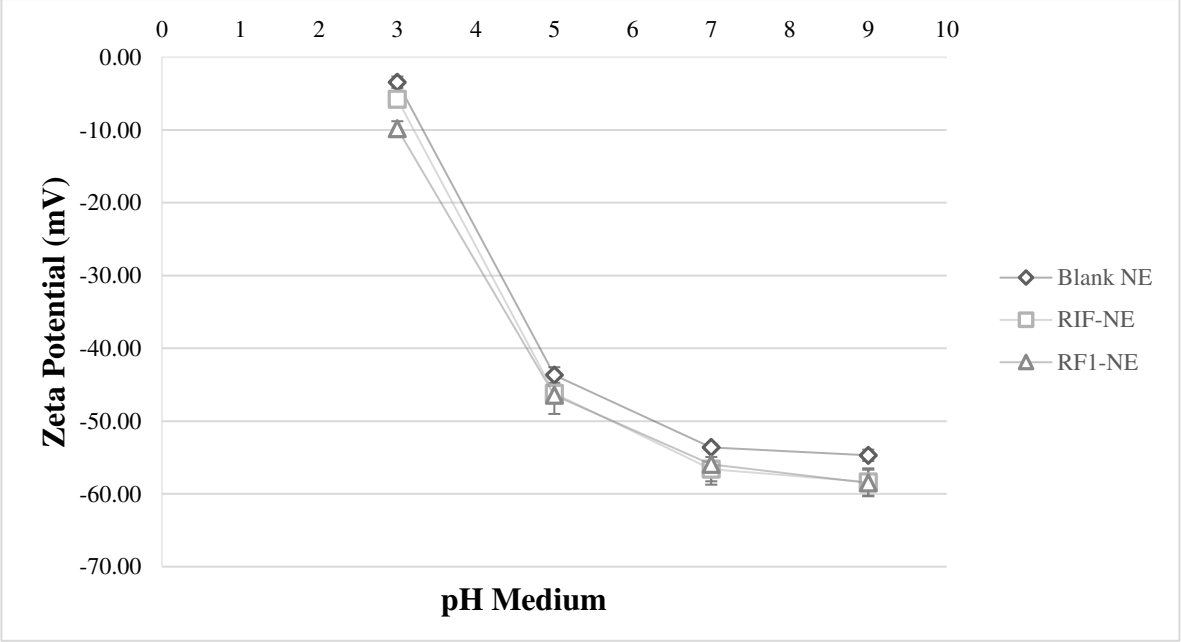

Figure 7. Effect of the pH of the dispersion medium of the nanoemulsions on the zeta potential: blank nanoemulsions (NE), containing rifampicin (RIF-NE) and containing the hexane fraction from roots of *Leucophyllum frutescens* (RF1-NE) ($\bar{X}\pm\sigma$, n=3).

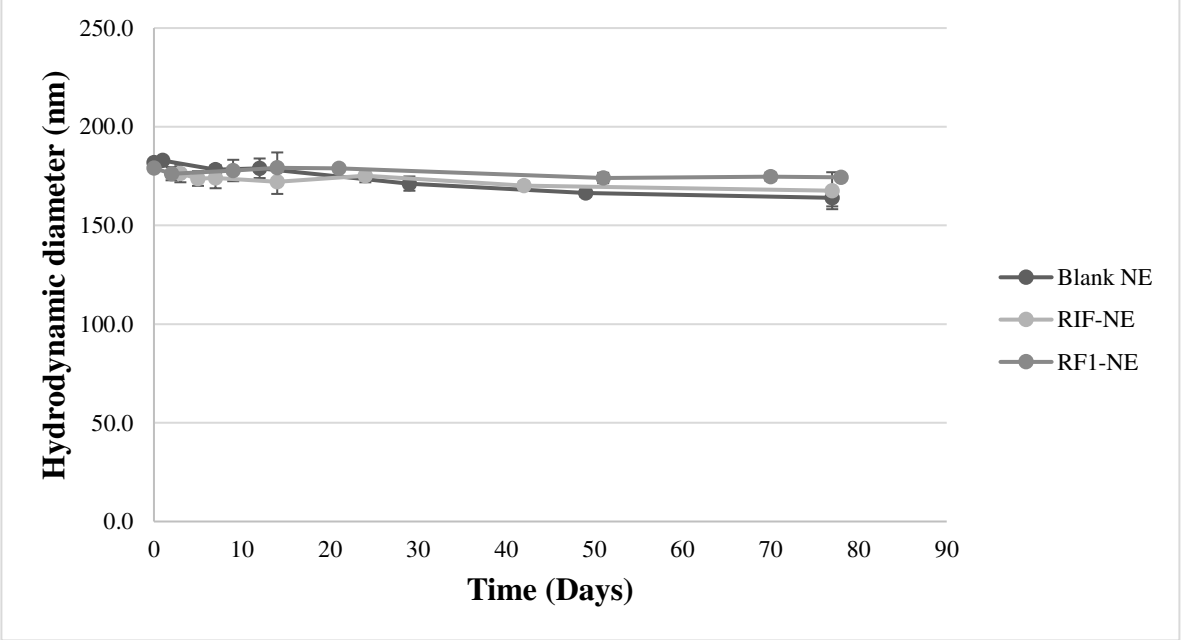

Figure 8. Stability of blank nanoemulsions (NE), containing rifampicin (RIF-NE) and containing the hexane fraction from roots of *Leucophyllum frutescens* (RF1-NE) ($\bar{X}\pm\sigma$, n=3).

Anti-*Mycobacterium tuberculosis* activity of the active fraction of *Leucophyllum frutescens* and rifampicin loaded nanoemulsions

Finally, the activity against *M. tuberculosis* of the three NE (blank NE, RIF-NE and RF1-NE) was evaluated by alamar blue microplate method. The test is based on the color change from blue to pink of the reagent. MIC of RIF and RF1 without encapsulation was 0.19 and 40 μg/mL, respectively. Blank NE showed inhibition when oleic acid and T80 were at 68.10 and 18.75 μg / mL, respectively. While the RIF-NE and RF1-NE showed inhibition when the actives were at a concentration of 0.19 and 0.39 μg/mL, respectively, but OA and T80 were at a concentration of 68.10 and 18.75 μg/mL, respectively, as in blank NE. Choi proved an unsaturated acid called linoleic acid (α and γ form) against M. tuberculosis, in both cases fatty acid forms obtained a MIC of 75 μg/mL (Choi, 2016). Therefore, in our study, the inhibition of blank NE can be explained by the presence of oleic acid. It was not possible to observe the effect of the activity of RIF and RF1 when they were in NE due to the presence of the fatty acid.

CONCLUSION

The effect of sonication time, surfactant concentration and oil/aqueous phase ratio on particle size, PDI, zeta potential and stability for NE optimization was tested. The optimal formulation was used for the encapsulation of RF1 and RIF having a diameter around 180 nm, homogenous size distribution, negatively charged and, they were stable for 77 days. Both formulations showed high efficiency of encapsulation. The anti-*M. tuberculosis* activity showed inhibition in the same concentrations including blank NE, this behavior can be attributed due to the presence of oleic acid as oil phase. The optimal NE characterized and tested are promising for their use against *M. tuberculosis*.

VIII. CONCLUSIONS

In this study some investigations with the extracts and fractions from *L. frutescens* were carried out in order to obtain a broader knowledge about the biological activity present in the plant. Likewise, the vegetable samples that showed activity were encapsulated in free systems of organic solvents. NP has shown to be a good alternative to load actives into nanoparticles. As good delivery systems, actives loaded into nanoparticles show stability, protection, controlled release and targeted. Different parameters during nanoprecipitation process can be modified to obtain a formulation with the desirable characteristics on the size, storage stability, active encapsulation and electrostatic charges.

Based on the antimycobacterial activity revealed by previous studies, the first part of this work was focused on testing the effect of *L. frutescens* against *M. tuberculosis* to propose it as a co-adjuvant of the drugs used for the tuberculosis treatment, such as RIF. To obtain the methanol extract from leaves and roots of *L. frutescens*, an ultrasound method was developed, which allowed a good performance to be obtained in a short time (2 h). Two different fractionation methods were developed in order to obtain the hexane fraction of leaves and roots, the percentage of yield obtained with both methods was close. However, method 2 was selected to continue with the following partitions because it is faster and easier to execute. The chromatographic profiles of the extracts and fractions were obtained through HPLC, these results reveal that there is the same number of peaks between the extract (leaves or roots) and the fractions obtained from it; in roots there is higher number of peaks than leaves.

The evaluation of the activity against *M. tuberculosis* of the extracts and fractions of *L. frutescens* revealed that in roots are more activity than in leaves, specifically, EMR, FHR and RF1 (MIC = 100, 40 and 40 µg/mL, respectively). Biodegradable NP of RIF and vegetable samples (EMR, FHR and RF1) of *L. frutescens* were prepared by nanoprecipitation. NP showed a size from 140 to 190 nm, with homogeneous distributions and negative zeta potential. RIF had a MIC of 0.20 µg/mL, but when RIF is encapsulated in NP-PLGA-PVAL, it enhanced its activity (0.10 µg/mL) against *M. tuberculosis*. On the other hand, the hexane fractions in NP had more activity than free. The most active formulation was NP-PLGA-FHR and NP-PLGA-RF1 with a MIC of 80 µg/mL for both.

The combination of FHR and RF! with RIF decreases the MIC value in both cases, demonstrating a better effect. Finally, the toxicity of the best samples was proved, at the active concentrations against *M. tuberculosis* RIF and NP-RIF did not present hemolysis. Whereas, RF1 and NP-RF1 showed hemolysis. However, when RF1 is combined with RIF, the concentrations decreased from 40 to 10 μg/mL for RF1 and from 80 to 20 μg/mL for RF1 loaded NP, and at these concentrations there is no presence of hemolysis. This suggested that the encapsulation of RF1 in NP favored the reduction of its toxicity. Therefore, an alternative to make use of the hexane fraction from roots of *L. frutescens* with potential activity against *M. tuberculosis*, at concentrations below the hemolytic effect, is to combine it with conventional antituberculosis drugs such as RIF, and thus, to enhance the activity.

Because of *L. frutescens* has been less studied for its antioxidant capacity, the second part of this work was focused on the antioxidant effect of the previously obtained extracts and fractions. The extracts and fractions of the *L. frutescens* plant showed a certain degree of protection, avoiding the lysis of RBC caused by the induced oxidation of AAPH reagent. FHH, EMR, FHR, RF1, RF2 and RF4 presented their maximum antioxidant activity at low concentrations and, subsequently, decreased when they were tested at higher concentrations due to a hemolysis effect. EMH, HF1, HF2, HF3, HF4, HF5 and RF5 were samples with antioxidant activity from 25 to 200 μg/mL and without hemolytic effect, being selected the fraction HF4 for the studies that proceeded. Suspensions of HF4 loaded NP were obtained by the nanoprecipitation technique, NP had a particle size around 200 nm with a homogeneous distribution. A chromatographic method was partially validated to be used for the quantification of the peaks-components present in HF4, from which the encapsulation of four peaks in NP was determined, it revealed a favorable incorporation of the *L. frutescens* fraction. Finally, when HF4 was incorporated in NP the antioxidant activity was conserved. For this reason, the incorporation of HF4 loaded NP is promising as an antioxidant agent because the encapsulation of the fraction is achieved, its properties are preserved, and it is non-toxic at the active concentrations.

An important part of the characterization of nanoparticulate systems is the determination of the percentage drug loading and encapsulation efficiency, for this raison a method of quantification by HPLC was developed and validated using the peaks-components of the plant as internal markers. Therefore, in this work we proposed a new strategy for the quantification of extracts or fractions of *L. frutescens*.

In the last part of the study, to make use of a sustained release system different of NP was proposed. Studies with NE were carried out testing the effect of sonication time, surfactant concentration and oil/water ratio on particle size, PDI, zeta potential and stability. The optimal formulation was selected for the encapsulation of RIF and the active fraction RF1 against *M. tuberculosis*. NE had a diameter around 180 nm, homogeneous size distribution, negatively charged and stable for 77 days. Both formulations showed high encapsulation efficiency. The anti-*M. tuberculosis* activity showed inhibition at the same concentrations including blank NE, this behavior can be attributed to the presence of oleic acid as oil phase. Thus, the optimal characterized and tested NE can be promising in the inhibition of *M. tuberculosis.*

With the results obtained in our work, the knowledge about the *L. frutescens* plant is extended, either by its activity against *M. tuberculosis* or by its antioxidant activity. Likewise, it is revealed that NP or NE are a promising alternative to load extracts or fractions of the plant, converting them into a viable formulation for its administration.

IX. PERSPECTIVES

Based on the results and conclusions obtained in this Doctoral Thesis, the perspectives are oriented in different directions.

In the Chapter 1, the results related to RIF, *L. frutescens*, NP and its activity against *M. tuberculosis* were shown. For this first section, future research would be about *in vitro* release studies of the active formulations obtained in order to know the time of release of the actives to the environment in which they would be in the body and, also, to propose their release mechanisms. Because the target organ of the formulations are macrophages, *in vitro* studies on macrophages would be promising. Likewise, from the favorable results obtained on the combination of the drug RIF and the formulation of NP-PLGA-RF1, we propose to work with the tests to determine the synergism effect. On the other hand, it would be interesting to know about the distribution of the active formulations in an organism, for which we suggest to carry out *in vivo* biodistribution studies of RIF and RF1 free and encapsulated into NP, individually and in combination. The final perspective to this chapter is to carry out the studies of isolation and identification of the compounds from the extracts and root fractions of *L. frutescens* that have the best activity against *M. tuberculosis*, encapsulation of the compounds in NP, the characterization of NP and studies of their effect on *M. tuberculosis*.

In the Chapter 2, the results related to *L. frutescens*, NP and its antioxidant activity were presented, due to the promising results obtained with the antioxidant effect of the plant, future investigations would be studies of *in vitro* release of the active encapsulated into formulations in order to know the time of release towards the environment in which they would be in the organism, also, to propose its release mechanisms and *in vivo* biodistribution studies.

Finally, in the Chapter 3, the results related to RIF, RF1, NE and their activity against *M. tuberculosis* were shown. Based on our research, it will be of great interest to

work on the formulation, determining the oil phase and aqueous phase that does not present activity in the microbiological studies.

For all the formulations obtained in this thesis work, other *in vitro* and *in vivo* methods should be carried out to expand knowledge about toxicity.

X. BIBLIOGRAPHY

INTRODUCTION

Booysen, L. L. Kalombo, L. Brooks, E. Hansen, R. Gilliland, J. Gruppo, V. Lungenhofer, P. Semete-Makokotlela, B. Swai, H. S. Kotze, A. F. Lenaerts, A. du Plessis, L. H. 2013. In Vivo/in Vitro Pharmacokinetic and Pharmacodynamic Study of Spray-Dried Poly-(Dl-Lactic-Co-Glycolic) Acid Nanoparticles Encapsulating Rifampicin and Isoniazid. *International Journal of Pharmaceutics* 444 (1–2):10–17.

Calleja-Avellanal, I. Dios-Viéitez, M. C. Ruz-Expósito N. Renedo-Omaechevarria, M. J. Blanco-Prieto, M. J. 2003. Desarrollo y caracterización de nanopartículas de rifampicina para su aplicación en el tratamiento de la tuberculosis. Tecnología Farmacéutica. Departamento de Farmacia y Tecnología Farmacéutica. Facultad de Farmacia. Univesidad de Navarra. Pamplona, España. 57 – 59.

Camacho-Corona, M. R. Favela-Hernández, J. M. J. González-Santiago, O. Garza-González, E. Molina-Salinas, G. Ma. Said-Fernández, S. Delgado, G. Luna-Herrera, J. 2009. Evaluation of Some Plant-Derived Secondary Metabolites Against Sensitive and Multidrug-Resistant Mycobacterium Tuberculosis. *Journal of the Mexican Chemical Society* 53 (2):71–75.

Maksimenko, O. O. Vanchugova, L. V. Shipulo, E. V. Shandrynk, G. A. Bondarenko, G. N. Gel'perina, S. É. Shvets, V. I. 2010. Effects of technical parameters on the physicochemical properties of rifampicina-containing polylactide nanoparticles. *Pharmaceutical Chemistry Journal* 44 (3): 151 – 156.

Martínez Rivas, C. Ja. Tarhini, M. Badri, W. Miladi, K. Greige-Gerges, H. Nazari, Q. A. Galindo Rodríguez, S. A. Álvarez Román, R. Fessi, H. Elaissari, A. 2017. Nanoprecipitation Process: From Encapsulation to Drug Delivery. *International Journal of Pharmaceutics* 532 (1): 66–81.

Molina-Salinas, G. M., Pérez-López, A. Becerril-Montes, P. Salazar-Aranda, R. Said-Fernández, S. Waksman de Torres, N. 2007. Evaluation of the Flora of Northern Mexico for in Vitro Antimicrobial and Antituberculosis Activity. *Journal of Ethnopharmacology* 109 (3):435–41.

Organización Mundial de la Salud (OMS). 2018. Nota descriptiva [Online]. Disponible en: http://www.who.int/mediacentre/factsheets/fs104/es/

Pandey, R. Khuller. G. K. 2006. Nanotechnology Based Drug Delivery System(s) for the Management of Tuberculosis. *Indian Journal of Experimental Biology* 44 (5):357–66.

Pandey, R. Sharma, A. Zahoor, A. Sharma, S. Khuller, G. K. Prasad. **B.** 2003. Poly (DL-Lactide-Co-Glycolide) Nanoparticle-Based Inhalable Sustained Drug Delivery System for Experimental Tuberculosis. *The Journal of Antimicrobial Chemotherapy* 52 (6):981–86.

Pilheu, J. A. Loro Marchese, J. Giannattasio, J. Falasco, M. Castagnino, J. M. 2007. Tuberculosis experimental y nanopartículas de las drogas específicas. *Revista de la Asociación Médica Argentina*. 120 (3): 31–33.

Ruiz-Manzano, J. Blanquer, R. Calpe, J. L. Caminero, J. A. Caylà, J. Domínguez, J. A. García, J. M. Vidal, R. 2008. Diagnóstico y tratamiento de la tuberculosis. *Archivos de Bronconeumología* 44 (10):551–66.

Uthaman, S. Snima, K. S. Annapoorna, M. Ravindranath K. C. Shanti, V. N. Vinoth-Kumar, L. 2012. Novel Boswellic Acids Nanoparticles Induces Cell Death in Prostate Cancer Cells. *Journal of Natural Products 0974-5211*, January, 100–108.

Yao, Q. Hou, S.-X. He, W.-L. Feng, J.-L. Wang, X.-C. Fei, H.-X. Chen, Z.-H. 2006. Study on the preparation of resveratrol chitosan nanoparticles with free amino groups on

the surface. *Zhongguo Zhong Yao Za Zhi = Zhongguo Zhongyao Zazhi = China Journal of Chinese Materia Medica* 31 (3):205–8.

Yolandy, L. Boitumelo, S. Laetitia, B. Lonji, K. Lebogang, K. Arwyn T. J. Cameron, A. Makobetsa, K. Hulda, S. S. Verschoor, J. A. 2010. Targeted nanodrug delivery systems for the treatment of Tuberculosis. University of Pretoria. *Drug Discovery Today*. *15 (23-24)*: *1098.*

CHAPTER 1

Amorim, Marcelo R. Rinaldo, Daniel. do Amaral, Fabiano P. Vilegas, Wagner. Magenta, Mara A. G. Vieira Jr, Gerardo M. dos Santos, Lourdes C. 2014. HPLC-DAD Based Method for the Quantification of Flavonoids in the Hydroethanolic Extract of Tonina Fluviatilis Aubl. (Eriocaulaceae) and Their Radical Scavenging Activity. *Química Nova* 37 (7):1122–27.

Avijgan, M. Mahboubi, M. Moheb Nasab, M. Ahmadi Nia, E. Yousefi, H. 2014. Synergistic Activity between Echinophora Platyloba DC Ethanolic Extract and Azole Drugs against Clinical Isolates of Candida Albicans from Women Suffering Chronic Recurrent Vaginitis. *Journal De Mycologie Medicale* 24 (2):112–16.

Booysen, L. L., Kalombo, L. Brooks, E. Hansen, R. Gilliland, J. Gruppo, V. Lungenhofer, P. Semete-Makokotlela, B. Swai, H. S. Kotze, A. F. Lenaerts, A. du Plessis, L. H. 2013. In Vivo/in Vitro Pharmacokinetic and Pharmacodynamic Study of Spray-Dried Poly-(Dl-Lactic-Co-Glycolic) Acid Nanoparticles Encapsulating Rifampicin and Isoniazid. *International Journal of Pharmaceutics* 444 (1–2):10–17.

Camacho-Corona, M. del R. Favela-Hernández, J.M. de J. González-Santiago, O. Garza-González, E. Molina-Salinas, G.M. Said-Fernández, S. Delgado, G. Luna-Herrera, J. 2009. Evaluation of Some Plant-derived Secondary Metabolites Against

Sensitive and Multidrug-resistant Mycobacterium tuberculosis. *Journal of the Mexican Chemical Society* 53: 71–75.

Dalpiaz, Alessandro. Sacchetti, Francesca. Baldisserotto, Anna. Pavan, Barbara. Maretti, Eleonora. Iannuccelli, Valentina. Leo, Eliana. 2016. Application of the 'in-Oil Nanoprecipitation' Method in the Encapsulation of Hydrophilic Drugs in PLGA Nanoparticles. *Journal of Drug Delivery Science and Technology*, Drug Delivery Research in Italy, 32, Part B:283–90.

Darvishi, Behrad. Manoochehri, Saeed. Kamalinia, Golnaz. Samadi, Nasrin. Amini, Mohsen. Mostafavi, Seyyed Hossein. Maghazei, Shahab. Atyabi, Fatemeh. Dinarvand, Rassoul. 2015. Preparation and Antibacterial Activity Evaluation of 18-β-Glycyrrhetinic Acid Loaded PLGA Nanoparticles. *Iranian Journal of Pharmaceutical Research* 14 (2): 373–83.

do Nascimento T. G. da Silva P. F. Azevedo L. F. da Rocha L. G. de Moraes Porto I. C. Lima E Moura T. F. Basílio-Júnior I. D. Grillo L. A. Dornelas C. B. Fonseca E. J. de Jesus Oliveira E. Zhang A. T. Watson D. G. 2016. Polymeric Nanoparticles of Brazilian Red Propolis Extract: Preparation, Characterization, Antioxidant and Leishmanicidal Activity. *Nanoscale Research Letters* 11 (1):301.

Fessi, H. Puisieux, F. Devissaguet, J. P. Ammoury, N. Benita, S. 1989. Nanocapsule formation by interfacial polymer deposition following solvent displacement. *International Journal of Pharmacetics* 55, R1–R4.

Fischer, Dagmar. Li, Youxin. Ahlemeyer, Barbara. Krieglstein, Josef. Kissel, Thomas. 2003. *In vitro* Cytotoxicity Testing of Polycations: Influence of Polymer Structure on Cell Viability and Hemolysis. *Biomaterials* 24 (7): 1121–31.

Gemechu, A. Giday, M. Worku, A. Ameni, G. 2013. In vitro Anti-mycobacterial activity of selected medicinal plants against Mycobacterium tuberculosis and Mycobacterium bovis Strains. *BMC Complementary and Alternative Medicine* 13, 291.

Glass, B. D. Agatonovic-Kustrin, S. Chen, Y.-J. Wisch, M. H. 2007. Optimization of a Stability-Indicating HPLC Method for the Simultaneous Determination of Rifampicin, Isoniazid, and Pyrazinamide in a Fixed-Dose Combination Using Artificial Neural Networks. *Journal of Chromatographic Science* 45 (1):38–44.

He, Xiaoye. Li, Jianke. Zhao, Wei. Liu, Run. Zhang, Lin. Kong, Xianghong. 2015. Chemical Fingerprint Analysis for Quality Control and Identification of Ziyang Green Tea by HPLC. *Food Chemistry* 171 (March): 405–11.

Honary, Soheyla. Zahir, Foruhe. 2013. Effect of Zeta Potential on the Properties of Nano-Drug Delivery Systems - A Review (Part 2). *Tropical Journal of Pharmaceutical Research* 12 (2): 265 – 273.

Huie, C.W. 2002. A review of modern sample-preparation techniques for the extraction and analysis of medicinal plants. *Analytical and Bioanalytical Chemistry* 373: 23–30.

International Coference on Harmonisation. ICH-Guidelines Q2(R1), Validation of Analytical Procedures: Text and Methodology [Online]. Disponible en: http://www.ich.org/fileadmin/Public_Web_Site/ICH_Products/Guidelines/Quality/Q2_R1/Step4/Q2_R1__Guideline.pdf

Jain, Narendra K. Mishra, Vijay. Mehra, Neelesh Kumar. 2013. Targeted Drug Delivery to Macrophages. *Expert Opinion on Drug Delivery* 10 (3): 353–67.

Kahaliw, W. Aseffa, A. Abebe, M. Teferi, M. Engidawork, E. 2017. Evaluation of the antimycobacterial activity of crude extracts and solvent fractions of selected Ethiopian medicinal plants. *BMC Complementary and Alternative Medicine* 17.

Kim, Jung-Hoon. Seo, Chang-Seob. Kim, Seong-Sil. Shin, Hyeun-Kyoo. 2015. "Quality Assessment of Ojeok-San, a Traditional Herbal Formula, Using High-Performance Liquid Chromatography Combined with Chemometric Analysis." *Journal of Analytical Methods in Chemistry* 2015 (October): e607252.

Liang, Y.-Z. Xie, P. Chan, K. 2004. Quality control of herbal medicines. *Journal of Chromatography B* 812, 53–70.

Maksimenko, O. O. Vanchugova, L. V. Shipulo, E. V. Shandrynk, G. A. Bondarenko, G. N. Gel'perina, S. É. Shvets, V. I. 2010. Effects of technical parameters on the physicochemical properties of rifampicina-containing polylactide nanoparticles. *Pharmaceutical Chemistry Journal* 44 (3): 151 – 156.

Martínez-Rivas, Claudia Janeth. Álvarez-Román, Rocío. Rivas-Morales, Catalina. Elaissari, Abdelhamid. Fessi, Hatem. Galindo-Rodríguez, Sergio Arturo. 2017. Quantitative Aspect of Leucophyllum Frutescens Fraction before and after Encapsulation in Polymeric Nanoparticles. *Journal of Analytical Methods in Chemistry* 2017.

Molina-Salinas, G. M., Pérez-López, A. Becerril-Montes, P. Salazar-Aranda, R. Said-Fernández, S. Waksman de Torres, N. 2007. Evaluation of the Flora of Northern Mexico for in Vitro Antimicrobial and Antituberculosis Activity. *Journal of Ethnopharmacology* 109 (3):435–41.

Moreno-Exebio, Luis. Grande-Ortiz, Miguel. 2014. Validación de Un Método de Cromatografía Líquida Para La Determinación de Rifampicina En Plasma Humano. *Revista Peruana de Medicina Experimental Y Salud Publica* 31 (1):56–61.

Mura, Simona. Hillaireau, Herve. Nicolas, Julien. Le Droumaguet, Benjamin. Gueutin, Claire. Zanna, Sandrine. Tsapis, Nicolas. Fattal, Elias. 2011. Influence of Surface Charge on the Potential Toxicity of PLGA Nanoparticles towards Calu-3 Cells. *International Journal of Nanomedicine* 6: 2591–2605.

Nahar, Manoj. Jain, Narendra K. 2009. Preparation, Characterization and Evaluation of Targeting Potential of Amphotericin B-Loaded Engineered PLGA Nanoparticles. *Pharmaceutical Research* 26 (12): 2588–98.

Nasiruddin, Mohammad. Neyaz, Md. Kausar. Das, Shilpi. 2017. Nanotechnology-Based Approach in Tuberculosis Treatment. *Tuberculosis Research and Treatment* 2017.

Nicolete, Roberto. dos Santos, Daiane F. Faccioli, Lúcia H. 2011. The Uptake of PLGA Micro or Nanoparticles by Macrophages Provokes Distinct *in vitro* Inflammatory Response. *International Immunopharmacology*, The role of Toll-like receptors in diseases, 11 (10): 1557–63.

Nguta, J. M. Appiah-Opong, R. Nyarko, A. K. Yeboah-Manu, D. Addo, P. G. A. Otchere, I. Kissi-Twum, A. 2016. Antimycobacterial and cytotoxic activity of selected medicinal plant extracts. J. Ethnopharmacol. 182, 10 – 5.

Nguyen Hoai, N. Dejaegher, B. Tistaert, C. Nguyen Thi Hong, V. Rivière, C. Chataigné, G. Phan Van, K. Chau Van, M. Quetin-Leclercq, J. Vander Heyden, Y. 2009. Development of HPLC fingerprints for Mallotus species extracts and evaluation of the peaks responsible for their antioxidant activity. *Journal of Pharmaceutical and Biomedical Analysis* 50, 753–63.

Norma Oficial Mexicana NOM-006-SSA2-1993 para la Prevención y Control de la Tuberculosis en la Atención Primaria a la Salud (1994).

NORMA UNE-EN ISO 10993-4:2009. Evaluación biológica de productos sanitarios. Parte 4: Selección de los ensayos para las interacciones con la sangre. (ISO 10993-4:2002, incluyendo Amd 1:2006).

Organización Mundial de la Salud (OMS). 2018. Nota descriptiva [Online]. Disponible en: http://www.who.int/mediacentre/factsheets/fs104/es/

Pandey, Rajesh. Khuller. G. K. 2006. Nanotechnology Based Drug Delivery System(s) for the Management of Tuberculosis. *Indian Journal of Experimental Biology* 44 (5):357–66.

Soares Melecchi, M. I. Péres, V. F. Dariva, C. Zini, C. A. Abad, F. C. Martinez, M. M. Caramão, E. B. 2006. Optimization of the sonication extraction method of Hibiscus tiliaceus L. flowers. *Ultrasonics Sonochemistry* 13, 242–50.

Sultana, B. Anwar, F. Ashraf, M. 2009. Effect of extraction solvent/technique on the antioxidant activity of selected medicinal plant extracts. *Molecules* 14, 2167–80.

Vega Menchaca, Maria del Carmen. Rivas Morales, Catalina. Verde Star, Julia. Oranday Cardenas, Azucena. Rubio Morales, Maria Eufemia. Nuñez Gonzalez, Maria Adriana. Serrano Gallardo, Luis Benjamin. 2013. Antimicrobial Activity of Five Plants from Northern Mexico on Medically Important Bacteria. *African Journal of Microbiology Research* 7 (43):5011–17.

Wiśniewska, M. Bogatyrov, V. Ostolska, I. Szewczuk-Karpisz, K. Terpiłowski, K. Nosal-Wiercińska, A. 2016. "Impact of Poly(vinyl Alcohol) Adsorption on the Surface Characteristics of Mixed Oxide Mn_xO_y–SiO_2. *Adsorption* 22 (4–6): 417–23.

Xie, Ying. Jiang, Zhi-Hong. Zhou, Hua. Cai, Xiong. Wong, Yuen-Fan. Liu, Zhong-Qiu. Bian, Zhao-Xiang. Xu, Hong-Xi. Liu, Liang. 2007. Combinative Method Using HPLC Quantitative and Qualitative Analyses for Quality Consistency Assessment of a Herbal Medicinal Preparation. *Journal of Pharmaceutical and Biomedical Analysis* 43 (1): 204–12.

Yang, Seung-Ok. Lee, Sang Won. Kim, Young Ock. Sohn, Sang-Hyun. Kim, Young Chang. Hyun, Dong Yoon. Hong, Yoon Pyo. Shin, Yu Su. 2013. HPLC-Based Metabolic Profiling and Quality Control of Leaves of Different Panax Species. *Journal of Ginseng Research* 37 (2): 248–53.

Yoo, Jin-Wook. Giri, Namita. Lee, Chi H. 2011. pH-Sensitive Eudragit Nanoparticles for Mucosal Drug Delivery. *International Journal of Pharmaceutics* 403 (1–2):262–67.

CHAPTER 2

Abajo, C. Boffill, M. A. del Campo, J. Méndez, M. A. González, Y. Mitjans, M. Vinardell M. P. 2004. *In vitro* Study of the Antioxidant and Immunomodulatory Activity of Aqueous Infusion of Bidens Pilosa. *Journal of Ethnopharmacology* 93 (2): 319–23.

Alanís-Garza, B. Salazar-Aranda, R. Ramírez-Durón, R. Garza-González, E. Waksman de Torres, N. 2012. A New Antimycobacterial Furanolignan from *Leucophyllum Frutescens*. *Natural Product Communications* 7 (5):597–98.

An, S. Park, H.-S. Kim, G.-H. 2014. Evaluation of the Antioxidant Activity of Cooked Gomchwi (Ligularia Fischeri) Using the Myoglobin Methods. *Preventive Nutrition and Food Science* 19 (1): 34–39.

Assunção, P. I. D. da Conceição, E. C. Borges, L. L. de Paula, J. A. M. 2017. Development and Validation of a HPLC-UV Method for the Evaluation of Ellagic Acid in Liquid Extracts of *Eugenia uniflora* L. (Myrtaceae) Leaves and Its Ultrasound-Assisted Extraction Optimization. *Evidence-Based Complementary and Alternative Medicine: eCAM* 2017.

Bian, Q. Yang, H. Chan, C.-O. Jin, D. Mok, D. K.-W., Chen, S. 2013. "Fingerprint Analysis and Simultaneous Determination of Phenolic Compounds in Extracts of

Curculiginis rhizoma by HPLC-Diode Array Detector." *Chemical & Pharmaceutical Bulletin* 61 (8): 802–8.

Christofoli, M. Candida Costa, E. C. Bicalho, K. U. de Cássia Domingues, V. Fernandes Peixoto, M. Fernandes Alves, C. C. Araújo, W. L. de Melo Cazal, C. 2015. Insecticidal Effect of Nanoencapsulated Essential Oils from *Zanthoxylum rhoifolium* (Rutaceae) in *Bemisia tabaci* Populations. *Industrial Crops & Products* Complete (70): 301–8.

Fessi, H. Puisieux, F. Devissaguet, J. P. Ammoury, N. Benita, S. 1989. Nanocapsule formation by interfacial polymer deposition following solvent displacement. *International Journal of Pharmacetics* 55, R1–R4.

International Coference on Harmonisation. ICH-Guidelines Q2(R1), Validation of Analytical Procedures: Text and Methodology [Online]. Disponible en: http://www.ich.org/fileadmin/Public_Web_Site/ICH_Products/Guidelines/Quality/Q2_R1/Step4/Q2_R1__Guideline.pdf

Jiang, R.-W. Lau, K.-M. Lam, H.-M. Yam, W.-S. Leung, L.-K. Choi, K.-L. Waye, M. M. Y. Mak, T. C. W. Woo, K.-S. Fung, K.-P. 2005. A comparative study on aqueous root extracts of *Pueraria thomsonii* and *Pueraria lobata* by antioxidant assay and HPLC fingerprint analysis. *Journal of Ethnopharmacol*ogy 96(1): 133–138.

Karimi, G. Aghasizadeh, M. Razavi, M. Taghiabadi, E. 2011. Protective Effects of Aqueous and Ethanolic Extracts of *Nigella sativa* L. and *Portulaca oleracea* L. on Free Radical Induced Hemolysis of RBCs. *DARU: Journal of Faculty of Pharmacy, Tehran University of Medical Sciences* 19 (4): 295–300.

Lobo, V. Patil, A. Phatak, A. Chandra, N. 2010. Free Radicals, Antioxidants and Functional Foods: Impact on Human Health. *Pharmacognosy Reviews* 4 (8): 118–26.

Mahapatro, A. Singh, D. K. 2011. Biodegradable Nanoparticles Are Excellent Vehicle for Site Directed *in-vivo* Delivery of Drugs and Vaccines. *Journal of Nanobiotechnology* 9 (November): 55.

Molina-Salinas, G. M., Pérez-López, A. Becerril-Montes, P. Salazar-Aranda, R. Said-Fernández, S. Waksman de Torres, N. 2007. Evaluation of the Flora of Northern Mexico for in Vitro Antimicrobial and Antituberculosis Activity. *Journal of Ethnopharmacology* 109 (3):435–41.

Molina-Salinas, G. M. Rivas-Galindo, V. M. Said-Fernández, S. Lankin, D. C. Muñoz, M. A. Joseph-Nathan, P. Pauli, G. F. Waksman, N. 2011. Stereochemical Analysis of Leubethanol, an Anti-TB-Active Serrulatane, from Leucophyllum Frutescens. *Journal of Natural Products* 74 (9):1842–50.

NORMA UNE-EN ISO 10993-4:2009. Evaluación biológica de productos sanitarios. Parte 4: Selección de los ensayos para las interacciones con la sangre. (ISO 10993-4:2002, incluyendo Amd 1:2006).

Özkan, G. Özcan, M. M. 2017. Antioxidant Activity of Some Medicinal Plant Extracts on Oxidation of Olive Oil. *Journal of Food Measurement and Characterization* 11 (2): 812–17.

Paiva-Martins, F. Gonçalves, P. Borges, J. E. Przybylska, D. Ibba, F. Fernandes, J. Santos-Silva A. 2015. Effects of the Olive Oil Phenol Metabolite 3,4-DHPEA-EDAH2 on Human Erythrocyte Oxidative Damage. *Food & Function* 6 (7): 2350–56.

Saeed, N. Khan, M. R. Shabbir, M. 2012. Antioxidant Activity, Total Phenolic and Total Flavonoid Contents of Whole Plant Extracts Torilis Leptophylla L. *BMC Complementary and Alternative Medicine* 12 (November): 221.

Sanna, V. Lubinu, G. Madau, P. Pala, N. Nurra, S. Mariani, A. Sechi, M. 2015. Polymeric Nanoparticles Encapsulating White Tea Extract for Nutraceutical Application. *Journal of Agricultural and Food Chemistry* 63 (7): 2026–32.

Wani, M. C. Taylor, H. L. Wall, M. E. Coggon, P. McPhail, A. T. 1971. Plant Antitumor Agents. VI. Isolation and Structure of Taxol, a Novel Antileukemic and Antitumor Agent from Taxus Brevifolia. *Journal of the American Chemical Society* 93 (9): 2325–27.

Zaragoza, O.Z. 2009. Guía de Árboles y Otras Plantas Nativas en la Zona Metropolitana de Monterrey. Fondo Editorial de NL.

CHAPTER 3

Ahmed, M. Ramadan, W. Rambhu, D. Shakeel, F. 2008. Potential of Nanoemulsions for Intravenous Delivery of Rifampicin. *Die Pharmazie* 63 (11): 806–11.

Alanís-Garza, B. Salazar-Aranda, R. Ramírez-Durón, R. Garza-González, E. Waksman de Torres, N. 2012. A New Antimycobacterial Furanolignan from *Leucophyllum Frutescens*. *Natural Product Communications* 7 (5):597–98.

Araújo, F. A. Kelmann, R. G. Araújo, B. V. Finatto, R. B. Teixeira, H. F. Koester, L. S. 2011. Development and Characterization of Parenteral Nanoemulsions Containing Thalidomide. *European Journal of Pharmaceutical Sciences: Official Journal of the European Federation for Pharmaceutical Sciences* 42 (3): 238–45.

Blanco-Padilla, A. Soto, K. M. Hernández Iturriaga, M. Mendoza, S. 2014. Food Antimicrobials Nanocarriers. *The Scientific World Journal*. 2014.

Choi, W. H. 2016. Evaluation of Anti-Tubercular Activity of Linolenic Acid and Conjugated-Linoleic Acid as Effective Inhibitors against *Mycobacterium tuberculosis*. *Asian Pacific Journal of Tropical Medicine* 9 (2): 125–29.

DeRuiter, J. 2005. Carboxylic Acid Structure and Chemistry: Part 2, in: Principles of Drug Action 1.

Devalapally, H. Silchenko, S. Zhou, F. McDade, J. Goloverda, G. Owen, A. Hidalgo, I.J. 2013. Evaluation of a Nanoemulsion Formulation Strategy for Oral Bioavailability Enhancement of Danazol in Rats and Dogs. *Journal of Pharmaceutical Sciences* 102 (10): 3808–15.

Donsì, F. Annunziata, M. Vincensi, M. Ferrari, G. 2012. "Design of Nanoemulsion-Based Delivery Systems of Natural Antimicrobials: Effect of the Emulsifier." *Journal of Biotechnology* 159 (4): 342–50.

Du, Z. Wang, C. Tai, X. Wang, G. Liu, X. 2016. Optimization and Characterization of Biocompatible Oil-in-Water Nanoemulsion for Pesticide Delivery. February 23, 2016.

Ghosh, V. Saranya, S. Mukherjee, A. Chandrasekaran, N. 2013. Cinnamon Oil Nanoemulsion Formulation by Ultrasonic Emulsification: Investigation of Its Bactericidal Activity. *Journal of Nanoscience and Nanotechnology* 13 (1): 114–22.

Gupta, A. Eral, H.B. Hatton, T.A. Doyle, P.S. 2016. Nanoemulsions: Formation, Properties and Applications. *Soft Matter* 12 (11): 2826–41.

Ha, T. V. A. Kim, S. Choi, Y. Kwak, H.-S. Lee, S. J. Wen, J. Oey, I. Ko, S. 2015. Antioxidant Activity and Bioaccessibility of Size-Different Nanoemulsions for Lycopene-Enriched Tomato Extract. *Food Chemistry* 178 (July): 115–21.

Hedgecock, L. W. 1970. Complexing of Fatty Acids by Triton WR1339 in Relation to Growth of *Mycobacterium tuberculosis*. *Journal of Bacteriology* 103 (2): 520–22

Hussain, A. Samad, A. Singh, S. K. Ahsan, M. N. Haque, M. W. Faruk, A. Ahmed, F. J. 2016. Nanoemulsion Gel-Based Topical Delivery of an Antifungal Drug: In Vitro Activity and in Vivo Evaluation. *Drug Delivery* 23 (2): 642–47.

Jaiswal, M. Dudhe, R. Sharma, P. K. 2015. "Nanoemulsion: An Advanced Mode of Drug Delivery System." *3 Biotech* 5 (2): 123–27.

Koroleva, M. Y. Yurtov, E. V. 2012. Nanoemulsions: The Properties, Methods of Preparation and Promising Applications. *Russian Chemical Reviews* 81 (1): 21.

Kumar, M. Misra, A. Babbar, A. K. Mishra, A. K. Mishra, P. Pathak, K. 2008. Intranasal Nanoemulsion Based Brain Targeting Drug Delivery System of Risperidone. *International Journal of Pharmaceutics* 358 (1–2): 285–91.

Laouini, A. Fessi, H. Charcosset, C. 2012. Membrane Emulsification: A Promising Alternative for Vitamin E Encapsulation within Nano-Emulsion. *Journal of Membrane Science* 423–424 (December): 85–96.

Manoharan, C. Basarkar, A. Singh, J. 2010. Various Pharmaceutical Disperse Systems, in: Kulshreshtha, A.K., Singh, O.N., Wall, G.M. (Eds.), Pharmaceutical Suspensions. Springer New York, pp. 1–37.

Mantena, A. D., Dontamsetti, B. R., Nerella, A. 2015. Formulation, Optimization and *in vitro* Evaluation of Rifampicin Nanoemulsions. International Journal of Pharmaceutical Sciences and Drug Research 7(6): 451–455.

Molina-Salinas, G. M., Pérez-López, A. Becerril-Montes, P. Salazar-Aranda, R. Said-Fernández, S. Waksman de Torres, N. 2007. Evaluation of the Flora of Northern

Mexico for in Vitro Antimicrobial and Antituberculosis Activity. *Journal of Ethnopharmacology* 109 (3):435–41.

Molina-Salinas, G. M. Rivas-Galindo, V. M. Said-Fernández, S. Lankin, D. C. Muñoz, M. A. Joseph-Nathan, P. Pauli, G. F. Waksman, N. 2011. Stereochemical Analysis of Leubethanol, an Anti-TB-Active Serrulatane, from Leucophyllum Frutescens. *Journal of Natural Products* 74 (9):1842–50.

Pubchem. Oleic acid | C18H34O2 – PubChem [Online]. Disponible en: https: //pubchem. ncbi.nlm.nih.gov/ compound/oleic_acid

Tsai, Y.-J. Chen, B.-H. 2016. "Preparation of Catechin Extracts and Nanoemulsions from Green Tea Leaf Waste and Their Inhibition Effect on Prostate Cancer Cell PC-3." *International Journal of Nanomedicine* 11: 1907–26.

APPENDIX 1
PUBLICATIONS

International Journal of Pharmaceutics 532 (2017) 66–81

Contents lists available at ScienceDirect

International Journal of Pharmaceutics

journal homepage: www.elsevier.com/locate/ijpharm

Review

Nanoprecipitation process: From encapsulation to drug delivery

Claudia Janeth Martínez Rivas[a,d], Mohamad Tarhini[a,b], Waisudin Badri[a,c], Karim Miladi[a], Hélène Greige-Gerges[b], Qand Agha Nazari[c], Sergio Arturo Galindo Rodríguez[d], Rocío Álvarez Román[d], Hatem Fessi[a], Abdelhamid Elaissari[a,*]

[a] University of Lyon, University Claude Bernard Lyon-1, CNRS, LAGEP UMR 5007, 43 boulevard du 11 novembre 1918, F-69100, Villeurbanne, France
[b] Lebanese University, Faculty of Sciences, B.P 906564, Jdaidet El-Matn, Lebanon
[c] Kabul University, Faculty of Pharmacy, Kabul, Afghanistan
[d] Universidad Autónoma de Nuevo León, Facultad de Ciencias Biológicas, Laboratorio de Química Analítica, Av. Pedro de Alba s/n, C.P. 66455, San Nicolás de los Garza, Nuevo León, Mexico

ARTICLE INFO

Article history:
Received 28 April 2017
Received in revised form 3 August 2017
Accepted 5 August 2017
Available online 9 August 2017

Keywords:
Nanoprecipitation
Encapsulation
Polymer
Drug delivery
In vitro
In vivo
Scale-up

ABSTRACT

Drugs encapsulation is a suitable strategy in order to cope with the limitations of conventional dosage forms such as unsuitable bioavailability, stability, taste, and odor. Nanoprecipitation technique has been used in the pharmaceutical and agricultural research as clean alternative for other drug carrier formulations. This technique is based on precipitation mechanism. Polymer precipitation occurs after the addition of a non-solvent to a polymer solution in four steps mechanism: supersaturation, nucleation, growth by condensation, and growth by coagulation that leads to the formation of polymer nanoparticles or aggregates. The scale-up of laboratory-based nanoprecipitation method shows a good reproducibility. In addition, flash nanoprecipitation is a good strategy for industrial scale production of nanoparticles. Nanoprecipitation is usually used for encapsulation of hydrophobic or hydrophilic compounds. Nanoprecipitation was also shown to be a good alternative for the encapsulation of natural compounds. As a whole, process and formulation related parameters in nanoprecipitation technique have critical effect on nanoparticles characteristics. Biodegradable or non-biodegradable polymers have been used for the preparation of nanoparticles intended to *in vivo* studies. Literature studies have demonstrated the biodistribution of the active loaded nanoparticles in different organs after administration *via* various routes. In general, *in vitro* drug release from nanoparticles prepared by nanoprecipitation includes two phases: a first phase of "burst release" which is followed by a second phase of prolonged release. Moreover, many encapsulated active molecules have been commercialized in the pharmaceutical market.

Contents

* Corresponding author.
E-mail addresses: abdelhamid.elaissari@univ-lyon1.fr, elaissari@lagep.univ-lyon1.fr (A. Elaissari).

http://dx.doi.org/10.1016/j.ijpharm.2017.08.064
0378-5173/

1. Introduction

Conventional drug delivery systems like tablets, capsules, solutions *etc.* are still the most used ways for medicines administration. Such formulations present many advantages such as, full control of preparation processes, common availability of manufacturing facilities and efficacy. Furthermore, major advances have been made to enhance drugs solubility and sustained release. Various excipients could be added to improve drugs properties and biodistribution. These advances enabled widening of used arsenal against diseases. However, in most cases, *in vivo* activity of conventional dosage forms remains limited to drug physicochemical properties. Consequently, stability, taste and absorption concerns are still observed. In addition, targeting specific tissue or cells could not be reached. For these reasons, encapsulation appeared as an interesting approach for drug delivery. In fact, major advances have been made, since the last decades, toward preparation of drug delivery systems that are based on entrapment of actives in various structures. Several techniques have also been used for encapsulation such as, emulsion solvent evaporation, nanoprecipitation, emulsion solvent diffusion, ethanol injection, ionic gelation *etc.* Major pharmaceutical forms prepared *via* these techniques are nanospheres, nanocapsules, microspheres, microcapsules and liposomes. Among these techniques, nanoprecipitation seems to be the most simple and reproducible. This made it one of the most commonly used approaches for the nanoparticles preparation. Several polymers are used to encapsulate drugs with nanoprecipitation. Among them, we could cite biodegradable polyesters such as, polylactide (PLA), polylactide-co-glycolide (PLGA) and poly-ε-caprolactone (PCL). Obtained particles could be either nanocapsules or nanospheres. Nanocapsules are vesicles with core-shell structure in which the drug is confined within a cavity surrounded by a polymeric membrane. Nanospheres are, however, particles in which the drug is either dissolved or dispersed within the polymer matrix (Mora-Huertas et al., 2010; Letchford and Burt, 2007). Nanoprecipitation is based on the interfacial deposition of a polymer following the displacement of a semi-polar solvent miscible with water from a lipophilic solution (Fessi et al., 1989). It is an easy and reproducible technique that has been widely used in the preparation of nanoparticles. In this review, the state of the art of this technique is performed. Definition of the method is provided. Nanoprecipitation mechanism and applications are also discussed.

2. Encapsulation of active pharmaceutical ingredients

Encapsulation has been broadly explored in the fields of pharmaceuticals, agriculture, food, cosmetics, and textile industries over the past decade (Ghosh, 2006). Modern technologies recently paved the way to the evolution of indigenous pharmaceuticals. Therefore, advanced drug deliveries are successively taking the place of conventional dosage forms that were less flexible and less sophisticated. The fact of overcoming these conventional dosage forms constraints attracted a special attention. Bioavailability, stability, taste, and odor could be among the aforementioned barriers. In this regard, encapsulation takes a crucial part in order to overwhelm these challenges (Iqbal et al., 2015). According to the biopharmaceutical classification system (BCS), 40% of the currently commercialized drug molecules on the market are poorly soluble while 90% of drug molecules in drug development pipeline are also categorized as poorly soluble (Loftsson and Brewster, 2010). In addition, drugs encapsulation could play an important role in prevention of active ingredients from degradation and obtaining of controlled or targeted drug release systems. In fact, following active molecule encapsulation, biodistribution would no longer be related to drug itself but to carriers physicochemical properties (Armendáriz-Barragán et al., 2016). Drug encapsulation as the best approach through the employing of biodegradable polymers may provide the biocompatible, easily administered, safe, comfortable and inert drug delivery system. Indeed, delivery system possessing such properties could be defined as an ideal drug delivery system (Kalani and Yunus, 2011). The adequate encapsulation method should be selected based on the hydrophobic or hydrophilic properties of

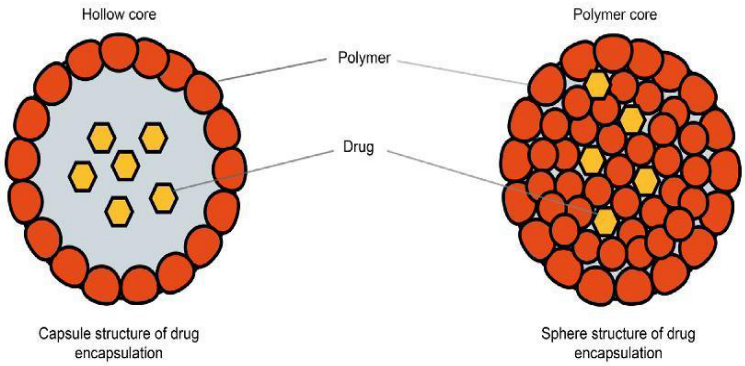

Fig. 1. Schematic representation of encapsulation forms.

drugs (Jelvehgari and Montazam, 2012). Fig. 1 shows examples of structures that could be obtained by encapsulation.

To resume, drugs encapsulation might be used for several reasons such as:

- Drug release prolongation,
- Design of targeted drug delivery,
- Mask unfavorable organoleptic properties (taste, odor, color),
- Protection of sensitive drugs from digestive tube contents degradation effect,
- Insurance of drug molecules stability toward environmental destructive factors such as, oxygen, temperature, moisture and light,
- Reducing the vaporization of volatile materials,
- Prevention of drugs incompatibility,
- Toxicity moderation,
- Hygroscopic characteristic decline of substances,
- Design of new dosage forms, (Singh et al., 2010)

3. Encapsulation based marketed products

The main aim of nanotherapeutics research and development in the pharmaceutical industry is to provide new approaches for the treatment of diseases. Some encapsulation based drug delivery systems are already marketed (see Table 1). Nevertheless, nanotherapeutics commercialization faces major challenges and hurdles such as: (a) deficit of quality control; (b) separation from unwanted nanostructures (*e.g.*, products and starting materials); (c) scalability related issues; (d) improvement of production scale; (e) batch to batch reproducibility in terms of particles distribution of size, charge, porosity, and mass; (f) high manufacturing price; (g) information shortage concerning nanosystems and living cell interaction (*e.g.*, biocompatibility and toxicity); (h) therapeutic capacity optimization of nanotherapeutics; (i) investment doubt by pharmaceutical industries on nanotherapeutics. (j) regular targeting of negative features of nanomaterials by media, in absence of clear scientific proof (Hafner et al., 2014).

4. Nanoprecipitation

Nanoprecipitation was patented by Fessi et al. in 1989 (Fessi et al., 1989). After its development, it was mostly employed for encapsulation of hydrophobic drug molecules (nanocapsule or nanosphere forms). To this end, several polymers, notably, biodegradable polyesters like polylactide (PLA), polylactide-co-glycolide (PLGA) and poly-ε-caprolactone (PCL), have been used (see Table 2). As reported by Fessi et al. (1989), in this method solvent and nonsolvent phases preparation is required which is followed by the addition of one phase to another under moderate magnetic stirring (See Fig. 2). Organic solvent evaporation at ambient temperature or with a rotavapor allows the obtaining of nanoparticles (NPs) suspension in water. Ultracentrifugation and freeze drying are two methods that could be employed in next step for aqueous phase removal. Basically, the solvent phase comprises a film-forming material, one or more drug molecules, a lipophilic surfactant, and one or more organic solvents. Solvent and nonsolvent phases are usually named as organic and aqueous phases, respectively. Film-forming materials could be natural, synthetic or semi-synthetic polymers. To provide nanocapsules instead of nanospheres, mineral oil or vegetable oil would be added. The NPs aggregation could be avoided by adding surfactants into the formulation (Miladi et al., 2016). Surfactants can affect NPs characteristics as well. For instance, D-α-tocopheryl polyethylene glycol 1000 succinate (TPGS) is broadly used in nanoprecipitation technique. It is recognized as an excellent emulsifier due to its bulky structure and large surface area (Zhu et al., 2016). This water-soluble derivative of a natural vitamin is also suggested as copolymer to form amphiphilic block biodegradable copolymers. Its potential to form polymeric NPs by self-ensemble effects is due to the hydrophobic-lipophilic interactions (Zeng et al., 2013). TPGS has been successfully co-ensembled to PLA (Wang et al., 2015; Zhu et al., 2016), PLGA (Tao et al., 2016, 2015) and PCL (Cao et al., 2015) for cancer treatment applications. In nanoprecipitation technique, parameters modification causes crucial change in physicochemical characteristics of NPs such as, size, drug encapsulation efficiency and so on. Process and formulation related parameters impacts are figured out in Table 3.

The most used solvents in nanoprecipitation method are ethanol, acetone, hexane, methylene chloride or dioxane. Mostly, non-solvent (or aqueous phase) is water. However, hydrophilic excipients could be also added to the nonsolvent phases. Transmission Electron Microscopy (TEM), Scanning Electron Microscopy (SEM) or dynamic light scattering (DLS) could be used in order to characterize produced particles in terms of size and surface morphology (Mora-Huertas et al., 2010; Miladi et al.,

Table 1
Examples of marketed drug delivery carriers with their composition and date of approval in EU and US (Bomgaars et al., 2004; Chang and Yeh, 2012; Mitchell, 2005; Schmidt et al., 2011; "Vincristine Liposomal—INEX," 2004; Wacker, 2013).

Encapsulated drug	Trade name	Drug carrier material	Carrier system	Administration route	Application	Approval
Leuprolide	Lupron Depot®	Poly lactic acid	Microparticles	Intramuscular	Analog of gonadotropin-releasing hormone	1989, USA
Amphotericin B	Ambisome®	Phospholipids	Liposomes	Intravenous	Visceral leishmaniasis treatment	1990, Europe 1997, USA
Doxorubicin	Doxil®	Phospholipids	Liposomes	Intravenous	Anticancer therapy	1995, USA 1996, Europe
Daunorubicin	DaunoXome®	Phospholipids	Liposomes	Intramuscular	Anticancer therapy	1996, Europe 1996, USA
Cytarabine	Depocyt®	Phospholipids	Liposomes	Intrathecal	Lymphomatous meningitis treatment	1999, USA
Doxorubicin	Myocet®	Phospholipids	Liposomes	Intravenous	Anticancer therapy	2000, Europe
Verteporfin	Visudyne®	Phospholipids	Liposomes	Intravenous	Photodynamic treatment of age-related macular degeneration	2000, USA
Morphine	DepoDUR®	Phospholipids	Liposomes	Epidural	Analgesia	2004, USA
Vincristine	Onco TCS®	Phospholipids	Liposomes	Intravenous	Anticancer therapy	2004, USA
Doxorubicin	Transdrug®	Poly-*iso*-hexyl-cyanoacrylate	Nanoparticles	Hepatic intra-arterial	Hepatocellular carcinoma treatment	2005, USA
Paclitaxel	Abraxane®	Human serum albumin	Nanoparticles	Intravenous	Anticancer therapy	2005, USA 2008, Europe

Table 2
Mostly used polymers in nanoparticles preparation by nanoprecipitation method.

Type	Group	Polymer Name (Common abbreviation)	References
Biodegradable	Polysaccharide	Starch	Qin et al. (2016)
		Chitosan	Luque-Alcaraz et al. (2016)
	Protein	Gelatin	Han et al. (2013)
		Bovine serum albumin (BSA)	Ge et al. (2012)
	Polyester	Polylactic acid (PLA)	Bazylińska et al. (2014)
		Poly ε-caprolactone (PCL)	Mazzarino et al. (2012)
		Polylactic-*co*-glycolic acid (PLGA)	Siqueira-Moura et al. (2013)
	Polyether	Polyethylene glycol (PEG)	Şimşek et al. (2013)
Non-Biodegradable	Polymethacrylate Acrylate	Eudragit®	Averina and Allémann (2013), Katara and Majumdar (2013), and Kumar et al. (2016)

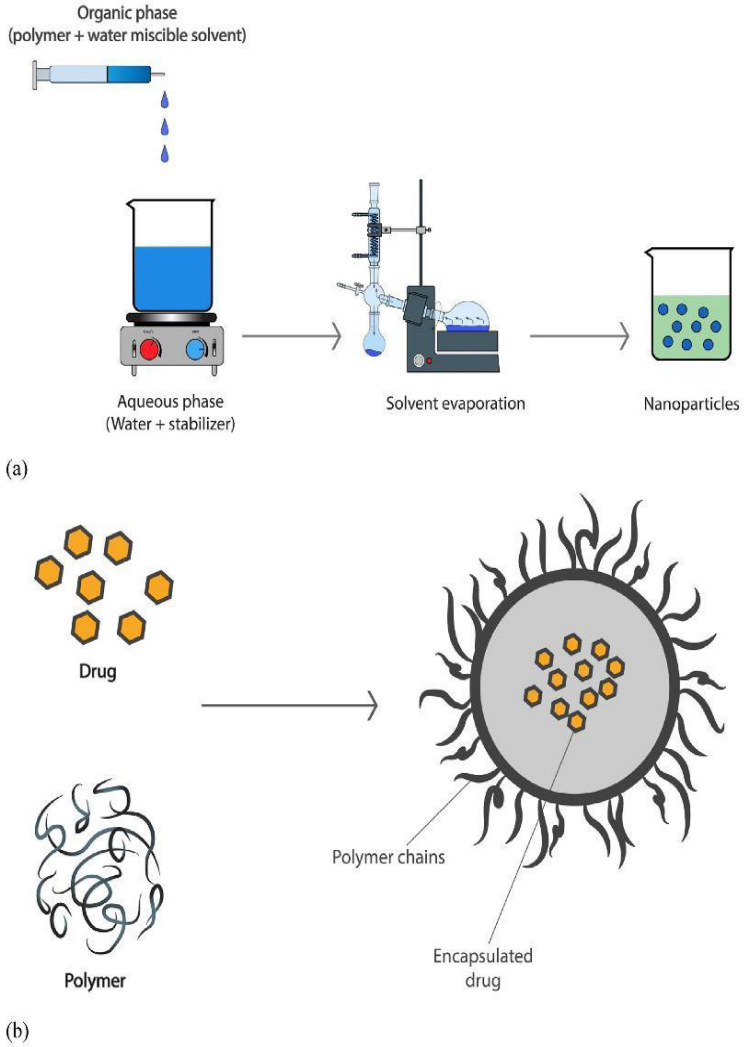

Fig. 2. (a). Nanoprecipitation schematic representation, (b). Illustration of drug encapsulation into a preformed polymer.

Table 3
Formulation and process dependent parameters effect on the characteristics of the nanoparticles (Miladi et al., 2016).

Affected Variable	Outcome	Parameter	Modification	Explanation	Reference
Size	Increases	Stirring rate	Increases	Faster diffusion rate will facilitate solvent diffusion	Asadi et al. (2011)
		Organic phase flow rate	Increases	High nucleation rates promotion that will reduce strongly the mean particle size.	Lince et al. (2008)
		Organic/ aqueous phase ratio	Volume of the aqueous phase increases	Increased diffusion of the water-soluble solvent in the aqueous phase. At a certain point, this diffusion of solvent to the aqueous phase becomes so rapid that the polymer immediately precipitates before agglomerating into particles.	Budhian et al. (2007)
	Increases, then decreases	Surfactant concentration	Increases	Prevents coalescence with each other. Increased viscosity of the aqueous phase reduces the net shear stress available for droplet breakdown	Budhian et al. (2007), Contado et al. (2013), and Zeng et al. (2013)
	Decreases	Polymer concentration	Increases	Favors particle growth with respect to particle nucleation. Higher organic solution viscosity.	Badri et al. (2017), Dong and Feng (2004), and Lince et al. (2008)
		Polymer molecular weight	Increases	Higher organic solution viscosity	Limayem Blouza et al. (2006) and Martín-Banderas et al. (2012)
Drug Encapsulation	Increases Efficiency	Polymer concentration	Increases	It is related to size, larger size higher drug entrapment	Chorny et al. (2002) and Dong and Feng (2004)
	Decreases	Organic/ aqueous phase ratio	Volume of the aqueous phases increases	Amount of drug that can dissolve in the aqueous phase increases, which increases the drug loss into the aqueous phase.	Budhian et al. (2007) and Limayem Blouza et al. (2006)
		Drug concentration	Increases	The polymer itself may have a limited capacity to encapsulate the specific amount of drug. Beyond its maximum capacity, more drug might be wasted during the fabrication process.	Dong and Feng (2004)

2016). In nanoprecipitation, many parameters modification cause crucial changes in the physical characteristics of NPs in terms of size, drug encapsulation efficiency and so on. Fig. 3 shows SEM images of NPs prepared *via* nanoprecipitation.

Another crucial measured parameter is the surface charge of NPs called zeta potential. It measures the magnitude of the electrostatic interactions. This parameter is too crucial for the stability of NPs and their behavior in a biological environment. The positive or negative zeta potential values could be determined by identifying towards which electrode particles are moving during electrophoresis. In fact, an electric field is applied and the electrophoretic mobility of the particles is measured by electrophoretic light scattering (Bhattacharjee, 2016). Loading and encapsulation efficiency are variables that are related to the quantification of the incorporated active ingredients within NPs. These parameters could be established by analytical methods such as UV–vis spectrophotometry, High Performance Liquid Chromatography or Gas Chromatography (for volatile actives *i.e.* essential oils). In addition, thermodynamic characterization of NPs could provide information about their chemical properties and it is carried out by the following methods:

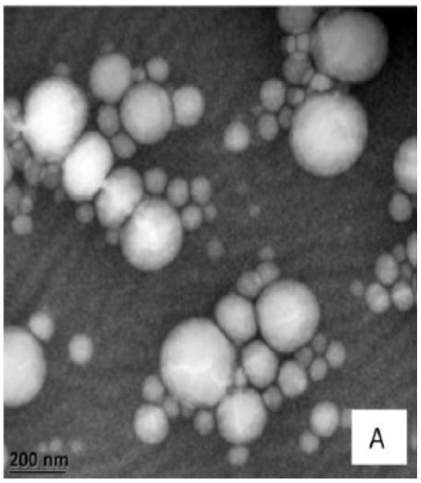

Fig. 3. TEM micrograph of typical PCL spheres prepared by solvent displacement process.
Reproduced with permission from Mora-Huertas et al. (2011).

i Thermal Gravimetric Analysis (TGA): determines endothermic and exothermic weight loss upon heating or cooling of NPs. In fact, TGA uses heat to force reactions and physical changes in materials. Thermogravimetric curves characterize specific compounds due to the unique sequence from physicochemical reactions occurring over the specific temperature ranges.
ii Differential Thermal Analysis (DTA): based on the principle that the substance upon heating undergoes reactions and phase changes that involve absorption or emission of heat. Identification of a substance is accomplished by comparing DTA curves obtained from the unknown substance with the DTA curves that are provided by known elements.
iii Differential Scanning Calorimetry (DSC): based on heat release from a chemical process, either a chemical reaction or a conformational alteration. The heat of reaction or $\Delta_r H$ is defined as the change in enthalpy associated with a chemical reaction (Singh, 2016).

Fourier Transform Infrared Spectroscopy or FT-IR is also a useful tool for the identification of drugs. It permits continuous monitoring of the spectral baseline and simultaneous analysis of different components of the same sample (Bansal et al., 2013). Molecular structure and composition of nanoparticle-forming polymers before and after nanoprecipitation could be analyzed *via* this technique (Qin et al., 2016; Wang and Tan, 2016).

5. Precipitation mechanism

Nanoprecipitation is based on the reduction of the quality of the solvent in which the main composition of NPs is dissolved. Such variation in solvent quality can be achieved by altering the pH, salt concentration, solubility conditions, or the addition of a non-solvent phase (Miladi et al., 2014). The non-solvent based precipitation process includes four steps: generation of supersaturation, nucleation, growth, and coagulation (see Fig. 4) (Joye and McClements, 2013). Supersaturation occurs when the solution contains more dissolved solute than that given by the equilibrium saturation value. In fact, the addition of non-solvent decreases solvent potency to dissolve the solute, which put the system in a supersaturation state. The supersaturation ratio (S_r) is expressed as follows:

$$S_r = \frac{C_s}{C_\infty}$$

Where C_s is the ratio of the particle solubility at the interface, and C_∞ is the bulk solubility. The supersaturation rate can affect final NPs properties where a higher supersaturation leads to a decrease in particle size.

After supersaturation, nucleation step starts in order to gain thermodynamic stability. It is induced when the supersaturation of the system reaches the boundaries of a critical level that is solvent/non-solvent specific. In other words, the energy barrier (ΔG) has to be overcome to form nuclei.

$$\Delta G = \frac{16\pi\sigma^3 v^3}{3K^2T^2(lnS_r)^2}$$

Where c is a constant, σ is the interfacial tension at the solid-liquid interface, v is the molar volume of solute, K is the Boltzmann constant, and T is the temperature (D'addio and Prud'homme, 2011).

The local fluctuations in the concentration caused by supersaturation lead to the formation of primary nuclei, which,by its turn, increases in size by the association of solute molecules until it reaches a critical size that is stable against dissolution (see Fig. 2). The nucleation step will carry on until the growth of earlier nuclei depletes the solution supersaturation. The nucleation rate (Nr) could be expressed by the following mathematical equation (D'addio and Prud'homme, 2011).

$$Nr = c.\exp\left[-\frac{16\pi\sigma^3 v^2}{3K^3T^3(lnS_r)^2}\right]$$

Nucleation stops when the solute concentration is reduced below the critical supersaturation concentration, and nuclei grow by either condensation or coagulation. Condensation is the addition of single molecules to the particle surface. It takes place in two steps: a diffusional step in which the solute is transported from the bulk fluid through the solution boundary layer adjacent to the nuclei surface, and a deposition step in which the adsorbed solute molecules are integrated into the nuclei matrix. When the non-adsorbed solute concentration is reduced below the equilibrium saturation concentration, condensation stops. The rate of condensation is decreased by coagulation (D'addio and Prud'homme, 2011).

On the other hand, coagulation is the adhesion of particles to each other's. It occurs when the attractive interactions (Van Der Waals, hydrophobic interactions, *etc.*) are stronger than the repulsive interactions (steric or electrostatic repulsion) (see Fig. 4). The factor that rules the coagulation step is the collision frequency, which depends on particle concentration, size, and motion. The number of collisions that leads to coagulation is called collision efficiency and depends on the attractive and repulsive ratio of interaction between particles. To protect particles from coagulation, stabilizing agents can be added during the preparation. Such agents could adsorb to NPs surface and introduce a repulsive interaction (Joye and McClements, 2013).

In addition to the precipitation with a non-solvent, pH-controlled precipitation is also an important approach to be discussed. In this method, the polymer switches from dissolved to

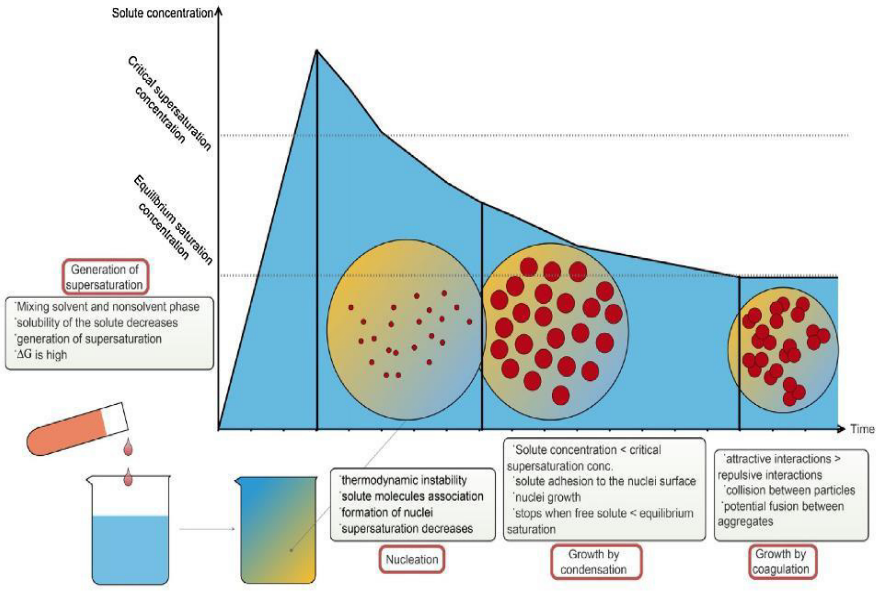

Fig. 4. Schematic illustration of non-solvent precipitation process.

non-dissolved phase by a simple pH variation in the medium. This will lead to the precipitation and formation of NPs (Pereira et al., 2006). Das et al. prepared Eudragit® RL100 based NPs using this method. Polymer was dissolved in organic phase of acetone and methanol, and the pH was adjusted to 4. The solution was later added to water where the precipitation occurs. Results showed that NPs were successfully prepared *via* pH-nanoprecipitation. In addition, due to unique particle size and positive zeta potential, particles have a good ocular retention property and a storage stability for 2 months (Das et al., 2010).

In another study, dexamethasone-loaded Eudragit® L100 based NPs were prepared by nanoprecipitation. Polymer was dissolved in organic phase of acetone and ethanol. In this case, aqueous phase pH was adjusted to 4. Obtained NPs showed no cytotoxic or oxidative stress on normal human keratinocytes. These results suggest that these particles are good candidates for the delivery of poorly soluble drugs to the skin (Sahle et al., 2017).

6. *In vitro* release profile

In vitro drug release from NPs prepared by nanoprecipitation generally consists of two phases: a first phase of "burst release" which is followed by a second phase of prolonged release. The first phase is due to the release of drug substance, which is adsorbed on NPs surface or which is dispersed near to the surface. The second phase is due to release of drug which is located in the core compartment (Wang and Tan, 2016). Many mathematical models have been also used to explain drug release mechanism. Most commonly used mathematical modeling that fitted drug delivery are the Higuchi model and Korsmeyer-Peppas model (Chourasiya et al., 2016; Das et al., 2010). The Higuchi model expresses cumulative percentage of released drug *versus* square root of time and it is presented by the following equation:

$$Q = k\sqrt{t}$$

Where Q is the absolute cumulative amount of released drug at time t and k is the constant reflecting the design variables of the system.

Higuchi model describes drug release as a diffusion process based on Fick's law. Therefore, when release kinetics fit this model, active release from particles would be mainly controlled by diffusion through polymer matrix (Sinha et al., 2004). However, Korsmeyer-Peppas model is presented by the following equation:

$$Q = kt^n$$

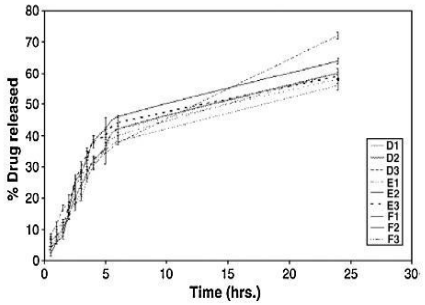

Fig. 5. *In vitro* drug-release profile of different nanoparticles formulations (D1, D2, D3, E1, E3, F1, F2, F3) through artificial membrane.
Reproduced with permission from Das et al. (2010).

Where Q is the cumulative amount of released drug at time t and n is the release exponent which is indicative of drug release mechanism. In Korsmeyer-Peppas model, n values of 0.43 indicate that the drug release is controlled by Fickian diffusion. Conversely, n values between 0.43 and 0.85 imply a non-Fickian diffusion process. The latter could be described as a combination of drug diffusion and polymer chain relaxation as long as the solvent diffuse into the polymeric matrix. However, if $n \geq 0.85$, this indicates that drug release is only governed by polymer relaxation (Puga et al., 2012). Fig. 5 shows an *in vitro* drug release profile of a drug encapsulated by nanoprecipitation technique.

Chourasiya et al. studied atenolol, which is used for cardiovascular disorders (Chourasiya et al., 2016). Atenolol loaded PLGA NPs, which are intended for the oral route, were prepared by nanoprecipitation. Different kinetics models were used to analyze *in vitro* drug release profile. In the case of *in vitro* drug release study of atenolol loaded PLGA NPs, dialysis bag diffusion method was used. Dialysis bag was immersed in a receptor compartment containing phosphate buffer (pH 7.4) stirred at 100 rpm and kept at a temperature of 37 ± 1 °C. To know the mechanism and kinetics of NPs drug release, *in-vitro* drug release data were fitted to various kinetic models such as first order, Higuchi, Hixson-Crowell and Korsmeyer-Peppas. The optimized formulation showed biphasic release profile comprising an initial burst release followed by sustained release. The preliminary fast release was due to drug molecules which are adsorbed on NPs surface. After a while, the release rate decreased which reflected the release of drug entrapped in the polymer. On the basis of best fit with the highest correlation (r^2) value, it is concluded that the formulation follows the Korsmeyer-Peppas model. Correlation value $r^2 = 0.99133$ and a release exponent value n of 0.650 were obtained. The magnitude of the release exponent n indicates that the release mechanism is an anomalous transport or non Fickian diffusion, which is related to a combination of both diffusion of the drug and dissolution of the polymer (Chourasiya et al., 2016).

Cosco et al. used the same technique for the encapsulation of 9-cis-retinoic acid (9-cis-RA) in poly (ethylene glycol)-coated PLGA. Such NPs were indicated for the treatment of undifferentiated tumor. Drug release of 9-cis-RA from PEG-PLGA NPs was evaluated by using the dynamic Franz-type diffusion cells separated by a cellulose acetate membrane. The receptor fluid was made up of a water/ethanol mixture (70:30 v:v). The PEG-PLGA NPs showed a prolonged release of the drug. An initial phase with a rapid drug release and a second phase with a more gradual release were observed (40 and 90% of released drug after 10 and 48 h, respectively).

Lie et al., investigated the encapsulation of green tea catechin derivative, lycopene, in PLGA NPs coated with chitosan. Lycopene-loaded NPs were prepared by nanoprecipitation followed by coating within chitosan to form a shell. Chitosan was coated onto the surface of lycopene NPs because chitosan exhibits pH-dependent behavior which allows to overcome the harsh environment. To understand the pH-dependent behavior effect on the release kinetics of lycopene, time-dependent release of lycopene in simulated gastric fluid and simulated intestinal fluid was studied. A known amount of lyophilized NPs was dispersed in simulated gastric juice or simulated intestinal fluid. In simulated gastric fluid, NPs released 5% of the total lycopene compared to 12% of total lycopene released in simulated intestinal fluid in 24 h. 7% of total lycopene was released in the burst-release phase from NPs in simulated gastric fluid compared to 16% of total lycopene released in simulated intestinal fluid in 24 h, both formulations showed pH-dependent release. Authors proposed that chitosan release is based on lysozyme degradation and swelling (Li et al., 2017).

7. Applications

7.1. Medicine

7.1.1. Synthetic compounds encapsulated in polymeric particles

Due to its easy manipulation, nanoprecipitation has become an important strategy in pharmaceutical development. Thus, particles for several drugs prepared by nanoprecipitation are in preclinical development (Chen et al., 2004). Paclitaxel, an anti-tumor, was loaded within poly (lactic-co-glycolic acid) (PLGA) NPs prepared by nanoprecipitation (Fonseca et al., 2002). It was shown that the 200 nm sized NPs have high EE towards paclitaxel (almost 100%). Moreover, by comparing paclitaxel loaded PLGA NPs to the already existing formulations such as, Taxol®, it was shown that PLGA NPs strongly enhanced the antitumor activity of paclitaxel. Such formulations did not have the same composition compared to marketed products. This could be important in cancer therapy by paclitaxel since commercially available formulations are accompanied with sever hypersensitivity reactions which are caused by the used excipients (Fonseca et al., 2002). Nanoprecipitation is stated as an efficient and usual method for hydrophobic drugs encapsulation (Miladi et al., 2015). However, hydrophilic drugs were considered incompatible with this method due to rapid migration and drug loss in the aqueous phase (Govender et al., 1999). Thus, the encapsulation of water-soluble drugs into NPs using nanoprecipitation method was investigated. Procaine hydrochloride loaded PLGA NPs were prepared by nanoprecipitation (Govender et al., 1999). The obtained NPs were spherical with a size of 210 nm and a low drug entrapment. However, the study showed that drug entrapment could be increased by changing variables in the method such as, by increasing the aqueous phase pH and replacing procaine hydrochloride with procaine dihydrate (Govender et al., 1999). In another study, sodium cromoglycate loaded PLA NPs were prepared by nanoprecipitation. Different technique related parameters were modified in order to increase entrapment efficiency of the hydrophilic drug into NPs. The pH also affected EE. By lowering the pH, drug entrapment increased from 10% to approximately 70% (Peltonen et al., 2004). These results show the ability of nanoprecipitation method to encapsulate hydrophilic drugs through optimization of the method parameters. Peltonen et al., studied several parameters to increase the loading of the hydrophilic sodium cromoglycate in PLA NPs (See Table 5). Specifically, salt addition (sodium chloride) to the inner or/and outer phase affected the osmotic gradient between phases (Peltonen et al., 2004). However, the best EE (70%) was achieved by adding HCl. In fact, aqueous phase pH affects the ionization of the drug substance and, hence, its solubility (Peltonen et al., 2004). Yordanov et al., prepared poly(butyl cyanoacrylate) (PBCA) nanospheres loaded with epirubicin hydrochloride (EPI·HCl) (Yordanov et al., 2012). Effect of aqueous phase pH and EPI·HCl concentration on drug loading efficiency was evaluated (Table 5). In this study, larger amount of EPI was loaded in PBCA at higher pH (7.4) (Yordanov et al., 2012). In another study, Miladi et al., encapsulated alendronate sodium in poly-ε-caprolactone (PCL) NPs. The effects of drug to polymer ratios, PCL molecular weights and organic to water phase ratio were determined (Table 5). EE reached 18.8% with PCL of 80,000 g/mol, 1:10 drug to polymer ratio and 1–2.5 organic: water phase (Miladi et al., 2015). Another key parameter to enhance entrapment is electrostatic charges of actives and polymers. In a comparative study, Zhou et al. encapsulated bovine serum albumin (BSA) in lactosylated PLGA and used ε-polylysine (ε-PL) used as an antiacidic agent (Zhou et al., 2015). All protein-loaded NPs had small sizes (<100 nm) with relatively uniform size distributions. The best EE of BSA was in Lac-PLGA/ε-PL. This could be explained by the fact that ε-PL has abundant positive charges indicating that the negatively charged proteins were easier to be loaded into Lac-PLGA/ε-PL NPs *via* electrical interaction. In addition, electrical attraction between ε-PL and BSA played an important role in the sustained release of BSA. The *in vitro* releases of BSA- and trypsin-loaded NPs were investigated in PBS solution (pH 7.4). Release of BSA was observed after 8 days, and 15.8% of BSA was released after 32 days. Moreover, BSA initial burst release was effectively avoided. Conversely, trypsin exhibited a faster release rate than trypsin-loaded Lac-PLGA NPs; more than 80% was released after 32 days (Zhou et al., 2015). Hydrophobic nature of the polymers can contribute to low entrapment efficiency (Arpicco et al., 2016). To overcome it, hydrophilic polymers can be used. Lee et al., prepared tizanidine hydrochloride, gatifloxacin and fluconazole-loaded gelatin NPs which were uncrosslinked or crosslinked with glutaraldehyde. EE was around 14% except for fluconazole which could not be loaded (Lee et al., 2012).

Modification of the method parameters can also affect the physicochemical characteristics of NPs prepared by nanoprecipitation. Polymer concentration, solvent and non-solvent nature, and solvent/non-solvent volume ratio can influence size, surface charge, size distribution. These variables were tested by Gonzalez et al. using BSA NP (Galisteo-González and Molina-Bolívar, 2014). It was shown that NPs characteristics could be modulated by altering BSA concentration, pH, salt concentration, temperature, ethanol volume, and ethanol addition rate. It was shown that these parameters have a huge effect on size and surface charge of NPs (Galisteo-González and Molina-Bolívar, 2014). In another study, PLGA NPs characteristics were also modified by changing method parameters (Bilati et al., 2005). Bian et al., encapsulated a synthetic triazole antifungal agent called itraconazole (ITZ) (Bian et al., 2013). They developed ITZ loaded poly (lactic-co-glycolic acid) (PLGA) nanospheres. The modified parameters are shown in Table 4. Optimal formulation were chosen considering particle size (178 nm), PDI (homogeneous distribution) and EE (72%) (Bian et al., 2013).

7.1.2. Natural compounds encapsulated in polymeric particles

Natural products are the source of most of the active ingredients of medicines (Harvey, 2008). Since prehistoric times, humans have used natural products, such as plants, in traditional treatments of various diseases (Bharali et al., 2011; Palombo, 2011). The focus on encapsulation of natural molecules is increased due to the interest for additionally conferring them enhanced stability and/or less volatility (Kayser et al., 2005; Asbahani et al., 2015). Nanoprecipitation was shown to be a good alternative to load these actives into NPs. Cucurbitacin I has a potent anticancer effect (Yuan et al., 2014). Alshamsan et al., used this triterpene hydrocarbon isolated from plants belonging to the species Cucurbitaceae and Cruciferae (Alshamsan, 2014). They compared the efficiency to encapsulate this polar water-insoluble drug by three emulsion based NPs formulations and nanoprecipitation. The different formulations were CI-NP1 (single emulsion o/w starting with 1000 μg of drug), CI-NP2 (double emulsion w/o/w starting with 250 μg of drug) and CI-NP3 (double emulsion w/o/w with 500 μg of drug) and CI-NP4 prepared by nanoprecipitation with 1000 μg of drug. EE was around 1%, 4%, 7% and 48%, respectively. These results showed nanoprecipitation is more efficient than emulsion solvent evaporation method to encapsulate cucurbitacin I (Alshamsan, 2014). Quercetin is another active ingredient obtained from fruits and vegetables. Sahu et al. proposed encapsulated quercetin as potential anti-cancer topical agent. *Ex vivo* study demonstrated drug release and retention in the skin (Sahu, 2013). Moreover, α-tocopherol (a form of vitamin E) is a commonly found compound in plants which has antioxidant effect (Ching and Mohamed, 2001). Noronha et al., prepared PCL nanocapsules containing α-tocopherol (Noronha et al., 2013). Table 4 shows the conditions studied to optimize formulation. In general, PCL

Table 4
Hydrophobic and hydrophilic active molecules loaded in polymeric nanoparticles prepared by nanoprecipitation and studied parameters during the process.

Active molecule	Nanoparticle-forming polymer	Parameter studied	Effect reported	Potential use	Reference
Itraconazol	PLGA	Surfactant concentration	Poloxamer 188 concentration increased, size increased.	Antifungal	Bian et al. (2013)
		Polymer:drug ratio	PLGA amount increased, size and EE% increased.		
Cucurbitacin I	PLGA	N/S	N/S	Anticancer	Alshamsan (2014)
Quercetin	Ethylcellulose	Polymer amount	Ethylcellulose amount increased, drug loading decreased, EE% increased and percentage *in vitro* release after 24 h decreased	Anticancer	Sahu (2013)
α-tocopherol	PCL	Drug amount	α-tocopherol amount increased, particle size increased and EE% decreased.	Antioxidant	Noronha et al. (2013)
		Lecithin concentration	Does not seem to exert any influence		
		Surfactant concentration	Pluronic F68 concentration increased, size increased		
Brazilian red propolis extract	PCL	N/S	N/S	Leishmanicidal	do Nascimento et al. (2016)
Zanthoxylum rhoifolium essential oil	PCL	Essential oil mount	*Zanthoxylum rhoifolium* essential oil increased, EE% decreased	Insecticidal	Christofoli et al. (2015)
Achyrocline satureioides essential oil	PLC	N/S	N/S	Hepatoprotective effect, antioxidant	Ritter et al. (2017)
Sodium cromoglycate	PLA	Drug percentage (related to the amount of polymer)	Drug percentage increased, EE% decreased	Preventive reducer of bronchoconstriction	Peltonen et al. (2004)
		Solvent and co-solvent selection	Combination of Dichloromethane and methanol, EE% increased		
		salt addition	Sodium chloride in the inner and outer phases, EE% increased		
		pH effect	Acid pH in the outer phase, EE% increased		
Epirubicin hydrochloride (EPI·HCl)	PBCA	pH effect	Higher pH, EE% increased	Anticancer	Yordanov et al. (2012)
		Drug concentration	EPI·HCl concentration increased, EE% decreased		
Alendronate sodium	PCL	Drug:polymer ratio	PCL amount increased particle size and EE% increased.	Osteoporosis treatment	Miladi et al. (2015)
		Polymer molecular weights	PCL molecular weight increased, particle size and EE% increased.		
		Organic:water phase ratio	Water phase increased, particle size and EE% decreased		
Bovine serum albumin (BSA)/Trypsin	Lactosylated PLGA	Negative or positive drug	Negative BSA with ε-polylysine, EE% and sustained release increased	Model proteins and cell culture	Zhou et al. (2015)
Tizanidine hydrochloride (TZN), gatifloxacin(GTX) and fluconazole	Gelatin	Uncrosslinked or crosslinked with glutaraldehyde	TZN crosslinked NPs, EE% increased. GTX uncrosslinked, EE% increased. No loading was observed for fluconazole	a^2-adrenergic agonist and myotonic muscle relaxant; antibacterial and antifungal, respectively	Lee et al. (2012)
Cocoa-derived polyphenolic extract	Gelatin	Polymer concentration	Gelatin concentration increased, size increased	Antioxidant	Quiroz-Reyes et al. (2014)
		Surfactant concentration	Tween 80 concentration increased, size decreased		
Protamine sulphate, diclofenac sodium and N6-cyclopentyladenosine (CPA)	PLGA/PLA	Drug amount	Drug amount increased, drug loading increased and EE% decreased. The size of the particles did not increase.	Anticoagulant activity inhibitor of heparin; anti-inflammatory, analgesic and antipyretic effect; selective agonist of adenosine A_1 receptors, respectively	Dalpiaz et al. (2016)
		PLGA substituted by PLA for CPA	PLGA substituted by PLA, EE% increased		

PLGA: polylactic-*co*-glicolic acid; PCL: poly-ε-caprolactone; PLA: polylactic acid; PBCA: poly(butyl cyanoacrylate).
N/S: not studied.
NPs: Nanoparticles.

nanocapsules showed a negative charge and homogeneous size distribution. The optimal formulation had an EE of 99.97% (Noronha et al., 2013). Other studies focused on the encapsulation of natural compounds obtained from extracts or essential oils. In fact, do Nascimento et al., who investigated propolis which is recollected by bees of the species *Apis mellifera* from plant exudates (do Nascimento et al., 2016). Propolis has been widely used in alternative and traditional medicine to treat several diseases. In this study, leishmanicidal activity against *Leishmania (V.) braziliensis* was proved. Red propolis raw material was collected and extracted by maceration, then the extract was loaded into NPs. The organic phase was composed by PCL and red propolis extract while the aqueous phase contained pluronic F-108 copolymer. Five formulations were prepared with values of particle size varying

between 208 and 280 nm (do Nascimento et al., 2016). Ritter et al., developed *Achyrocline satureioides* essential oil loaded nanocapsules (Ritter et al., 2017). When tested, nanocapsules showed potency to protect hepatic tissue against cytotoxic damage caused by *Trypanosoma evansi* (Ritter et al., 2017). Essential oils could also have insecticidal activity. Their encapsulation into NPs can potentially improve their activity, offer better protection against degradation and oxidation processes by light and heat. Essential oils could also be used against agricultural pests such as *Bemisia tabaci* (Christofoli et al., 2015). Due to large number of compounds that constitute an extract or an essential oil, some researchers quantified the major component and used the obtained data to determine EE or loading rate of the essential oil (do Nascimento et al., 2016). Quiroz-Reyes et al. (2014) obtained cocoa-derived polyphenolic extract in gelatin NPs. They dissolved the polyphenolic extract in a water-methanol solution, adding a specific quantity of gelatin. The mixture was then stirred and maintained at 45 °C for 30 min. The resulting solution was added dropwise to an ethanolic solution of tween 80. Finally, glutaraldehyde was added as a crosslinking agent. With 2% w/v of tween 80 and gelatin, it was possible to obtain a formulation with a loading efficiency of 77% (Quiroz-Reyes et al., 2014). Another strategy is used by Dalpiaz et al., who dissolved protamine sulphate, diclofenac sodium and N^6-cyclopentyladenosine (CPA) and PLGA in acetone phase and added them drop-wise to the cottonseed oil (oil phase) and tween 80 (Dalpiaz et al., 2016). For CPA, authors substituted PLGA with PLA, which is characterized by a lower hydrophilicity. Using PLA instead of PLGA increased CPA loading when 5 mg of drug were used as the initial amount, doubling the EE value (from 7% to 15%) (Dalpiaz et al., 2016).

7.1.3. Protein based particles

Proteins constitute an important class of biopolymers that gained lately importance in drug delivery field. Proteins have several advantages. They are biocompatible, biodegradable, and their biodegradation products are often non-toxic. Moreover, since they are derived from animals or plant sources, they are lacking of monomers or initiators found in synthetic polymers (Pathak and Thassu, 2009). Because of their importance, protein based nanoparticle systems are already found in the market, such as albumin bound paclitaxel NPs (Abraxane™) (Langer et al., 2008). Protein based NPs prepared by nanoprecipitation method could be often found in literature. Lee et al. prepared gelatin based NPs by nanoprecipitation (Lee et al., 2012). Water and ethanol were used as solvent and non-solvent, respectively. It was shown that the non-crosslinked particles have an irregular shape due to particle aggregation. However, the cross linked particles have a unimodal size of 251 nm, low polydispersity index (0.096), and uniformly round shape (Lee et al., 2012). This suggests that nanoprecipitation is a suitable method for the preparation of gelatin NPs. In another study, curcumin loaded zein NPs were prepared by nanoprecipitation. Results showed that the average particle size can be controlled through the solvent system and the zein/curcumin ratio. This formulation enhanced the stability of curcumin at all physiological pH and following UV irradiation. The formulation was also found stable in the gastrointestinal tract. Furthermore, due to the fact that zein is an edible protein, the ability to use such formulation by including it in oral products was suggested (Patel et al., 2010). Whey protein were also used to prepare NPs. Ethanol was used as non-solvent and added at a speed rate of 1 ml/min in order to achieve a solvent/non-solvent volume ratio of 1:5. Obtained particles were spherical with a relatively small size (less than 100 nm). These particle properties are obtainable at pH3, a desirable pH for food applications. Moreover, it was found that particle size can be controlled by a combination of heating and homogenization (Gülseren et al., 2012). These results show that nanoprecipitation is a successful and promising approach for the preparation of NPs using the natural, biodegradable, non-toxic proteins as starting materials.

7.2. Applications in agricultural and food industry

The success of nanoprecipitation method in the pharmaceutical field shed the light on the application of this technique in the agricultural industry. In fact, the growth of world population requires food sources increase which leads to an augmentation of fertilizers and pesticides use. However, this could result in soil depletion and environmental pollution (Bareras-Urbina et al., 2016). Thus, the need of a controlled release system is crucial to reduce environmental problems associated with the use of pesticides (Boehm et al., 2003). For this reason, nanoprecipitation has been used to prepare polymeric NPs as an insecticide formulation (Boehm et al., 2003). Eudragit® S100 based NPs showed small size and high EE, but they did not provide a controlled release of the active ingredient. However, they enhanced the penetration of the active in the plant due to their small size (Boehm et al., 2003). Nanoprecipitation is also important in the food industry since particles could be prepared by natural food compound such as, starch or proteins (Castro-Enríquez et al., 2012). Moreover, α-tocopherol loaded poly ε-caprolactone NPs were prepared. These particles showed high values of recovery and EE. They could potentially be used as food antioxidants and preservatives in food packaging (Noronha et al., 2013).

8. *In vivo* testing

In vivo studies give a closer idea about NPs action in the human body (Popov et al., 2016). Biodegradable and biocompatible polymers as PLA, PGA, PCL, poly(γ-valerolactone) and copolymers such as, PLGA (Nicolas et al., 2013) are used for preparation of NPs by nanoprecipitation. In *vivo* studies could give relevant information about drug transportation up to the targeted organs. For example, Sharma et al. demonstrated that intranasal NPs can potentially transport the encapsulated drug *via* nose-to-brain (Sharma et al., 2015). They used diazepam (DZP), which is widely used as sedative hypnotic, antianxiety, and antiepileptic drug. The administration routes were intranasal and intravenous in Sprague-Dawley rats. DZP was labeled using technetium-99m-labeled (^{99m}Tc), loaded into PLGA NPs (DNP) and applied. Gamma scintigraphy and biodistribution study were carried out to follow DNP and DZP solution (DS) in rats. The scintigraphy images indicated the high uptake of ^{99m}Tc-DNP into the brain. Presence of high radioactivity was observed in rat brain after administration of ^{99m}Tc-DNP intranasally compared to intravenous ^{99m}Tc-DS and intranasal ^{99m}Tc-DS. Biodistribution studies showed significantly higher brain uptake of intranasal ^{99m}Tc-DNP as compared to intranasal ^{99m}Tc-DS and intravenous ^{99m}Tc-DS (Sharma et al., 2015). After intravenous administration, it has been demonstrated that these particles provided sustained drug delivery. Bian et al. (2013) showed that systemic bioavailability of itraconazol (ITZ) loaded PLGA nanospheres was more important than Sporanox® formulation. This is consistent with the observed sustained plasma drug level for up to 24 h after administration by PLGA-ITZ-NS formulation (Bian et al., 2013). NPs have been found in spleen, liver and lungs (Zhou et al., 2015). Intratracheal instillation in male mice has been used to evaluate pulmonary delivery by Popov et al. (2016). Fluticasone propionate (FP) was loaded in poly(lactide)-based particles of around 200 nm diameter prepared by nanoprecipitation. NPs pulmonary residence was assessed by measuring FP levels in mouse lungs over 24 h. Higher FP levels were observed with PLA-based NPs during 24 h while free FP was rapidly eliminated from lungs following instillation (Popov et al., 2016).

These studies demonstrated the presence of active loaded NPs in different organs. Jeannot et al., administrated intravenously and intrapulmonary NPs in healthy mice, H358-tumor bearing mice or A549-tumor bearing mice (Jeannot et al., 2016). Two different sizes of NPs, 30 and 300 nm (NP30 and NP300, respectively), were prepared by nanoprecipitation. NP30 and NP300 were internalized in H358 and A549 cells and cell labeling and internalization were stronger with NP30 than NP300. In both lung tumor models, intrapulmonary nebulized NPs were accumulated in lungs, but not in the tumor nodules. This means that direct administration of these NPs into the airways failed to increase their uptake by tumors. Despite a significant liver capture, intravenous injection led to a better accumulation of the NPs in the lung tumors compared with the surrounding healthy lung tissues. The pharmacokinetic constants were calculated, and the theoretical distribution and elimination half-lives for NP30 were higher than for NP300, which showed that NP30 had longer circulation times than NP300 (Jeannot et al., 2016). The *in vivo* distribution and the cellular uptake of NP depended on their size (Dufort et al., 2012).

Focusing on natural products, *in vivo* study has carried out for *Achyrocline satureioides* essential oil loaded PCL nanocapsules (AS-NC) proving their capacity to protect liver. Here, Ritter et al., infected female Wistar rats with *Trypanosoma evansi*, a widely distributed protozoan that parasites the blood of wild and domestic animals, and rarely humans (Ritter et al., 2017). Four groups administrated by oral gavage were used: uninfected/saline, uninfected/AS-NC, infected/saline and infected/AS-NC. Infected/AS-NC group showed lower parasitemia than animals of the infected/saline group. Moreover, *T. evansi* infection causes decreased cell viability on hepatic tissue after excessive production of reactive oxygen species (ROS) and nitric oxide metabolites. Treatment with AS-NC was able to protect the hepatic tissue against cytotoxic effect caused by parasite due to the capacity of to avoid exacerbated production of ROS. Thus, the protective effect of AS-NC might be related to antioxidant properties of *A. satureioides* essential oil (Ritter et al., 2017). Studies of Danhier et al., has proved that NPs can be an effective anticancer drug delivery system for cancer chemotherapy (Danhier et al., 2009). Paclitaxel (PTX) a major anticancer drug isolated from the plant *Taxus brevifolia* was loaded in PEGylated PLGA NPs. NPs inhibited tumor growth more efficiently than Taxol® (commercial product of PTX) (Danhier et al., 2009). Oral administration of Eudragit® E PO based NPs loaded with meloxicam prepared by nanoprecipitation resulted in an enhanced anti-inflammatory effect and in a decrease of the adverse effects associated with the treatment (Khachane et al., 2011). Singh and Pai prepared Eudragit® RL 100 based NPs for encapsulation of trans-resveratrol with mean particle size around 180 nm (Singh and Pai, 2014). These NPs showed higher plasma levels than free resveratrol. Active accumulation in the brain, heart, liver, lungs, kidneys and spleen after oral administration over a period of 24 h was also higher than pure drug and marketed formulation (Singh and Pai, 2014). Eudragit® RL 100 was used for encapsulation of amphotericin-B (AmB), a polyene antifungal antibiotic that has broad-spectrum activity (Das et al., 2010). NPs sizes ranged from 134 to 290 nm. The selected formulation administered *via* ocular route in male albino rabbits showed no eye irritation. *In vivo* study suggests that AmB NPs could have potent ocular antifungal effect with minimal eye-irritating effect (Das et al., 2010). Fig. 6 depicts most common administration routes and targeted organs for NPs prepared by nanoprecipitation.

9. Clinical trials of drug loaded nanoparticles prepared by nanoprecipitation

In general, FDA drug approval process can be separated into preclinical, clinical, and post-marketing phases. The gathered data

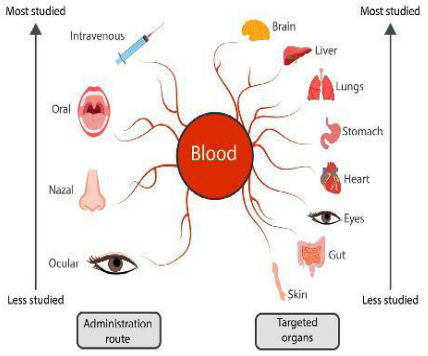

Fig. 6. Most common administration routes and targeted organs for nanoparticles prepared by nanoprecipitation.

during the preclinical phase is used to support an Investigational New Drug (IND). If during the clinical phase, the drug is considered safe and efficacious, the manufacturer files a New Drug Application (NDA) (see Fig. 7) (Eifler and Thaxton, 2011). Despite the potential advantages of these new drug delivery systems, few NPs formulations are approved for clinical use and face challenges and hurdles at different stages of development (Desai, 2012).

The following features are studied during formulation development process and have to be well known before clinical trials:

- Adequate particle size
- Stability of the nanosystem
- Drug release from the complex matrix
- Targeting
- Efficacy of biological activity
- Toxicology in cell lines and animals
- Pharmacology
- Scale up (manufacturing process)
- Production of sterile forms at laboratory and scale up

Mostly clinical studies are focused on cancer therapy (see Table 5).

The *in vivo* findings, showed that loaded NPs prepared by nanoprecipitation gave satisfactory results. Due to the versatility of nanoprecipitation technique, a broad range of polymeric materials which have already been approved by FDA could be used. Dong and Feng elaborated paclitaxel-loaded NPs of poly(D,L-lactide)/methoxy poly(ethylene glycol)-polylactide (PLA/MPEG-PLA) blends of various blend ratio from 100/0 to 0/100 by the nanoprecipitation method to control the release of paclitaxel. NPs with hydrodynamic diameter of 230 to 74 nm, encapsulation efficiency of 69–55% and zeta potential of 19.6–0.3 mV were obtained. DSC analysis suggested the miscibility of PLA and MPEG-PLA. The pure PLA NPs (100/0) exhibited the slowest drug release rate with 37.3% of encapsulated drug released from the NPs for 14 days. MPEG-PLA NPs (0/100) provided the fastest drug release with 95.9% drug release in the same period (Dong and Feng, 2004). Genexol-PM® Cremophor EL-free based on paclitaxel loaded methoxy-PEG-polylactide NPs is marketed in Europe and Korea for breast cancer and small cell lung cancer (Lohcharoenkal et al., 2014; Pillai, 2014). Based on its simplicity and versatility, nanoprecipitation is chosen as encapsulation method for the development of new nanoparticle-forming polymers with potential used in biomedical field. An example is poly(*N*-(2-hydroxypropyl) methacrylamide) (PHPMA), which is in clinical phase. This polymer is water-soluble, synthetic, vinyl-based polymer with

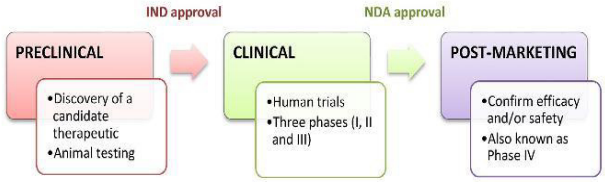

Fig. 7. Phases of drug development and approval by the US Food and Drug Administration. Reproduced with permission from Eifler and Thaxton (2011).

Table 5
Polymeric nanosystems in clinical use for anticancer therapy.

Product name	Polymer-forming nanoparticle	Active molecule	Reported Clinical Phase	Cancer type	Reference
NK105	PEG–poly(aspartic acid) block copolymer	Paclitaxel	I	Pancreatic, bile duct, gastric and colonic cancer	Hamaguchi et al. (2007)
			II	Gastric Cancer	Kato et al. (2012)
NK911	PEG–poly(aspartic acid) block copolymer	Doxorubicin	I	Metastatic pancreatic cancer	Matsumura et al. (2004)
CRLX101	PEG–Cyclodextrin copolymer	Camptothecin	II	Various types (non-small cell lung)	Svenson et al. (2011)
NC-6004	PEG-poly(glutamic acid) block co-polymer	Cisplatin	I	Various types (*i.e.* colon and lung)	Plummer et al. (2011)

singular nonimmunogenic and nontoxic characteristics (Yan et al., 2017).

In the pharmaceutical industry, the production of nanoparticles by nanoprecipitation has not been applied due to the organic solvent usage issue. Nevertheless, the production equipment for large-scale has been marketed (Tran et al., 2016). Despite the employment of organic solvent within the process, pre-clinical and clinical studies have suggested to this technique as a potential preparation technique of nanoparticles in order to be applied in organism. Thus, nanoprecipitation could be a recommended technique for the nanoparticles preparation.

10. Industrial scale-up of nanoprecipitation method

The transition from laboratory to industrial grade is crucial for any clinically approved formulation. However, this transition should be controlled by a scale-up strategy in order to create industrial scale parameters that lead to the mass production of laboratory-like formulations (Galindo-Rodríguez et al., 2005). Scaling-up of NPs formulations is often successful and have advantages over laboratory scale production. Smaller polymers amounts are needed to produce NPs in pilot-scale than in

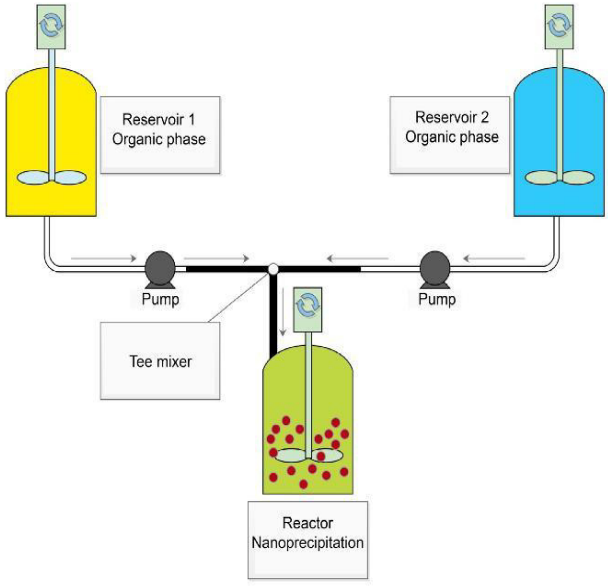

Fig. 8. Experimental set-up for pilot-scale nanoprecipitation.

laboratory-scale. In addition, pilot-scale processes are more reproducible than laboratory-scale ones. Moreover, polymer precipitation during NPs production is more efficient in pilot-scale since formulation parameters are well controlled (Marchisio et al., 2006).

The success of nanoprecipitation depends on the way the aqueous and organic phases are mixed together to lead to polymer precipitation and create NPs. It is known that the mixing time must be faster than the time required to induce nanoparticle formation (Johnson and Prud'homme, 2003). In lab scale, the mixing conditions are ideal since the amount of solutions is relatively small (in ml), and the initial conditions are maintained stable during the whole process. However, in industrial scale, the production of large amount of NPs needs large amounts of both phases. This is where the keeping of the ideal conditions during the whole process becomes difficult.

Galindo-Rodriguez et al., assessed a scaling-up procedure for ibuprofen loaded poly(vinyl alcohol) NPs prepared by nano-precipitation (Galindo-Rodríguez et al., 2005). Particles were prepared at laboratory scale and at pilot scale by increasing the volume 20 fold from 60 ml to 1.5 l. The scale-up of nano-precipitation was performed using the experimental set up showed in Fig. 8. This set-up consists of two reservoirs, one for the aqueous phase and another for the organic one. Each reservoir is connected to an independent pump that continuously supplies the two phases. The two phases meet at the "Tee mixer" where the precipitation occurs instantaneously. Finally, the set up includes a reactor where particles are maintained under agitation (see Fig. 7).

Laboratory and pilot-scale NPs were compared. It was found that the particles prepared by laboratory scale have a bigger size (141 nm) than the ones prepared by pilot scale (105 nm). However, the polydispersity index at pilot scale (0.130) is higher than the laboratory scale (0.082). This could be caused by the higher turbulence generated in the pilot scale which improves the diffusion of solvent and, by its turn, leads to smaller NPs. In addition, drug loading and entrapment efficiency at lab scale (4.5% and 50% respectively) were higher than pilot scale (3.2% and 39% respectively). Moreover, the pilot batches show reproducibility and each batch requires 120 min to be produced. These results show that the pilot scale production of polymer NPs by nanoprecipitation method was successful. However, the major drawback of this method is related to the low concentration of polymer, which leads to a difficult NPs recovery in the final dispersion (Galindo-Rodríguez et al., 2005).

Another approach of precipitation optimization is flash nano-precipitation (FNP) method. This modified version of nano-precipitation is based on stimulating the supersaturation conditions required for the precipitation using a jet mixer to mix the two phases (See Fig. 9) (Pustulka et al., 2013). In this method, the characteristic mixing time of the two phases is in the order of milliseconds. Such rapid mixing induces a high supersaturation that initiates precipitation (Johnson and Prud'-homme, 2003). Zhang et al. prepared polystyrene NPs using FNP method (Zhang et al., 2012). It was found that formulations have a comparative size distribution when the diameter of particles was less than 150 nm. In addition, NPs size was tunable by modifying the polymer concentration. An increase in polymer concentration leads to an increase in particle size (Zhang et al., 2012). FNP as an enhanced version of nanoprecipitation could lead to more accurate and reproductive results. In addition, an advantage of this method is that it could be run at laboratory scale with small amounts of solutions, and the process performance could be easily duplicated at a pilot-scale (Johnson and Prud'homme, 2003).

11. Advantages and disadvantages of nanoprecipitation

Nanoprecipitation technique is based on the interfacial deposition of polymers following the displacement of a semi-polar solvent miscible with water from a lipophilic solution. Generally, actives loaded into nanoparticles show stability, controlled release or targeting potential. Different parameters during nanoprecipitation process can be modified to obtain a formulation with the desirable characteristics in terms of size, storage stability, active encapsulation and electrostatic charges. Advantages of nanoprecipitation over other encapsulation techniques are: (1) simplicity (2) ease of scalability (3) good reproducibility (4) safety (large amounts of toxic solvents are avoided) (5) obtaining of submicron particle sizes with narrow size distribution

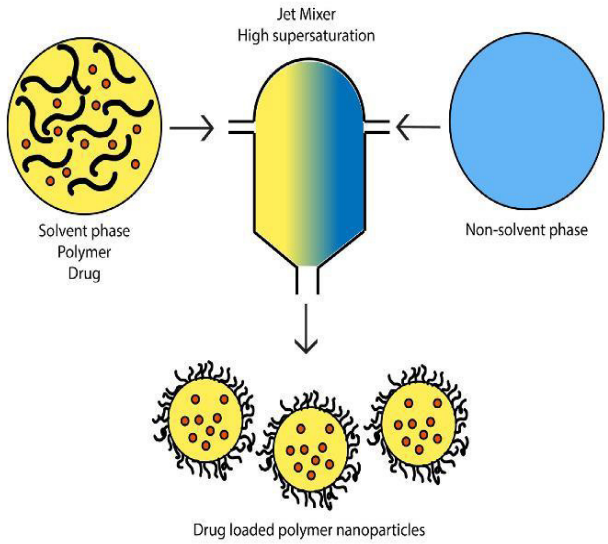

Fig. 9. Flash nanoprecipitation method.

Table 6
Advantages and drawbacks of nanoprecipitation method (Miladi et al., 2016; Paliwal et al., 2014).

No	Advantages	Drawbacks
1	Rapid	Not adequate method for water soluble molecules
2	Profitable	Particles growth controlling complication
3	Simple	
3	Production of colloidal dispersion with a narrow size distribution	
4	Easy to scale-up	
5	Satisfying reproducibility	
6	Formulations with good stability	
7	Preparation of nanospheres and nanocapsules	

and (6) Low energy input (7) (Miladi et al., 2016). Table 6. depicts major advantages and drawbacks of this method.

Nanoprecipitation has become an important strategy in pharmaceutical, agricultural, food and cosmetic industry. In agricultural industry, the need of a controlled release system is crucial to reduce the environmental and health problems associated with the use of pesticides. Possibly the most investigated field is medicine and encapsulated actives for application in pharmaceutical industry attract a special attention. Based on nanoprecipitation simplicity and versatility, it is a potential preparation method of polymeric nanosystems for pre-clinical and clinical studies.

12. Conclusion

Several drugs could present bioavailability, stability or taste limitations. Encapsulation of such molecules in NPs could be a relevant alternative to circumvent such problems. This contributes to the enhancement of the efficacy of actives and promotes patient compliance. Nanoprecipitation is a simple and reproducible technique that has been widely used for the preparation of polymeric NPs intended for several biomedical applications. Operating conditions management is a key point to obtain NPs with suitable properties. Several research works have been carried out to use nanoprecipitation in a conventional way while other works focused on the enhancement of its scalability, reproducibility and safety *via* scale-up. Tee mixer and flash nanoprecipitation are among the techniques that were introduced to achieve such purposes. Advantages of submicron carriers prepared by nanoprecipitation in the biomedical and agricultural fields have been confirmed by numerous studies. These achievements include enhanced bioavailability, better targeting and tolerance, sustained release and enhanced absorption of the drug through biological barriers. Nanoprecipitation has been widely used to prepare NPs. Although several advances have been recorded, more *in vivo* testing in human is needed. Such investigations along with scale-up approach would be highly relevant to promote the clinical applications of nanoprecipitation technique.

References

Alshamsan, A., 2014. Nanoprecipitation is more efficient than emulsion solvent evaporation method to encapsulate cucurbitacin I in PLGA nanoparticles. Saudi Pharm. J. SPJ 22, 219–222. doi:http://dx.doi.org/10.1016/j.jsps.2013.12.002.

Armendáriz-Barragán, B., Zafar, N., Badri, W., Galindo-Rodríguez, S.A., Kabbaj, D., Fessi, H., Elaissari, A., 2016. Plant extracts: from encapsulation to application. Expert Opin. Drug Deliv. 13, 1165–1175. doi:http://dx.doi.org/10.1080/17425247.2016.1182487.

Arpicco, S., Battaglia, L., Brusa, P., Cavalli, R., Chirio, D., Dosio, F., Gallarate, M., Milla, P., Peira, E., Rocco, F., et al., 2016. Recent studies on the delivery of hydrophilic drugs in nanoparticulate systems. J. Drug Deliv. Sci. Technol. 32, 298–312.

Asadi, H., Rostamizadeh, K., Salari, D., Hamidi, M., 2011. Preparation of biodegradable nanoparticles of tri-block PLA-PEG-PLA copolymer and determination of factors controlling the particle size using artificial neural network. J. Microencapsul. 28, 406–416. doi:http://dx.doi.org/10.3109/02652048.2011.576784.

Asbahani, A.E., Miladi, K., Badri, W., Sala, M., Addi, E.H.A., Casabianca, H., Mousadik, A.E., Hartmann, D., Jilale, A., Renaud, F.N.R., Elaissari, A., 2015. Essential oils: from extraction to encapsulation. Int. J. Pharm. 483, 220–243. doi:http://dx.doi.org/10.1016/j.ijpharm.2014.12.069.

Averina, E., Allémann, E., 2013. Encapsulation of alimentary bioactive oils of the Baikal Lake area into pH-sensitive micro- and nanoparticles. LWT–Food Sci. Technol. 53, 271–277. doi:http://dx.doi.org/10.1016/j.lwt.2013.01.020.

Badri, W., Miladi, K., Nazari, Q.A., Fessi, H., Elaissari, A., 2017. Effect of process and formulation parameters on polycaprolactone nanoparticles prepared by solvent displacement. Colloids Surf. Physicochem. Eng. Asp. 516, 238–244. doi:http://dx.doi.org/10.1016/j.colsurfa.2016.12.029.

Bansal, R., Guleria, A., Acharya, P.C., 2013. FT-IR method development and validation for quantitative estimation of zidovudine in bulk and tablet dosage form. Drug Res. 63, 165–170.

Bareras-Urbina, C.G., Ramírez-Wong, B., López-Ahumada, G.A., Burruel-Ibarra, S.E., Martínez-Cruz, O., Tapia-Hernández, J.A., Rodríguez Félix, F., 2016. Nano- and micro-particles by nanoprecipitation: possible application in the food and agricultural industries. Int. J. Food Prop. 19, 1912–1923. doi:http://dx.doi.org/10.1080/10942912.2015.1089279.

Bazylińska, U., Lewińska, A., Lamch, Ł., Wilk, K.A., 2014. Polymeric nanocapsules and nanospheres for encapsulation and long sustained release of hydrophobic cyanine-type photosensitizer. Colloids Surf. Physicochem. Eng. Asp. 442, 42–49. doi:http://dx.doi.org/10.1016/j.colsurfa.2013.02.023 Selected papers from the 26th European Colloid and Interface Society conference (26th ECIS 2012).

Bharali, D.J., Siddiqui, I.A., Adhami, V.M., Chamcheu, J.C., Aldahmash, A.M., Mukhtar, H., Mousa, S.A., 2011. Nanoparticle delivery of natural products in the prevention and treatment of cancers: current status and future prospects. Cancers 3, 4024–4045. doi:http://dx.doi.org/10.3390/cancers3044024.

Bhattacharjee, S., 2016. DLS and zeta potential ? What they are and what they are not?. J. Controlled Release 235, 337–351.

Bian, X., Liang, S., John, J., Hsiao, C.-H., Wei, X., Liang, D., Xie, H., 2013. Development of PLGA-based itraconazole injectable nanospheres for sustained release. Int. J. Nanomed. 8, 4521–4531.

Bilati, U., Allémann, E., Doelker, E., 2005. Development of a nanoprecipitation method intended for the entrapment of hydrophilic drugs into nanoparticles. Eur. J. Pharm. Sci. 24, 67–75. doi:http://dx.doi.org/10.1016/j.ejps.2004.09.011.

Boehm, A.L., Martinon, I., Zerrouk, R., Rump, E., Fessi, H., 2003. Nanoprecipitation technique for the encapsulation of agrochemical active ingredients. J. Microencapsul. 20, 433–441. doi:http://dx.doi.org/10.1080/0265204021000058410.

Bomgaars, L., Geyer, J.r., Franklin, J., Dahl, G., Park, J., Winick, N.j., Klenke, R., Berg, S.l., Blaney, S.m., 2004. Phase I trial of intrathecal liposomal cytarabine in children with neoplastic meningitis. J. Clin. Oncol. 22, 3916–3921.

Budhian, A., Siegel, S.J., Winey, K.I., 2007. Haloperidol-loaded PLGA nanoparticles: systematic study of particle size and drug content. Int. J. Pharm. 336, 367–375. doi:http://dx.doi.org/10.1016/j.ijpharm.2006.11.061.

Castro-Enríquez, D.D., Rodríguez-Félix, F., Ramírez-Wong, B., Torres-Chávez, P.I., Castillo-Ortega, M.M., Rodríguez-Félix, D.E., Armenta-Villegas, L., Ledesma-Osuna, A.I., 2012. Preparation, characterization and release of urea from wheat gluten electrospun membranes. Materials 5, 2903–2916. doi:http://dx.doi.org/10.3390/ma5122903.

Chang, H.-I., Yeh, M.-K., 2012. Clinical development of liposome-based drugs: formulation, characterization, and therapeutic efficacy. Int. J. Nanomedicine 7, 49–60.

Chen, J.-F., Zhou, M.-Y., Shao, L., Wang, Y.-Y., Yun, J., Chew, N.Y., Chan, H.-K., 2004. Feasibility of preparing nanodrugs by high-gravity reactive precipitation. Int. J. Pharm. 269, 267–274.

Ching, L.S., Mohamed, S., 2001. Alpha-tocopherol content in 62 edible tropical plants. J. Agric. Food Chem. 49, 3101–3105.

Chorny, M., Fishbein, I., Danenberg, H.D., Golomb, G., 2002. Lipophilic drug loaded nanospheres prepared by nanoprecipitation: effect of formulation variables on size, drug recovery and release kinetics. J. Control. Release 83, 389–400.

Chourasiya, V., Bohrey, S., Pandey, A., 2016. Formulation, optimization, characterization and in-vitro drug release kinetics of atenolol loaded PLGA nanoparticles using 33 factorial design for oral delivery. Mater. Discov. 5, 1–13. doi:http://dx.doi.org/10.1016/j.md.2016.12.002.

Christofoli, M., Costa, E.C.C., Bicalho, K.U., de Cássia Domingues, V., Peixoto, M.F., Alves, C.C.F., Araújo, W.L., de Melo Cazal, C., 2015. Insecticidal effect of nanoencapsulated essential oils from Zanthoxylum rhoifolium (Rutaceae) in

Bemisia tabaci populations. Ind. Crops Prod. 70, 301–308. doi:http://dx.doi.org/10.1016/j.indcrop.2015.03.025.
Contado, C., Vighi, E., Dalpiaz, A., Leo, E., 2013. Influence of secondary preparative parameters and aging effects on PLGA particle size distribution: a sedimentation field flow fractionation investigation. Anal. Bioanal. Chem. 405, 703–711. doi:http://dx.doi.org/10.1007/s00216-012-6113-5.
D'addio, S.M., Prud'homme, R.K., 2011. Controlling drug nanoparticle formation by rapid precipitation. Adv. Drug Deliv. Rev. 63, 417–426.
Dalpiaz, A., Sacchetti, F., Baldisserotto, A., Pavan, B., Maretti, E., Iannuccelli, V., Leo, E., 2016. Application of the in-oil nanoprecipitation method in the encapsulation of hydrophilic drugs in PLGA nanoparticles. J. Drug Deliv. Sci. Technol. Drug Deliv. Res. Italy 32 Part B 283–290. doi:http://dx.doi.org/10.1016/j.jddst.2015.07.020.
Danhier, F., Lecouturier, N., Vroman, B., Jérôme, C., Marchand-Brynaert, J., Feron, O., Préat, V., 2009. Paclitaxel-loaded PEGylated PLGA-based nanoparticles: in vitro and in vivo evaluation. J. Control. Release 133, 11–17. doi:http://dx.doi.org/10.1016/j.jconrel.2008.09.086.
Das, S., Suresh, P.K., Desmukh, R., 2010. Design of Eudragit RL 100 nanoparticles by nanoprecipitation method for ocular drug delivery. Nanomed. Nanotechnol. Biol. Med. 6, 318–323. doi:http://dx.doi.org/10.1016/j.nano.2009.09.002.
Desai, N., 2012. Challenges in development of nanoparticle-based therapeutics. AAPS J 14 (2), 282–295.
do Nascimento, T.G., da Silva, P.F., Azevedo, L.F., da Rocha, L.G., de Moraes Porto, I.C. C., Lima E Moura, T.F.A., Basílio-Júnior, I.D., Grillo, L.A.M., Dornelas, C.B., da S. Fonseca, E.J., de Jesus Oliveira, E., Zhang, A.T., Watson, D.G., 2016. Polymeric nanoparticles of brazilian red propolis extract: preparation, characterization, antioxidant and leishmanicidal activity. Nanoscale Res. Lett. 11, 301. doi:http://dx.doi.org/10.1186/s11671-016-1517-3.
Dong, Y., Feng, S.-S., 2004. Methoxy poly(ethylene glycol)-poly(lactide)(MPEG-PLA) nanoparticles for controlled delivery of anticancer drugs. Biomaterials 25, 2843–2849. doi:http://dx.doi.org/10.1016/j.biomaterials.2003.09.055.
Dufort, S., Sancey, L., Coll, J.-L., 2012. Physico-chemical parameters that govern nanoparticles fate also dictate rules for their molecular evolution. Adv. Drug Deliv. Rev. Biol. Interact. Nanopart. 64, 179–189. doi:http://dx.doi.org/10.1016/j.addr.2011.09.009.
Eifler, A.C., Thaxton, C.S., 2011. Nanoparticle therapeutics: FDA approval, clinical trials, regulatory pathways, and case study, in: biomedical nanotechnology. Methods in Molecular Biology. Humana Press, pp. 325–338.
Fessi, H., Puisieux, F., Devissaguet, J.P., Ammoury, N., Benita, S., 1989. Nanocapsule formation by interfacial polymer deposition following solvent displacement. Int. J. Pharm. 55, R1–R4. doi:http://dx.doi.org/10.1016/0378-5173(89)90281-0.
Fonseca, C., Simões, S., Gaspar, R., 2002. Paclitaxel-loaded PLGA nanoparticles: preparation, physicochemical characterization and in vitro anti-tumoral activity. J. Control. Release 83, 273–286.
Gülseren, I., Fang, Y., Corredig, M., 2012. Whey protein nanoparticles prepared with desolvation with ethanol: characterization, thermal stability and interfacial behavior. Food Hydrocolloids 29, 258–264. doi:http://dx.doi.org/10.1016/j.foodhyd.2012.03.015.
Galindo-Rodríguez, S.A., Puel, F., Briançon, S., Allémann, E., Doelker, E., Fessi, H., 2005. Comparative scale-up of three methods for producing ibuprofen-loaded nanoparticles. Eur. J. Pharm. Sci. 25, 357–367. doi:http://dx.doi.org/10.1016/j.ejps.2005.03.013.
Galisteo-González, F., Molina-Bolívar, J.A., 2014. Systematic study on the preparation of BSA nanoparticles. Colloids Surf. B Biointerfaces 123, 286–292. doi:http://dx.doi.org/10.1016/j.colsurfb.2014.09.028.
Ge, J., Neofytou, E., Lei, J., Beygui, R.E., Zare, R.N., 2012. Protein–polymer hybrid nanoparticles for drug delivery. Small 8, 3573–3578. doi:http://dx.doi.org/10.1002/smll.201200889.
Ghosh, S.K., 2006. Functional Coatings: By Polymer Microencapsulation. John Wiley & Sons.
Govender, T., Stolnik, S., Garnett, M.C., Illum, L., Davis, S.S., 1999. PLGA nanoparticles prepared by nanoprecipitation: drug loading and release studies of a water soluble drug. J. Control. Release 57, 171–185.
Hafner, A., Lovrić, J., Lakoš, G.P., Pepić, I., 2014. Nanotherapeutics in the EU: an overview on current state and future directions. Int. J. Nanomed. 9, 1005–1023 [WWW Document], URL https://www.dovepress.com/nanotherapeutics-in-the-eu-an-overview-on-current-state-and-future-dir-peer-reviewed-article-IJN. (Accessed 25 January 2017).
Han, S., Li, M., Liu, X., Gao, H., Wu, Y., 2013. Construction of amphiphilic copolymer nanoparticles based on gelatin as drug carriers for doxorubicin delivery. Colloids Surf. B Biointerfaces 102, 833–841. doi:http://dx.doi.org/10.1016/j.colsurfb.2012.09.010.
Harvey, A.L., 2008. Natural products in drug discovery. Drug Discov. Today 13, 894–901. doi:http://dx.doi.org/10.1016/j.drudis.2008.07.004.
Iqbal, M., Zafar, N., Fessi, H., Elaissari, A., 2015. Double emulsion solvent evaporation techniques used for drug encapsulation. Int. J. Pharm. 496, 173–190. doi:http://dx.doi.org/10.1016/j.ijpharm.2015.10.057.
Jeannot, V., Mazzaferro, S., Lavaud, J., Vanwonterghem, L., Henry, M., Arboléas, M., Vollaire, J., Josserand, V., Coll, J.-L., Lecommandoux, S., Schatz, C., Hurbin, A., 2016. Targeting CD44 receptor-positive lung tumors using polysaccharide-based nanocarriers: influence of nanoparticle size and administration route. Nanomed. Nanotechnol. Biol. Med. 12, 921–932. doi:http://dx.doi.org/10.1016/j.nano.2015.11.018.
Jelvehgari, M., Montazam, S.H., 2012. Comparison of microencapsulation by emulsion-solvent extraction/evaporation technique using derivatives cellulose and acrylate-methacrylate copolymer as carriers. Jundishapur J. Nat. Pharm. Prod. 7, 144–152.
Johnson, B.K., Prud'homme, R.K., 2003. Mechanism for rapid self-assembly of block copolymer nanoparticles. Phys. Rev. Lett. 91, 118302.
Joye, I.J., McClements, D.J., 2013. Production of nanoparticles by anti-solvent precipitation for use in food systems. Trends Food Sci. Technol. 34, 109–123. doi:http://dx.doi.org/10.1016/j.tifs.2013.10.002.
Kalani, M., Yunus, R., 2011. Application of supercritical antisolvent method in drug encapsulation: a review. Int. J. Nanomed. 6, 9–42.
Katara, R., Majumdar, D.K., 2013. Eudragit RL 100-based nanoparticulate system of aceclofenac for ocular delivery. Colloids Surf. B Biointerfaces 103, 455–462. doi:http://dx.doi.org/10.1016/j.colsurfb.2012.10.056.
Kayser, O., Lemke, A., Hernández-Trejo, N., 2005. The impact of nanobiotechnology on the development of new drug delivery systems. Curr. Pharm. Biotechnol. 6, 3–5.
Khachane, P., Date, A.A., Nagarsenker, M.S., 2011. Eudragit EPO nanoparticles: application in improving therapeutic efficacy and reducing ulcerogenicity of meloxicam on oral administration. J. Biomed. Nanotechnol. 7, 590–597.
Kumar, S., Kesharwani, S.S., Mathur, H., Tyagi, M., Bhat, G.J., Tummala, H., 2016. Molecular complexation of curcumin with pH sensitive cationic copolymer enhances the aqueous solubility, stability and bioavailability of curcumin. Eur. J. Pharm. Sci. 82, 86–96. doi:http://dx.doi.org/10.1016/j.ejps.2015.11.010.
Langer, K., Anhorn, M.G., Steinhauser, I., Dreis, S., Celebi, D., Schrickel, N., Faust, S., Vogel, V., 2008. Human serum albumin (HSA) nanoparticles: reproducibility of preparation process and kinetics of enzymatic degradation. Int. J. Pharm. 347, 109–117. doi:http://dx.doi.org/10.1016/j.ijpharm.2007.06.028.
Lee, E.J., Khan, S.A., Park, J.K., Lim, K.-H., 2012. Studies on the characteristics of drug-loaded gelatin nanoparticles prepared by nanoprecipitation. Bioprocess Biosyst. Eng. 35, 297–307. doi:http://dx.doi.org/10.1007/s00449-011-0591-2.
Letchford, K., Burt, H., 2007. A review of the formation and classification of amphiphilic block copolymer nanoparticulate structures: micelles, nanospheres, nanocapsules and polymersomes. Eur. J. Pharm. Biopharm. 65, 259–269. doi:http://dx.doi.org/10.1016/j.ejpb.2006.11.009.
Limayem Blouza, I., Charcosset, C., Sfar, S., Fessi, H., 2006. Preparation and characterization of spironolactone-loaded nanocapsules for paediatric use. Int. J. Pharm. 325, 124–131. doi:http://dx.doi.org/10.1016/j.ijpharm.2006.06.022.
Li, W., Yalcin, M., Lin, Q., Ardawi, M.-S.M., Mousa, S.A., 2017. Self-assembly of green tea catechin derivatives in nanoparticles for oral lycopene delivery. J. Controlled Release 248, 117–124.
Lince, F., Marchisio, D.L., Barresi, A.A., 2008. Strategies to control the particle size distribution of poly-epsilon-caprolactone nanoparticles for pharmaceutical applications. J. Colloid Interface Sci. 322, 505–515. doi:http://dx.doi.org/10.1016/j.jcis.2008.03.033.
Loftsson, T., Brewster, M.E., 2010. Pharmaceutical applications of cyclodextrins: basic science and product development. J. Pharm. Pharmacol. 62, 1607–1621. doi:http://dx.doi.org/10.1111/j.2042-7158.2010.01030.x.
Lohcharoenkal, W., Wang, L., Chen, Y.C., Rojanasakul, Y., 2014. Protein nanoparticles as drug delivery carriers for cancer therapy. BioMed Res. Int..
Luque-Alcaraz, A.G., Lizardi-Mendoza, J., Goycoolea, F.M., Higuera-Ciapara, I., Argüelles-Monal, W., 2016. Preparation of chitosan nanoparticles by nanoprecipitation and their ability as a drug nanocarrier. RSC Adv. 6, 59250–59256. doi:http://dx.doi.org/10.1039/C6RA06563E.
Marchisio, D.L., Rivautella, L., Barresi, A.A., 2006. Design and scale-up of chemical reactors for nanoparticle precipitation. AIChE J. 52, 1877–1887. doi:http://dx.doi.org/10.1002/aic.10786.
Martín-Banderas, L., Álvarez-Fuentes, J., Durán-Lobato, M., Prados, J., Melguizo, C., Fernández-Arévalo, M., Holgado, M.Á., 2012. Cannabinoid derivate-loaded PLGA nanocarriers for oral administration: formulation, characterization, and cytotoxicity studies. Int. J. Nanomed. 7, 5793–5806. doi:http://dx.doi.org/10.2147/IJN.S34633.
Mazzarino, L., Travelet, C., Ortega-Murillo, S., Otsuka, I., Pignot-Paintrand, I., Lemos-Senna, E., Borsali, R., 2012. Elaboration of chitosan-coated nanoparticles loaded with curcumin for mucoadhesive applications. J. Colloid Interface Sci. 370, 58–66. doi:http://dx.doi.org/10.1016/j.jcis.2011.12.063.
Miladi, K., Ibraheem, D., Iqbal, M., Sfar, S., Fessi, H., Elaissari, A., 2014. Particles from preformed polymers as carriers for drug delivery. EXCLI J. 13, 28–57.
Miladi, K., Sfar, S., Fessi, H., Elaissari, A., 2015. Encapsulation of alendronate sodium by nanoprecipitation and double emulsion: from preparation to in vitro studies. Ind. Crops Prod. 72, 24–33. doi:http://dx.doi.org/10.1016/j.indcrop.2015.01.079 Special issue derived from International Conference on Bio-based Materials and Composites.
Miladi, K., Sfar, S., Fessi, H., Elaissari, A., 2016. Nanoprecipitation process: from particle preparation to in vivo applications. In: Vauthier, C., Ponchel, G. (Eds.), Polymer Nanoparticles for Nanomedicines. Springer International Publishing, pp. 17–53.
Mora-Huertas, C.E., Fessi, H., Elaissari, A., 2010. 2010. Polymer-based nanocapsules for drug. Delivery. Int. J. Pharm 385, 113–142. https://doi.org/10.1016/j.ijpharm.2009.10.018.
Mora-Huertas, C.E., Fessi, H., Elaissari, A., 2011. Influence of process and formulation parameters on the formation of submicron particles by solvent displacement and emulsification–diffusion methods: critical comparison. Adv. Colloid Interface Sci. 163, 90–122. doi:http://dx.doi.org/10.1016/j.cis.2011.02.005.
Nicolas, J., Mura, S., Brambilla, D., Mackiewicz, N., Couvreur, P., 2013. Design, functionalization strategies and biomedical applications of targeted biodegradable/biocompatible polymer-based nanocarriers for drug delivery. Chem. Soc. Rev. 42, 1147–1235. doi:http://dx.doi.org/10.1039/c2cs35265f.

Noronha, C.M., Granada, A.F., de Carvalho, S.M., Lino, R.C., de O.B. Maciel, M.V., Barreto, P.L.M., 2013. Optimization of α-tocopherol loaded nanocapsules by the nanoprecipitation method. Ind. Crops Prod. 50, 896–903. doi:http://dx.doi.org/10.1016/j.indcrop.2013.08.015.

Paliwal, R., Babu, R.J., Palakurthi, S., 2014. Nanomedicine scale-up technologies: feasibilities and challenges. AAPS PharmSciTech 15, 1527–1534. doi:http://dx.doi.org/10.1208/s12249-014-0177-9.

Palombo, E.A., 2011. Traditional medicinal plant extracts and natural products with activity against oral bacteria: potential application in the prevention and treatment of oral diseases. Nat. Med. 2011 doi:http://dx.doi.org/10.1093/ecam/nep067.

Patel, A.R., Hu, Y., Tiwari, J.K., Velikov, K.P., 2010. Synthesis and characterisation of zein-curcumin colloidal particles. Soft Matter 6, 6192–6199. doi:http://dx.doi.org/10.1039/C0SM00800A.

Pathak, Y., Thassu, D., 2009. Drug Delivery Nanoparticles Formulation and Characterization, Drugs and the Pharmaceutical Sciences, First Edition doi: http://dx.doi.org/10.1111/j.1600-0854.2005.00260.x.

Peltonen, L., Aitta, J., Hyvönen, S., Karjalainen, M., Hirvonen, J., 2004. Improved entrapment efficiency of hydrophilic drug substance during nanoprecipitation of poly(l)lactide nanoparticles. AAPS PharmSciTech 5 doi:http://dx.doi.org/10.1208/pt050116.

Pereira, R., Julianto, T., Yuen, K., Abdul Majeed, A., 2006. Anionic Eudragit nanoparticles as carriers for oral administration of peptidomimetic drugs. 2006 International Conference on Nanoscience and Nanotechnology, IEEE, pp. 298–301. doi:http://dx.doi.org/10.1109/ICONN.2006.340611.

Popov, A., Schopf, L., Bourassa, J., Chen, H., 2016. Enhanced pulmonary delivery of fluticasone propionate in rodents by mucus-penetrating nanoparticles. Int. J. Pharm. 502, 188–197. doi:http://dx.doi.org/10.1016/j.ijpharm.2016.02.031.

Puga, A.M., Rey-Rico, A., Magariños, B., Alvarez-Lorenzo, C., Concheiro, A., 2012. Hot melt poly-ε-caprolactone/poloxamine implantable matrices for sustained delivery of ciprofloxacin. Acta Biomater. 8, 1507–1518. doi:http://dx.doi.org/10.1016/j.actbio.2011.12.020.

Pustulka, K.M., Wohl, A.R., Lee, H.S., Michel, A.R., Han, J., Hoye, T.R., McCormick, A.V., Panyam, J., Macosko, C.W., 2013. Flash nanoprecipitation: particle structure and stability. Mol. Pharm. 10, 4367–4377. doi:http://dx.doi.org/10.1021/mp400337f.

Qin, Y., Liu, C., Jiang, S., Xiong, L., Sun, Q., 2016. Characterization of starch nanoparticles prepared by nanoprecipitation: influence of amylose content and starch type. Ind. Crops Prod. 87, 182–190. doi:http://dx.doi.org/10.1016/j.indcrop.2016.04.038.

Quiroz-Reyes, C.N., Jesús, E.R., Duran-Caballero, N.E., Aguilar-Méndez, M.Á., 2014. Development and characterization of gelatin nanoparticles loaded with a cocoa-derived polyphenolic extract. Fruits 69, 481–489. doi:http://dx.doi.org/10.1051/fruits/2014034.

Ritter, C.S., Baldissera, M.D., Grando, T.H., Souza, C.F., Sagrillo, M.R., da Silva, A.P.T., Moresco, R.N., Guarda, N.S., da Silva, A.S., Stefani, L.M., Monteiro, S.G., 2017. Achyrocline satureioides essential oil-loaded in nanocapsules reduces cytotoxic damage in liver of rats infected by Trypanosoma evansi. Microb. Pathog. 103, 149–154. doi:http://dx.doi.org/10.1016/j.micpath.2016.12.023.

Sahle, F.F., Gerecke, C., Kleuser, B., Bodmeier, R., 2017. Formulation and comparative in vitro evaluation of various dexamethasone-loaded pH-sensitive polymeric nanoparticles intended for dermal applications. Int. J. Pharm. 516, 21–31. doi:http://dx.doi.org/10.1016/j.ijpharm.2016.11.029.

Sahu, S., 2013. Biocompatible nanoparticles for sustained topical delivery of anticancer Phytoconstituent quercetin*Sneha Sahu, Swarnlata Saraf, Chanchal Deep Kaur and Shailendra Saraf Shri Rawatpura Sarkar Institute of Pharmacy, Kumhari, Durg, CG, India University Institute of Pharmacy, Pt. Ravishankar Shukla UniversityRaipur, 492010 CG, India. Pak. J. Biol. Sci. 16, 601–609.

Sharma, D., Sharma, R.K., Sharma, N., Gabrani, R., Sharma, S.K., Ali, J., Dang, S., 2015. Nose-to-brain delivery of PLGA-diazepam nanoparticles. AAPS PharmSciTech 16, 1108–1121. doi:http://dx.doi.org/10.1208/s12249-015-0294-0.

Şimşek, S., Eroğlu, H., Kurum, B., Ulubayram, K., 2013. Brain targeting of Atorvastatin loaded amphiphilic PLGA-b-PEG nanoparticles. J. Microencapsul. 30, 10–20. doi:http://dx.doi.org/10.3109/02652048.2012.692400.

Singh, G., Pai, R.S., 2014. In-vitro/in-vivo characterization of trans-resveratrol-loaded nanoparticulate drug delivery system for oral administration. J. Pharm. Pharmacol. 66, 1062–1076. doi:http://dx.doi.org/10.1111/jphp.12232.

Singh, M.N., Hemant, K.S.Y., Ram, M., Shivakumar, H.G., 2010. Microencapsulation: a promising technique for controlled drug delivery. Res. Pharm. Sci. 5, 65–77.

Sinha, V.R., Bansal, K., Kaushik, R., Kumria, R., Trehan, A., 2004. Poly-epsilon-caprolactone microspheres and nanospheres: an overview. Int. J. Pharm. 278, 1–23. doi:http://dx.doi.org/10.1016/j.ijpharm.2004.01.044.

Siqueira-Moura, M.P., Primo, F.L., Espreafico, E.M., Tedesco, A.C., 2013. Development, characterization, and photocytotoxicity assessment on human melanoma of chloroaluminum phthalocyanine nanocapsules. Mater. Sci. Eng. C 33, 1744–1752. doi:http://dx.doi.org/10.1016/j.msec.2012.12.088.

Vincristine liposomal—INEX., 2004. lipid-encapsulated vincristine, onco TCS, transmembrane carrier system–vincristine, vincacine, vincristine sulfate liposomes for injection, VSLI, Drugs RD 5, 119–123.

Wacker, M., 2013. Nanocarriers for intravenous injection–the long hard road to the market. Int. J. Pharm. 457, 50–62. doi:http://dx.doi.org/10.1016/j.ijpharm.2013.08.079.

Wang, T., Zhu, D., Liu, G., Tao, W., Cao, W., Zhang, L., Wang, L., Chen, H., Mei, L., Huang, L., Zeng, X., 2015. DTX-loaded star-shaped TAPP-PLA- b -TPGS nanoparticles for cancer chemical and photodynamic combination therapy. RSC Adv. 5, 50617–50627.

Wang, Y., Tan, Y., 2016. Enhanced drug loading capacity of 10-hydroxycamptothecin-loaded nanoparticles prepared by two-step nanoprecipitation method. J. Drug Deliv. Sci. Technol. 36, 183–191. doi:http://dx.doi.org/10.1016/j.jddst.2016.09.012.

Yan, X., Ramos, R., Hoibian, E., Soulage, C., Alcouffe, P., Ganachaud, F., Bernard, J., 2017. Nanoprecipitation of PHPMA (Co)polymers into nanocapsules displaying tunable compositions, dimensions, and surface properties. ACS Macro Lett. 6, 447–451.

Yordanov, G., Skrobanska, R., Evangelatov, A., 2012. Entrapment of epirubicin in poly (butyl cyanoacrylate) colloidal nanospheres by nanoprecipitation: formulation development and in vitro studies on cancer cell lines. Colloids Surf. B Biointerfaces 92, 98–105. doi:http://dx.doi.org/10.1016/j.colsurfb.2011.11.029.

Yuan, G., Yan, S.-F., Xue, H., Zhang, P., Sun, J.-T., Li, G., 2014. Cucurbitacin I induces protective autophagy in glioblastoma in vitro and in vivo. J. Biol. Chem. 289, 10607–10619. doi:http://dx.doi.org/10.1074/jbc.M113.528760 jbc.M113.528760.

Zhang, X., Zhang, X., Wang, S., Liu, M., Tao, L., Wei, Y., 2012. Surfactant modification of aggregation-induced emission material as biocompatible nanoparticles: facile preparation and cell imaging. Nanoscale 5, 147–150. doi:http://dx.doi.org/10.1039/C2NR32698A.

Zhou, P., An, T., Zhao, C., Li, Y., Li, R., Yang, R., Wang, Y., Gao, X., 2015. Lactosylated PLGA nanoparticles containing ε-polylysine for the sustained release and liver-targeted delivery of the negatively charged proteins. Int. J. Pharm. 478, 633–643. doi:http://dx.doi.org/10.1016/j.ijpharm.2014.12.017.

Hindawi
Journal of Analytical Methods in Chemistry
Article ID 9086467

Research Article

Quantitative Aspect of *Leucophyllum frutescens* Fraction before and after Encapsulation in Polymeric Nanoparticles

Claudia Janeth Martínez-Rivas,[1,2] Rocío Álvarez-Román,[3] Catalina Rivas-Morales,[1] Abdelhamid Elaissari,[2] Hatem Fessi,[2] and Sergio Arturo Galindo-Rodríguez[1]

[1]*Facultad de Ciencias Biológicas, Laboratorio de Nanotecnología, Universidad Autónoma de Nuevo León, Av. Pedro de Alba s/n, 66455 San Nicolás de los Garza, NL, Mexico*
[2]*CNRS, LAGEP UMR 5007, University Claude Bernard Lyon 1, 43 Boulevard du 11 Novembre 1918, 69100 Villeurbanne, France*
[3]*Facultad de Medicina, Departamento de Química Analítica, Universidad Autónoma de Nuevo León, Av. Fco. I. Madero y Dr. E. Aguirre Pequeño s/n, 64460 Monterrey, NL, Mexico*

Correspondence should be addressed to Sergio Arturo Galindo-Rodríguez; sagrod@yahoo.com.mx

Received 18 May 2017; Revised 11 September 2017; Accepted 13 September 2017

Academic Editor: Anna V. Queralt

The interest on plants has been focalized due to their biological activities. Extracts or fractions from plants in biodegradable polymeric nanoparticles (NP) provide many advantages on application studies. The encapsulation of the extract or fraction in NP is determined for the establishment of the test dose. HPLC method is an alternative to calculate this parameter. An analytical method based on HPLC for quantification of a hexane fraction from *L. frutescens* was developed and validated according to ICH. Different concentrations of the hexane fraction from leaves (HFL) were prepared (100–600 μg/mL). Linearity, limit of detection, limit of quantification, and intra- and interday precision parameters were determined. HFL was encapsulated by nanoprecipitation technique and analyzed by HPLC for quantitative aspect. The method was linear and precise for the quantification of the HFL components. NP size was 190 nm with homogeneous size distribution. Through validation method, it was determined that the encapsulation of components (1), (2), (3), and (4) was 44, 74, 86, and 97%, respectively. A simple, repeatable, and reproducible methodology was developed for the propose of quantifying the components of a vegetable material loaded in NP, using as a model the hexane fraction of *L. frutescens* leaves.

1. Introduction

Since prehistoric times, medicinal plants have been used as treatments for numerous human diseases [1, 2]. Recently, research articles have proved biological activities of some plant extracts as antioxidant [3, 4], anti-inflammatory [4], antimicrobial [5, 6], and anticancer [7] activity. Organic solvents are used in the extraction process to obtain the active plant material [8] and as carrier in the assays for extract application. However, for *in vivo* administration, an organic solvent would result in toxicity for the organism [9].

Different carriers as nanocomposite films [10], microparticles [11], and nanoparticles [12, 13] have been a good alternative as drug delivery systems. Particularly, polymeric nanoparticles (NP) are promising as carriers which present sustained release and protection to the active [14] and targeting to specific organs [15, 16]. During NP preparation the organic solvent has to be eliminated. Researches in natural products encapsulation have demonstrated beneficial effects. *Arrabidaea chica* is a plant with healing properties employed in folk medicine for wound healing, inflammation, and gastrointestinal colic. Servat-Medina et al. studied the antiulcerogenic activity. *A. chica* hydroalcoholic extract was incorporated in chitosan-sodium tripolyphosphate NP. An *in vitro* study in human skin fibroblasts showed biocompatibility. *In vivo* study proved that *A. chica* hydroalcoholic extract-loaded NP enhances its antiulcerogenic activity [17]. Similar behaviors were obtained by Kwon et al. They investigated

Table 1: Validation parameters for the four peaks-components in hexane fraction from *Leucophyllum frutescens* leaves.

Peak-component	Regression equation	Correlation coefficient (r)	LOD (μg/mL)	LOQ (μg/mL)	Intraday precision (RSD, %)	Interday precision (RSD, %)
(1)	$y = 5.5199x - 22.689$	0.99	53.73	162.83	4.10	6.08
(2)	$y = 3.3057x - 23.667$	0.99	60.00	181.81	6.93	6.41
(3)	$y = 11.692x - 209.84$	0.99	44.27	134.15	7.30	7.28
(4)	$y = 4.8221x - 74.844$	0.99	101.47	307.49	9.34	10.51

Table 2: Characterization of hexane fraction from *L. frutescens* leaves loaded biodegradable polymeric nanoparticles.

Size (nm)	PDI	Peak-component	Quantification % L	% EE
189.7 ± 3.81	0.138 ± 0.026	(1)	4.01 ± 0.48	44.23 ± 5.35
		(2)	6.74 ± 0.64	74.34 ± 6.97
		(3)	7.87 ± 0.78	86.78 ± 8.62
		(4)	8.81 ± 0.34	97.03 ± 3.44

Mean ± SD ($n = 3$).

different activities of the aqueous extract of *Centella asiatica* loaded gelatin NP. Encapsulated aqueous extract presented lower toxicity in human skin fibroblasts. Extract-loaded NP displayed a stronger inhibition of enzymatic activity that affects dermal tissues, flux through mouse skin, and retention. These results showed the potential use of aqueous extract of *C. asiatica* loaded NP in cosmetic industry [18].

As well as drug encapsulation, extract encapsulation involves the NP characterization, loading (% L), and encapsulation efficiency (% EE). Besides, being two of the main parameters determined for NP characterization [19], in *in vitro* and *in vivo* studies, it is important to establish the test dose in treatments. UV-Vis spectrophotometry has been used for extract-loaded NP quantification [17, 20]. However, quantification of low concentrations is limited for its poor sensitivity. High performance liquid chromatography (HPLC) is a method used to separate the marker compounds in extracts or fractions for their subsequent quantification [21, 22]. Sangthong and Weerapreeyakul identified two compounds (sulforaphene and sulforaphane) in *Raphanus sativus* L. var. *caudatus* Alef extracts. Quantification of both molecules was carried out through a validated HPLC method [23]. Thus, development and validation of a method based on separation of known molecules in the plant and their quantification in NP are promising.

However, there are plants less studied as *Leucophyllum frutescens*, Scrophulariaceae family, is commonly known as "cenizo." This plant is the bush par excellence of Nuevo León, while, in Texas, it is called the "bush barometer" due to its surprising flowering depending on the humidity in the environment and precipitation rain [24]. *L. frutescens* has received attention for its anti-*M. tuberculosis* activity. Methanol extract from leaves has presented biological activity against multidrug-resistant (MDR) *M. tuberculosis* strains [25] and two new active compounds from hexane fraction of *L. frutescens* against these bacteria have been described [26, 27]. We posed hexane fraction loaded NP as promising agent against multidrug-resistant (MDR) strain and NP administration in systems involves knowing the fraction encapsulation. In this context, the aim of this study was to propose the development and validation of an analytical method by HPLC using internal marker compounds for the quantification of the hexane fraction from *L. frutescens* leaves (HFL) loaded in NP.

2. Materials and Methods

2.1. Plant Material and Reagents. *L. frutescens* was collected in Monterrey; N. L. Methanol (Tedia, USA), formic acid (purity: 90%, Millipore, USA), and acetonitrile (J.T. Baker, USA) were HPLC-grade. Purified water was from a Milli-Q water-purification system (Millipore, USA). Poly-L-lactide acid (PLA) (PURASORB, PURAC biochem BV, Gorinchem, HOL) as the NP-formed polymer and polyvinyl alcohol (PVAL, Clariant, Mexico) as stabilizer. Other solvents used were of analytical grade.

2.2. Chromatographic Analysis. High performance liquid chromatography assay was performed with a photodiode array detector (HPLC-DAD) (Varian 9065, 9012, ProStar 410, USA). A Synergi™ 4 μm Fusion-RP 80 Å (150 mm × 2.0 mm × 4 μm) column was used with a flow rate of 0.2 mL/min and maintained at 30°C. Two methods were carried out; for method 1, the mobile phase was formic acid 0.1% v/v (A) and methanol (B). Gradient conditions were as follows: a gradual change from 45 : 55 (A : B) to 100 (B) was completed during 0–20 min, and then 100 (B) was maintained for 20–35 min. For method 2, the mobile phase was an isocratic elution with 45 : 55 (A : B) during 40 min. Detection wavelength was set at 210, 215, 220, and 229 nm. The peaks at 210 nm were detected, based on peak areas at the maximum wavelength.

2.3. Preparation of Calibration Curve. The leaves of *L. frutescens* (50 g) were dried at room temperature, pulverized, and extracted with methanol (350 mL) with sonication (Ultrasonic Cleaners, VWR Symphony, USA). The methanol extract was evaporated under reduced pressure (Laborota 4003 control, Heidolph). Liquid-liquid partition was carried out with hexane. The hexane fraction from leaves (HFL) was evaporated under reduced pressure. For the preparation of stock solution, the total semisolid HFL was weighed and dissolved in methanol. Then, this solution was filtered through a 0.45 μm membrane filter (Millipore, USA). The working solutions were prepared in a concentration range from 100 to 600 μg/mL in triplicate and filtered for their HPLC-DAD analysis to obtain the calibration curve.

2.4. Method Validation. The method was validated for linearity, limit of detection (LOD), limit of quantification (LOQ), and intra- and interday precision according to International Conference on Harmonisation [28]. For the establishment of linearity, five levels of concentration were prepared in a range from 100 to 600 μg/mL in triplicate, while the LOD and LOQ were calculated from the calibration curve according to

$$\text{LOD} = \frac{3.3\sigma}{S}, \qquad \text{LOQ} = \frac{10\sigma}{S}, \tag{1}$$

where σ is the standard deviation of the response and S is the slope of the calibration curve. The residual standard deviation of a line regression or the standard deviation of y-intercepts of lines regression may be used as the standard deviation. Finally, the intra- and interday precision were determined analyzing three concentrations with six replicates each one, during a single day and on three different days, respectively.

Once the chromatographic method was established and validated, NP were prepared according to the procedure of nanoprecipitation technique developed by Fessi et al. [29]. Briefly, the organic phase was prepared by dissolving 30 mg of PLA and 3 mg of hexane fraction in 3 mL of an organic solvent mixture (acetone : methanol). The organic solution was added to 10 mL of aqueous phase containing PVAL (1%, w/w) and stirred magnetically. The organic solvent was evaporated at reduced pressure. NP characterization was carried out determining size and size distribution index (PDI) by dynamic light scattering (DLS) (Zetasizer Nano ZS90, Malvern Instruments, UK). The morphology of the NP was observed using a FEI Quanta 250 FEG Microscope at the "*Centre Technologique des Microstructures*" (CTμ, Claude Bernard University Lyon 1, France). For the preparation of SEM samples, a drop of diluted aqueous suspension was deposited on a flat metallic holder and dried at room temperature. The sample was finally coated under vacuum by cathodic sputtering with platinum. The samples were observed by SEM under an accelerating voltage of 10 kV. For encapsulation loading (% L) and encapsulation efficiency (% EE), NP dispersions were centrifuged at 25,000 rpm (Allegra 64R, Beckman Coulter, USA) and obtained pellets were lyophilized (Freeze Dry System, LABCONCO, USA). Lyophilized NP were dissolved in acetonitrile-methanol. Solutions were analyzed by HPLC to quantify the encapsulated peaks by the parameters: % L and % EE, according to the following:

$$\%\ L = \frac{\text{Amount of peak/component in NP}}{\text{Mass of lyophilized NP}} \times 100, \qquad \%\ \text{EE} = \frac{\text{Amount of peak/component in NP}}{\text{Total amount of peak/component}} \times 100. \tag{2}$$

3. Results and Discussion

3.1. Development of the Chromatographic Method by HPLC. In medicinal plants, there are hundreds of unknown components. Variability within the same herbal materials [21] depends on the collection station and the origin of the plant, among other factors [30]. For this reason, the determination of the chromatographic profile is a useful tool for the quality control of plant extract samples [31–34]. HPLC analysis is carried out for knowledge of the chromatographic profile of the vegetal samples [21].

L. frutescens is a plant less studied that has demonstrated to be promising for its use against tuberculosis. In this way, to obtain the chromatographic profile using the hexane fraction of *L. frutescens* leaves increases the knowledge about the plant. Method 1 was developed to obtain the chromatographic profile HFL. Figure 1(a) shows 16 peaks at a concentration of 400 μg/mL of the fraction and the main peaks are (1)–(4). Method 2 was developed to separate these four main peaks and validated for quantification of peaks (Figure 1(b)). In both chromatograms each peak corresponds to one component of the fraction [35]. Method 2 was validated to quantify the components in the hexane fraction loaded NP.

To increase the knowledge about the plant, a searching for some compounds found in *L. frutescens* family called Scrophulariaceae was performed; three compounds, quercetin [36], luteolin, and apigenin [37], were selected and analyzed by HPLC method 2. The HPLC analysis was carried out and retention time of each one was obtained (Figure 1(c)). Compared with the retention time of the four components in HFL observed by the same method, peak-component (1) (15.48 min) would be apigenin (16.07 min). It is necessary to analyze HFL by spectroscopic methods to assign the presence of this compound.

3.2. Validation of Analytical Procedure: Linearity, Limit of Detection, Limit of Quantification, and Intra- and Interday Precision. The developed HPLC-DAD method has demonstrated to be simple, sensitive, specific, and adequate for the simultaneous quantification [38]. The validation was performed to know the linearity and the precision of the chromatographic method (method 2) for the quantification of the peaks-components of HFL loaded NP. For the establishment of linearity, a minimum of 5 concentrations is recommended by the ICH [28]. A calibration curve of the semisolid HFL in acetonitrile-methanol at a concentration range from 100 to 600 μg/mL was prepared. The area

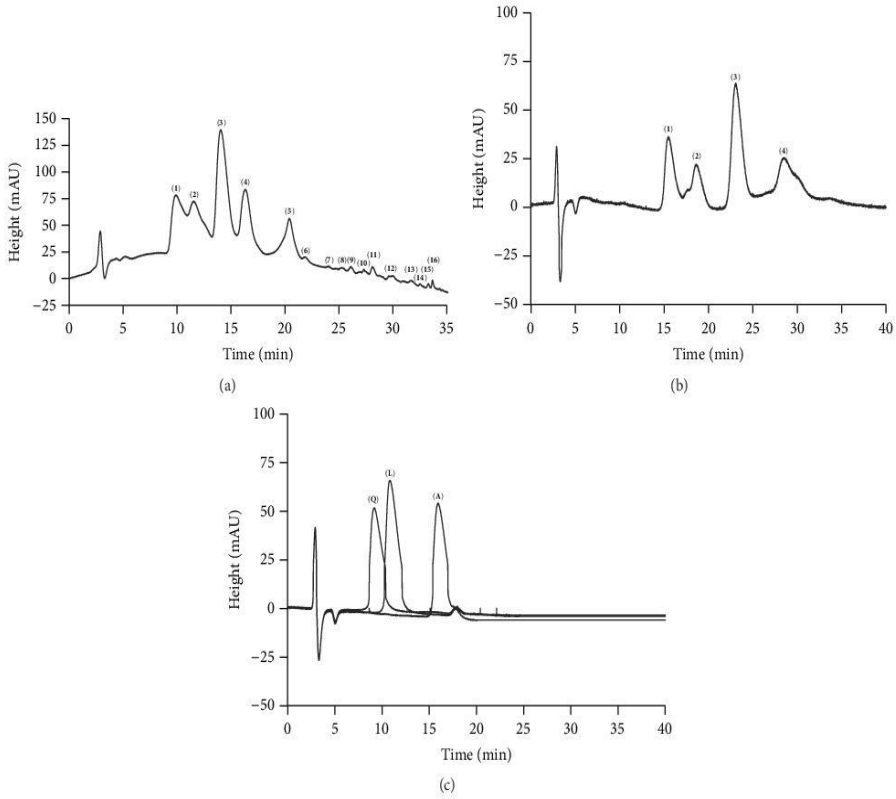

FIGURE 1: Chromatographic profile of hexane fraction from *L. frutescens* leaves (400 μg/mL) by HPLC (a) method 1: chromatogram shows 16 peaks-components with a retention time of 9.88, 11.50, 14.04, 16.34, 20.40, 21.88, 24.04, 25.30, 26.11, 27.32, 28.11, 29.94, 31.62, 32.52, 33.27, and 33.66 min. (b) Method 2: chromatogram shows 4 peaks-components with a retention time of 15.48, 18.61, 23.05, and 28.49 min. (c) Quercetin (Q), luteolin (L), and apigenin (A) with retention time of 9.31, 10.97, and 16.07 min, respectively, analyzed by method 2.

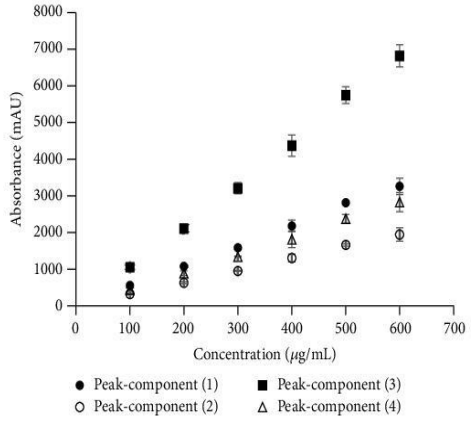

FIGURE 2: Calibration curve for the four peaks-components present in the hexane fraction from *L. frutescens* leaves (Mean ± SD, $n = 3$).

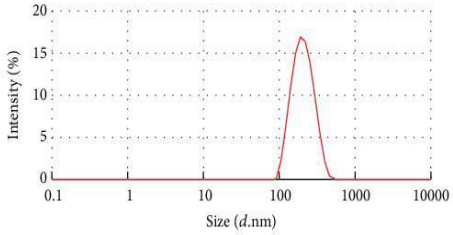

Figure 3: Size distribution of HFL loaded NP measured by the DLS technique.

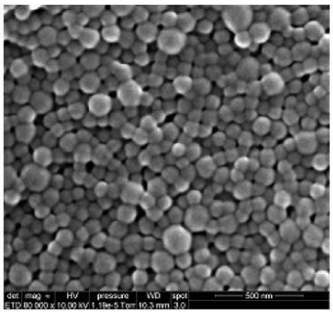

Figure 4: SEM image of PLA nanoparticles prepared by the nanoprecipitation method (scale bar represents 500 nm).

under the curve in each concentration level of each peak-component was analyzed to obtain Figure 2. Consequently, regression equation, correlation coefficient, LOD, and LOQ of each peak-component were established (Table 1). The acceptance criterion for linearity is given by the correlation coefficient [28, 39]. For quantification of content or active ingredient, the coefficient must be greater than or equal to 0.99 [39].

As shown in Table 2, correlation coefficients for calibration curve of each peak-component are greater than 0.99. LOD and LOQ for peaks-components (1), (2), (3), and (4) were determined, being 53.73 and 162.83, 60.00 and 181.80, 44.27 and 134.15, and 101.47 and 307.49 μg/mL, respectively. Da Silva et al. quantified simultaneously quercetin and rosmarinic acid in sage and savoury (*Salvia* sp. and *Satureja montana*, resp.) from a calibration curve with standard compounds. LOD and LOQ were found to be 20 and 80 μg/mL for rosmarinic acid, respectively. For quercetin, they were 30 and 90 μg/mL, respectively [40]. In our study, higher values have been determined due to LOD and LOQ values and have been established with respect to the concentration of total HFL.

Intra- and interday precision of the chromatographic method were determined analyzing three concentrations with six replicates each one, during a single day and on three different days; in order to obtain their RSD, results of these parameters are shown in Table 1. Intra- and interday variations were around 9.34% and 10.51%, respectively. Ying et al. used *Angelica sinensis*, a famous traditional Chinese medicinal herb. Many kinds of compounds have been isolated and identified from the plant. They validated a method for the simultaneous quantification of six active compounds present in *A. sinensis* (ferulic acid, senkyunolide I, senkyunolide H, coniferyl ferulate, Z/E-ligustilide, and Z/E-butylidenephthalide) from a mixture of standards. The precision of the quantification method had an intraday RSD below 2.43% and interday below 5.00% [41].

3.3. Preparation and Characterization of the Hexane Fraction from L. frutescens Incorporated in Polymeric Nanoparticles. Nanoprecipitation technique described by Fessi et al. was used for NP preparation. The size of obtained NP formulation was 189.70 ± 3.80 nm with homogeneous distribution (Figure 3). SEM was used to visualize the morphology. Particles were evaluated on the basis of shape and presence of interparticulate bridging. Under SEM observation, the submicron particles produced had spherical shapes and showed a homogenous particle size distribution (Figure 4). After that, lyophilized pellet of HFL loaded NP was dissolved in acetonitrile/methanol and solutions were analyzed by HPLC. The area under the curve obtained from each peak-component was replaced in its regression equation (Table 1), in order to obtain the concentration of four peak-components in NP. Consequently, equations (2) were used to determine % L and % EE of each peak-component (Table 2). The encapsulation of the peaks-components in NP was 44, 74, 86, and 97% of peaks (1), (2), (3), and (4), respectively. Based on the separation of peaks by HPLC method, first peak is the less hydrophobic, in NP representing the lowest encapsulation. The most hydrophobic peak in NP represents the highest

encapsulation. Studies have reported that nanoprecipitation method is highly favorable in the encapsulation of the hydrophobic compounds [42]. Dalpiaz et al. mentioned that, compared PLGA with PLA, PLA has a lower hydrophilicity [43]. In this study, the method of NP preparation as well as the NP-formed polymer permits higher encapsulation percentage of the hydrophobic peaks-components.

4. Conclusions

L. frutescens is a plant with potential use. Chromatographic profile is part of characterization of extracts or fractions obtained from plants. In this study, we developed a chromatographic method to obtain the chromatographic profile of hexane fraction of *L. frutescens* leaves. The chromatographic method was validated based on the presence of the peaks-components in HFL, in order to quantify them in NP. HFL loaded NP suspension around 190 nm was obtained. NP-formed polymer and nanoprecipitation method were favorable to encapsulate the hydrophobic components of *L. frutescens* extract.

Conflicts of Interest

The authors declare that there are no conflicts of interest regarding the publication of this article.

Acknowledgments

The authors gratefully acknowledge the financial supports by PRODEP-SEP Networks, Mexico, DSA/103.5/15/14156, AIRD, France (JEAI-2011, NANOBIOSA), PN-CONACYT, Mexico, 2014-248560, and PAICYT-UANL, Mexico. Claudia Janeth Martínez-Rivas is thankful for CONACyT scholarship, Mexico, no. 280112.

References

[1] D. J. Bharali, I. A. Siddiqui, V. M. Adhami et al., "Nanoparticle delivery of natural products in the prevention and treatment of cancers: Current status and future prospects," *Cancers*, vol. 3, no. 4, pp. 4024–4045, 2011.

[2] E. A. Palombo, "Traditional medicinal plant extracts and natural products with activity against oral bacteria: potential application in the prevention and treatment of oral diseases," *Evidence-Based Complementary and Alternative Medicine*, vol. 2011, Article ID 680354, 15 pages, 2011.

[3] V. Kraujaliene, A. Pukalskas, P. Kraujalis, and P. R. Venskutonis, "Biorefining of *Bergenia crassifolia* L. roots and leaves by high pressure extraction methods and evaluation of antioxidant properties and main phytochemicals in extracts and plant material," *Industrial Crops and Products*, vol. 89, pp. 390–398, 2016.

[4] J. Malik, J. Tauchen, P. Landa et al., "*In vitro* antiinflammatory and antioxidant potential of root extracts from Ranunculaceae species," *South African Journal of Botany*, vol. 109, pp. 128–137, 2017.

[5] S. Akroum, "Antifungal activity of acetone extracts from *Punica granatum* L., *Quercus suber* L. and *Vicia faba* L," *Journal de Mycologie Médicale*, vol. 27, no. 1, pp. 83–89, 2017.

[6] A. A. Mostafa, A. A. Al-Askar, K. S. Almaary, T. M. Dawoud, E. N. Sholkamy, and M. M. Bakri, "Antimicrobial activity of some plant extracts against bacterial strains causing food poisoning diseases," *Saudi Journal of Biological Sciences*, 2016.

[7] R. B. Villacorta, K. F. J. Roque, G. A. Tapang, and S. D. Jacinto, "Plant extracts as natural photosensitizers in photodynamic therapy: *in vitro* activity against human mammary adenocarcinoma MCF-7 cells," *Asian Pacific Journal of Tropical Biomedicine*, vol. 7, no. 4, pp. 358–366, 2017.

[8] M. N. Alam, N. J. Bristi, and M. Rafiquzzaman, "Review on *in vivo* and *in vitro* methods evaluation of antioxidant activity," *Saudi Pharmaceutical Journal*, vol. 21, no. 2, pp. 143–152, 2013.

[9] J. Maes, L. Verlooy, O. E. Buenafe, P. A. M. de Witte, C. V. Esguerra, and A. D. Crawford, "Evaluation of 14 Organic Solvents and Carriers for Screening Applications in Zebrafish Embryos and Larvae," *PLoS ONE*, vol. 7, no. 10, Article ID e43850, 2012.

[10] L. Floroian, C. Ristoscu, G. Candiani et al., "Antimicrobial thin films based on ayurvedic plants extracts embedded in a bioactive glass matrix," *Applied Surface Science*, vol. 417, pp. 224–233, 2016.

[11] T. Klein, R. Longhini, M. L. Bruschi, and J. C. P. De Mello, "Microparticles containing Guaraná extract obtained by spray-drying technique: Development and characterization," *Revista Brasileira de Farmacognosia*, vol. 25, no. 3, pp. 292–300, 2015.

[12] T. G. do Nascimento, P. F. da Silva, L. F. Azevedo et al., "Polymeric Nanoparticles of Brazilian red propolis extract: preparation, characterization, antioxidant and leishmanicidal activity," *Nanoscale Research Letters*, vol. 11, no. 1, article 301, 2016.

[13] Y. Zhou, C. Guo, H. Chen, Y. Zhang, X. Peng, and P. Zhu, "Determination of sinomenine in cubosome nanoparticles by HPLC technique," *Journal of Analytical Methods in Chemistry*, vol. 2015, Article ID 931687, 2015.

[14] J.-W. Yoo, N. Giri, and C. H. Lee, "pH-sensitive Eudragit nanoparticles for mucosal drug delivery," *International Journal of Pharmaceutics*, vol. 403, no. 1-2, pp. 262–267, 2011.

[15] O. O. Maksimenko, L. V. Vanchugova, E. V. Shipulo et al., "Effects of technical parameters on the physicochemical properties of rifampicin-containing polylactide nanoparticles," *Pharmaceutical Chemistry Journal*, vol. 44, no. 3, pp. 151–156, 2010.

[16] R. Pandey and G. K. Khuller, "Nanotechnology based drug delivery system(s) for the management of tuberculosis," *Indian Journal of Experimental Biology (IJEB)*, vol. 44, no. 5, pp. 357–366, 2006.

[17] L. Servat-Medina, A. González-Gómez, F. Reyes-Ortega et al., "Chitosan–tripolyphosphate nanoparticles as *Arrabidaea chica* standardized extract carrier: Synthesis, characterization, biocompatibility, and antiulcerogenic activity," *International Journal of Nanomedicine*, vol. 10, pp. 3897–3909, 2015.

[18] M. C. Kwon, W. Y. Choi, Y. C. Seo et al., "Enhancement of the Skin-Protective Activities of *Centella asiatica* L. Urban by a Nano-encapsulation Process," *Journal of Biotechnology*, vol. 157, no. 1, pp. 100–106, 2012.

[19] A. C. de Mattos, N. M. Khalil, and R. M. Mainardes, "Development and validation of an HPLC method for the determination of fluorouracil in polymeric nanoparticles," *Brazilian Journal of Pharmaceutical Sciences*, vol. 49, no. 1, pp. 117–126, 2013.

[20] R. Renuka, P. Sandhya, B. N. Vedha Hari, and D. Ramya Devi, "Design of polymeric nanoparticles of *Emblica officinalis* extracts and study of *in vitro* therapeutic effects," *Current Trends in Biotechnology and Pharmacy*, vol. 7, no. 3, pp. 716–724, 2013.

[21] Y.-Z. Liang, P. Xie, and K. Chan, "Quality control of herbal medicines," *Journal of Chromatography B*, vol. 812, no. 1-2, pp. 53–70, 2004.

[22] B. Medeiros-Neves, F. M. Corrêa De Barros, G. L. Von Poser, and H. F. Teixeira, "Quantification of coumarins in aqueous extract of *Pterocaulon balansae* (Asteraceae) and characterization of a new compound," *Molecules*, vol. 20, no. 10, pp. 18083–18094, 2015.

[23] S. Sangthong and N. Weerapreeyakul, "Simultaneous quantification of sulforaphene and sulforaphane by reverse phase HPLC and their content in *Raphanus sativus* L. var. caudatus Alef extracts," *Food Chemistry*, vol. 201, pp. 139–144, 2016.

[24] O. Z. Zaragoza, "Guía de árboles y otras plantas nativas en la zona metropolitana de monterrey," *Fondo Editorial de NL*, 2009.

[25] G. M. Molina-Salinas, A. Pérez-López, P. Becerril-Montes, R. Salazar-Aranda, S. Said-Fernández, and N. W. D. Torres, "Evaluation of the flora of Northern Mexico for *in vitro* antimicrobial and antituberculosis activity," *Journal of Ethnopharmacology*, vol. 109, no. 3, pp. 435–441, 2007.

[26] B. Alanís-Garza, R. Salazar-Aranda, R. Ramírez-Durón, E. Garza-González, and N. W. De Torres, "A new antimycobacterial furanolignan from *Leucophyllum frutescens*," *Natural Product Communications (NPC)*, vol. 7, no. 5, pp. 597-598, 2012.

[27] G. M. Molina-Salinas, V. M. Rivas-Galindo, S. Said-Fernández et al., "Stereochemical analysis of leubethanol, an anti-TB-active serrulatane, from *Leucophyllum frutescens*," *Journal of Natural Products*, vol. 74, no. 9, pp. 1842–1850, 2011.

[28] International Coference on Harmonisation (ICH), Validation of Analytical Procedures: Text and Methodology, [Online]. Available: https://www.ich.org/fileadmin/Public_Web_Site/ICH_Products/Guidelines/Quality/Q2_R1/Step4/Q2_R1__Guideline.pdf, 2005.

[29] H. Fessi, F. Piusieux, J. P. Devissaguet, N. Ammoury, and S. Benita, "Nanocapsule formation by interfacial polymer deposition following solvent displacement," *International Journal of Pharmaceutics*, vol. 55, no. 1, pp. R1–R4, 1989.

[30] N. Nguyen Hoai, B. Dejaegher, C. Tistaert et al., "Development of HPLC fingerprints for *Mallotus* species extracts and evaluation of the peaks responsible for their antioxidant activity," *Journal of Pharmaceutical and Biomedical Analysis*, vol. 50, no. 5, pp. 753–763, 2009.

[31] X. He, J. Li, W. Zhao, R. Liu, L. Zhang, and X. Kong, "Chemical fingerprint analysis for quality control and identification of Ziyang green tea by HPLC," *Food Chemistry*, vol. 171, pp. 405–411, 2015.

[32] Y. Xie, Z.-H. Jiang, H. Zhou et al., "Combinative method using HPLC quantitative and qualitative analyses for quality consistency assessment of a herbal medicinal preparation," *Journal of Pharmaceutical and Biomedical Analysis*, vol. 43, no. 1, pp. 204–212, 2007.

[33] S.-O. Yang, S. W. Lee, Y. O. Kim et al., "HPLC-based metabolic profiling and quality control of leaves of different *Panax* species," *Journal of Ginseng Research*, vol. 37, no. 2, pp. 248–253, 2013.

[34] J.-H. Kim, C.-S. Seo, S.-S. Kim, and H.-K. Shin, "Quality assessment of Ojeok-san, a traditional herbal formula, using high-performance liquid chromatography combined with chemometric analysis," *Journal of Analytical Methods in Chemistry*, vol. 2015, Article ID 607252, 11 pages, 2015.

[35] J. Zaiyou, W. Wenquan, X. Guifang, M. Li, and H. Junling, "Comprehensive quality evaluation of Chishao by HPLC," *Nutrición Hospitalaria*, vol. 28, no. 5, pp. 1681–1687, 2013.

[36] A. Grigore, S. Colceru-Mihul, S. Litescu, M. Panteli, and I. Rasit, "Correlation between polyphenol content and anti-inflammatory activity of *Verbascum phlomoides* (mullein)," *Pharmaceutical Biology*, vol. 51, no. 7, pp. 925–929, 2013.

[37] M. Nikolova, R. Gevrenova, and S. Ivancheva, "External flavonoid aglycones from *Veronica chamaedrys* L. (Scrophulariaceae)," *Acta Pharmaceutica*, vol. 53, no. 2, pp. 145–149, 2003.

[38] F.-C. Chen, L.-H. Wang, J. Guo, X.-Y. Shi, and B.-X. Fang, "Simultaneous Determination of Dexamethasone, Ondansetron, Granisetron, Tropisetron, and Azasetron in Infusion Samples by HPLC with DAD Detection," *Journal of Analytical Methods in Chemistry*, vol. 2017, Article ID 6749087, 2017.

[39] Secretaria de Salud (SSA), Criterios para la validación de métodos Fisicoquímicos, [Online], Available: http://www.cofepris.gob.mx/TyS/Documents/TercerosAutorizados/cvfq032011.pdf, 2011.

[40] S. B. Da Silva, A. Oliveira, D. Ferreira, B. Sarmento, and M. Pintado, "Development and validation method for simultaneous quantification of phenolic compounds in natural extracts and nanosystems," *Phytochemical Analysis*, vol. 24, no. 6, pp. 638–644, 2013.

[41] L. Ying, W. Si-Wang, T. Hong-Hai, and C. Wei, "Simultaneous quantification of six main active constituents in Chinese Angelica by high-performance liquid chromatography with photodiode array detector," *Pharmacognosy Magazine*, vol. 9, no. 34, pp. 114–119, 2013.

[42] D. B. Shenoy and M. M. Amiji, "Poly(ethylene oxide)-modified poly(ε-caprolactone) nanoparticles for targeted delivery of tamoxifen in breast cancer," *International Journal of Pharmaceutics*, vol. 293, no. 1-2, pp. 261–270, 2005.

[43] A. Dalpiaz, F. Sacchetti, A. Baldisserotto et al., "Application of the "in-oil nanoprecipitation" method in the encapsulation of hydrophilic drugs in PLGA nanoparticles," *Journal of Drug Delivery Science and Technology*, vol. 32, pp. 283–290, 2016.

APPENDIX II
PARTICIPATION IN CONGRESSES

"Cuantificación de rifampicina incorporada en nanopartículas poliméricas por CLAR para su potencial aplicación biológica". XXIX Congreso Nacional de Química Analítica y XIX Simposio Estudiantil. Villahermosa, Tabasco, Mexico. June-Jully 2016. Poster.

"Desarrollo y validación de un método por cromatografía de líquidos de alta resolución para la cuantificación de rifampicina incorporada en nanopartículas poliméricas". XXVIII Congreso Nacional de Química Analítica y XVIII Simposio Estudiantil. Guerrero, Mexico. June 2015. Poster.

"Caracterización de extractos de Leucophyllum frutescens (cenizo) obtenidos mediante dos métodos de extracción". 10ª. Reunión Internacional en Investigación de Productos Naturales. Yucatán, Mexico. May 2014. Poster.